Temporal Lobe - Sylvian Region

Last Updated: July 5, 2021

ABSTRACT

OBJECTIVE: We present observations of the anatomy of the sylvian fissure region and their clinical application in neuroimaging, microsurgery for middle cerebral artery aneurysms and insular lesions, frontobasal resections, and epilepsy surgery.

METHODS: Sixty adult cadaveric hemispheres and 12 adult cadaveric heads were studied after perfusion of the arteries and veins with colored latex. The anatomic information was applied in more than 200 microsurgeries in and around the sylvian fissure region in the past 15 years.

RESULTS: The sylvian fissure extends from the basal to the lateral surface of the brain and presents 2 compartments on each surface, 1 superficial (temporal stem and its ramii) and 1 deep (anterior and lateral operculoinsular compartments). The temporal operculum is in opposition to the frontal and parietal opercula (planum polare versus inferior frontal and precentral gyri, Heschl's versus postcentral gyri, planum temporale versus supramarginal gyrus). The inferior frontal, precentral, and postcentral gyri cover the anterior, middle, and posterior thirds of the lateral surface of the insula, respectively. The pars triangularis covers the apex of the insula, located immediately distal to the genu of the middle cerebral artery. The clinical application of the anatomic information presented in this article is in angiography, middle cerebral artery aneurysm surgery, insular resection, frontobasal resection, and amygdalohippocampectomy, and hemispherotomy.

CONCLUSION: The anatomic relationships of the sylvian fissure region can be helpful in preoperative planning and can serve as reliable

intraoperative navigation landmarks in microsurgery involving that region.

INTRODUCTION

The sylvian fissure is the most prominent and complex fissure of the brain, and the surgical approaches through the sylvian fissure are among the most popular approaches in contemporary neurosurgery (28, 31, 32, 34–36).

Although some of the pertinent anatomy of the sylvian fissure and its contents have been described previously (5, 10, 12–14, 19, 20, 22, 25, 30, 34), we believe that different viewpoints on the anatomy of the sylvian fissure could be added to the literature.

We work in academic institutions and have observed that with the advances in imaging and targeting technologies over the years, the capacity of younger neurosurgeons to interpret angiography has diminished drastically. Also, it is sometimes difficult, especially for novice surgeons, to process, convert, and apply the complex anatomic information in their daily neurosurgical practice.

Therefore, in this article, after a brief review of the current concept of the sylvian fissure, we display some additional observations on the anatomy of the sylvian fissure region and demonstrate some of the clinical applications of that anatomic knowledge in the first author's (HTW) microneurosurgical practice over the past 15 years.

ANATOMIC CONSIDERATIONS

The sylvian fissure is a fissure formed by the infolding of the frontal, parietal, and temporal opercula over the insula. The insula has been described as a pyramid-shaped structure with its apex pointing downward, surrounded by the superior, inferior, and anterior limiting or circular sulci (20, 22, 30). It presents lateral and anterior surfaces. The lateral surface of the insula is divided by the central sulcus of the insula into a larger anterior zone and a small posterior zone. The anterior zone is composed of the anterior, middle, and posterior short gyri that converge and fuse with each other in the apex of the insula, which is the most convex or

prominent portion of the insula. The posterior zone usually consists of one long gyrus that bifurcates posteriorly. The long gyrus courses anteroinferiorly to reach the most anteroinferior aspect of the insula pole.

The anterior surface of the insula is composed of one vertically oriented and laterally placed gyrus, an accessory gyrus, and a short transversely oriented and medially placed gyrus, the transverse gyrus of Eberstaller. Both gyri converge inferiorly and become fused with each other at the insular pole. The insular pole is exclusively derived from the gyri originating from the anterior zone and from the anterior surface of the insula. The limen insulae or the falciform fold is composed of fibers of uncinate fasciculus covered by a thin layer of gray matter that presents itself as an arched ridge of variable prominence extending from the anterior end of the long gyrus, where it fuses with the temporal pole, passing through the medial part of the insular pole, and ends at the middle of the posterior orbital gyrus.

The temporal operculum that constitutes the inferior wall of the sylvian fissure is the superior surface of the temporal lobe. It comprises, from posterior to anterior, the planum temporale, Heschl's gyrus, and planum polare.

The planum temporale is usually composed of 2 transverse temporal gyri: the middle and the posterior. The planum temporale is a flat, triangular-shaped area with its apex pointing medially.

The Heschl's gyrus or anterior transverse temporal gyrus is located anterior to the planum temporale and is separated from the latter by the Heschl's sulcus. The Heschl's gyrus is directed medially to laterally and posteriorly to anteriorly, and it is fused with the superior temporal gyrus on the lateral surface of the cerebrum.

The planum polare is a depression that constitutes the superior surface of the anterior portion of the temporal lobe; it is located between the Heschl's gyrus posteriorly and the uncus antero medially (Fig. 1A).

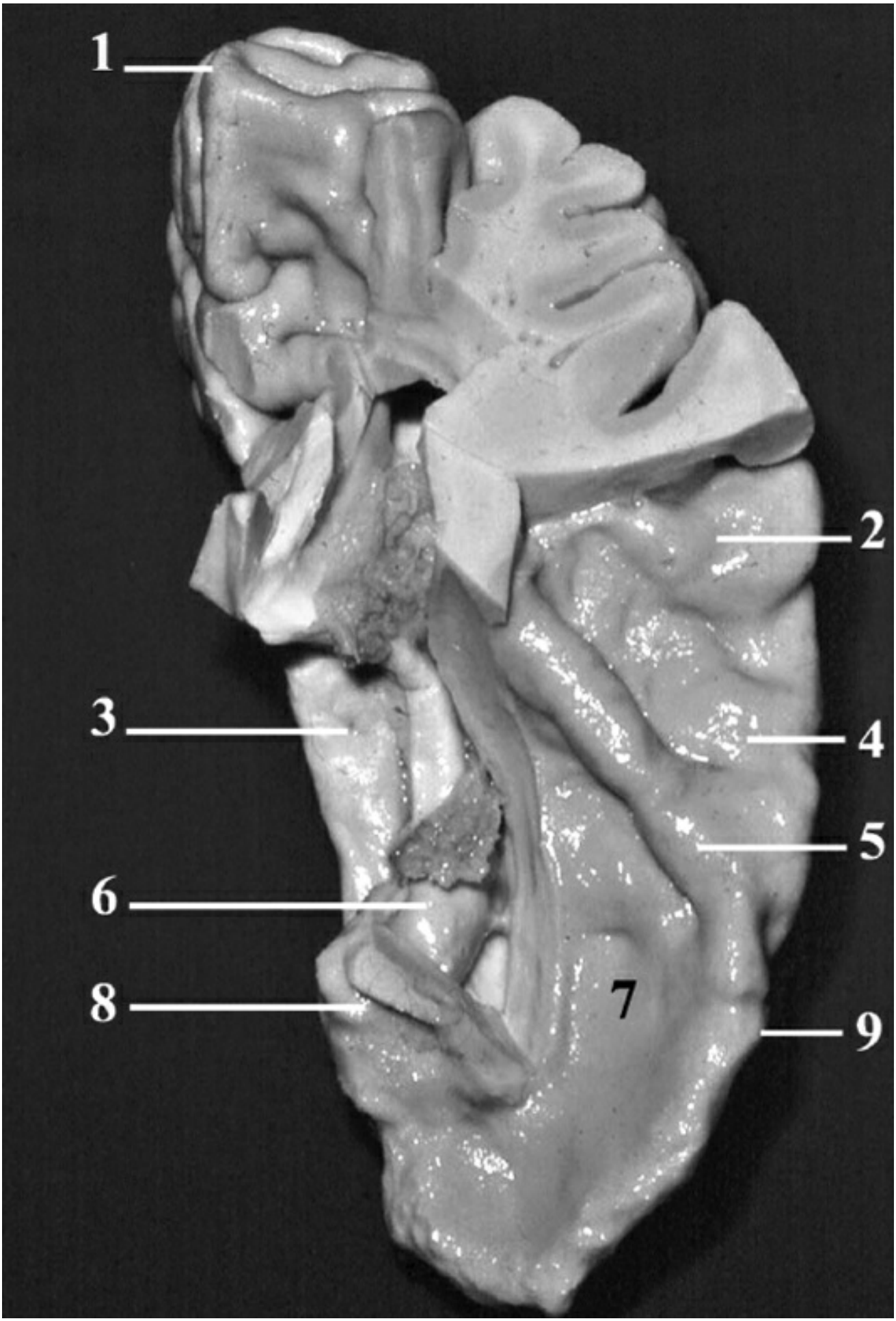

Figure 1. Superior view of the left temporal lobe. 1, cuneus; 2, posterior transverse temporal gyrus; 3, parahippocampal gyrus; 4, middle

transverse temporal gyrus; 5, Heschl's gyrus (anterior transverse temporal gyrus); 6, head of the hippocampus; 7, planum polare; 8, anteromedial surface of the uncus; 9, superior temporal gyrus, where the anterior portion of the temporal lobe starts to deviate medially. (Images courtesy of AL Rhoton, Jr.)

The gyri of the frontal lobe that constitute the sylvian fissure are lateral and posterior medial orbital gyri on the basal surface of the hemisphere and the pars orbitalis, triangularis, pars opercularis, and precentral gyrus on the lateral surface. The gyri of the parietal lobe that constitute the sylvian fissure are postcentral and supramarginal gyri.

Sylvian Fissure

According to Gibo et al. (5), the sylvian fissure presents a superficial part and a deep part: the sylvian fissure stem and the 3 main rami (anterior horizontal, anterior ascending, and posterior rami) form the superficial part. The stem is located on the basal surface, and the 3 rami are located on the lateral surface. The sphenoidal and the operculoinsular compartments of the sylvian fissure form the deep part. The sphenoidal compartment is located on the basal surface, and the operculoinsular is located on the lateral surface.

Szikla et al. (19) also described the sylvian fissure in a similar way, but with different terminology: superficial, intermediate, and deep planes. The superficial plane corresponds to that described by Gibo et al. (5), the intermediate plane matches the opercular compartment, and the deep plane is the insular compartment.

The sylvian fissure stem starts just lateral to the anterior perforated substance, between the lateral olfactory stria and the rhinal incisura or temporal incisura (10, 22, 30), and proceeds laterally and anteriorly toward the lateral surface of the brain. During this trajectory, it stays behind the lesser wing of the sphenoid bone. The temporal stem is covered anteriorly by the arachnoid membrane, the frontotemporal arachnoid reflection that covers the frontal lobe, and continues on the surface of the temporal lobe (30).

On the lateral surface of the cerebrum, the stem of the sylvian fissure divides into the anterior horizontal, anterior ascending, and posterior rami. The anterior horizontal and the anterior ascending rami delimit the pars triangularis of the inferior frontal gyrus. The junction of these 3 rami is located at the tip of the pars triangularis. The posterior ramus of the sylvian fissure is the longest one; it is directed posteriorly and superiorly, separating the frontal and parietal lobes superiorly from the temporal lobe inferiorly. The sphenoidal compartment arises in the region of the limen insulae at the lateral margin of the anterior perforated substance. It is a narrow space posterior to the sphenoid ridge between the frontal and temporal lobes that communicates medially with the carotid cistern. The operculoinsular compartment is located deep to the superficial rami of the sylvian fissure on the lateral surface.

The intermediate or opercular compartment of the sylvian fissure is composed of the opercula from the frontal and parietal lobes superiorly and those from the temporal lobe inferiorly. The pars orbitalis also is called the fronto-orbital operculum; the pars triangularis is called the frontal operculum; pars opercularis, and the precentral and postcentral gyri are collectively called frontoparietal operculum; and the supramarginal gyrus is called the parietal operculum (2).

Yaşargil et al. (31) described an intraoperative finding of 4 different types of the intermediate plane of the anterior sylvian fissure.

The insular compartment described by both Szikla et al. (19) and Gibo et al. (5) is located on the lateral surface of the insula. The insular compartment contains the M2 segment of middle cerebral artery (MCA) and insular veins.

The MCA is divided into 4 segments. The M1 segment extends from the carotid bifurcation to the limen of the insula (31) or to the genu of the MCA (5, 13). The M2 segment turns around the pole of the insula to form the genu of the MCA and continues on the lateral surface of the insula to reach the superior and inferior limiting sulci. It then turns downward to follow the inner surface of the frontal, parietal, and temporal opercula to

become the M3 segment, which runs between the frontal and parietal opercula above and the temporal operculum below. The M4 segment exits the sylvian fissure to constitute the cortical branches of the MCA.

During its trajectory on the lateral surface of the insula, the M2 segment sends off branches to the insula, extreme capsule, and occasionally the claustrum and the external capsule. The lenticulostriate arteries supply the structures of the central core of the hemisphere located medially to the claustrum (12, 26). At the posterior portion of the insula, the M2 segment can send off branches the corona radiata (23).

MATERIALS AND METHODS

The anatomic part of the study was performed in 2 locations: between 1993 and 1996, 12 formalin-fixed adult cadaveric heads with vessels injected with colored latex were dissected in the microneurosurgical anatomy laboratory at the Department of Neurological Surgery, University of Florida, for photographic documentation. Subsequently, between 1996 and 1998, 60 additional formalin-fixed adult cadaveric hemispheres were dissected in the microsurgery laboratory at the Hospital Beneficência Portuguesa, São Paulo, Brazil, for additional observation.

The lessons learned from the anatomic laboratory studies were applied in more than 200 surgeries using transsylvian approaches performed from 1996 to 2007 by a single surgeon (HTW) at the Hospital das Clínicas, College of Medicine, University of São Paulo, and the Hospital Samaritano, in São Paulo, Brazil.

RESULTS

Additional Anatomic Observations

Temporal Operculum

The junction between the Heschl's gyrus and the superior temporal gyrus usually occurs in the coronal plane at the level of the external acoustic meatus (Fig. 2, A and B). This junctional point is usually not very evident on the surface of the cerebrum, making its intraoperative identification

difficult. However, the Heschl's gyrus can be promptly identified on its opercular portion because of its characteristic hump (Fig. 2C). Medially, the Heschl's gyrus is directed toward the pulvinar of the thalamus, and it constitutes the posterior wall of the retroinsular space.

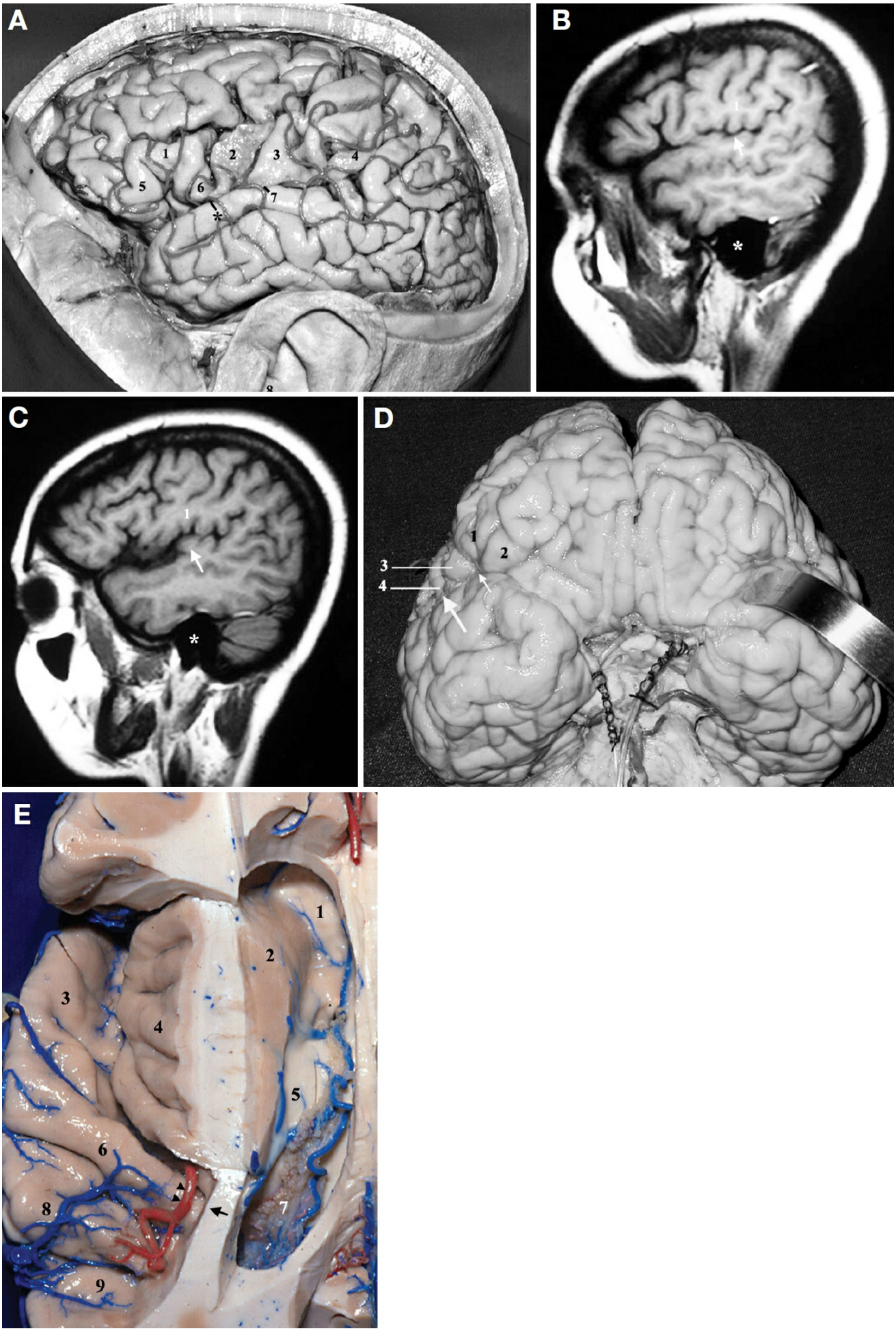

Figure 2. A, lateral view of the left cerebral hemisphere. 1, pars triangularis of the inferior frontal gyrus; 2, precentral gyrus; 3,

postcentral gyrus; 4, supramarginal gyrus; 5, pars orbitalis; 6, pars opercularis; 7, junction between the superior temporal gyrus and the Heschl's gyrus; 8, external acoustic meatus. Asterisk, at this point, the planum polare starts to deviate medially. Note the large space in the sylvian fissure between the structures 1, 5, and 6. B, sagittal magnetic resonance imaging (MRI) scan at the surface of the left hemisphere. 1, postcentral gyrus. Asterisk, projection of the external acoustic meatus over the petrous temporal bone. Heschl's gyrus (arrow). C, sagittal MRI scan at the opercular level of the left hemisphere. 1, postcentral gyrus. Asterisk, projection of the external acoustic meatus over the petrous temporal bone. Heschl's gyrus (arrow). D, anterobasal view of the cerebrum. 1, pars triangularis; 2, pars orbitalis; 3, pars opercularis; 4, precentral gyrus. The large arrow indicates where the medial deviation of the planum polare begins. The small arrow indicates where the medial deviation of the planum polare intensifies. E, superior view of the left hemisphere. An axial cut has been made to expose the lateral ventricle. The frontal and parietal opercula have been removed to expose the insula and the temporal opercula. 1, rostrum of the corpus callosum; 2, head of the caudate nucleus; 3, planum polare; 4, insula; 5, thalamus; 6, Heschl's gyrus; 7, choroid plexus of the atrium of the lateral ventricle covering the pulvinar of the thalamus; 8, middle transverse temporal gyrus; 9, posterior transverse temporal gyrus. The arrow indicates the medial end of the Heschl's gyrus that points toward the posterior limb of the internal capsule and toward the atrium of the lateral ventricle. The arrowheads indicate the location of the angiographic sylvian point. (Images courtesy of AL Rhoton, Jr.)

The planum polare can be divided into 2 parts: the first part extends from the Heschl's gyrus to the level of the anterior edge of the precentral gyrus and presents its main axis oriented anteroposteriorly. The second part starts at the level of the anterior edge of the precentral gyrus, soon deviates medially like the rest of the anterotemporal structures, and has its axis oriented lateromedially. This medial deviation is more evident from the level of the pars triangularis (Fig. 2, A and D).

The medial deviation of the planum polare in addition to the usual upward

retraction of the pars triangularis leaves a formidable space in the lateral sylvian fissure (Fig. 2A).

The Heschl's gyrus and the planum temporale form a triangular area with its apex pointing medially toward the retroinsular region, the posterior portion of the posterior limb, and the retrolentiform parts of the internal capsule. The apex of that area also points indirectly toward the atrium of the lateral ventricle and toward its anterior wall, which is the ventricular portion of the pulvinar of the thalamus (Fig. 2E).

Fronto-orbital Operculum

The pars orbitalis of the inferior frontal gyrus occupies not only the lateral surface of the cerebrum, but also the most lateral and most posterior aspect of the orbital surface of the frontal lobe, formed by the posterior part of the lateral orbital gyrus and the lateral part of the posterior orbital gyrus (Fig. 3).

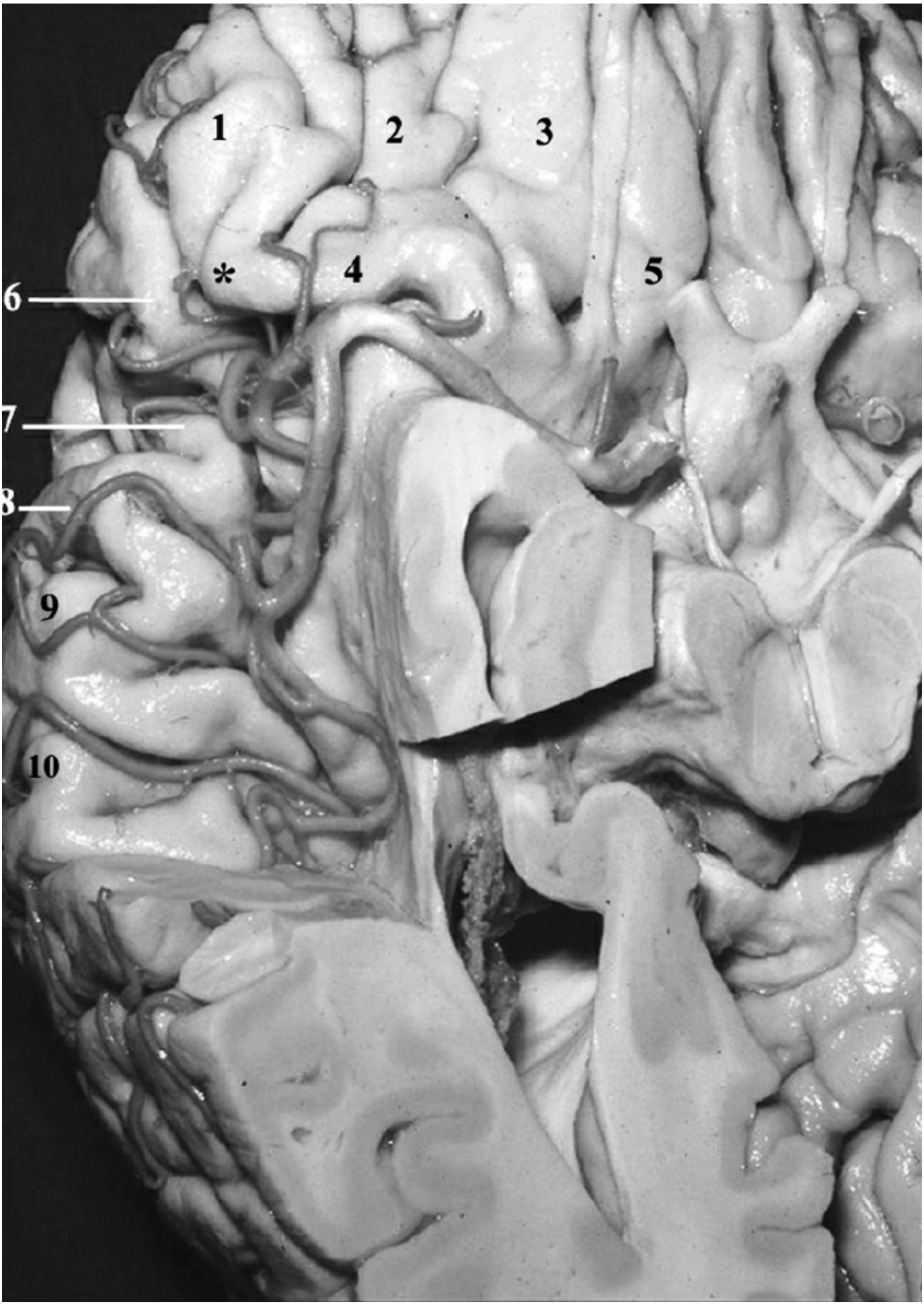

Figure 3. Basal view of the right hemisphere. The temporal operculum has been removed to expose the frontal and parietal opercula. 1, lateral orbital gyrus; 2, anterior orbital gyrus; 3, medial orbital gyrus; 4, posterior orbital gyrus; 5, rectus gyrus; 6, pars triangularis; 7, pars opercularis; 8,

precentral gyrus; 9, postcentral gyrus; 10, supramarginal gyrus. Asterisk, pars orbitalis. (Images courtesy of AL Rhoton, Jr.)

Parietal Opercula

The postcentral gyrus consistently overlies the Heschl's gyrus (anterior transverse temporal gyrus). The precentral gyrus, pars opercularis, and pars triangularis are in opposition to the planum polare, and the supramarginal gyrus (composed of middle and posterior transverse parietal gyri) overlies the planum temporale (composed of middle and posterior transverse temporal gyri) (Figs. 2, B and C, and 4, A–F).

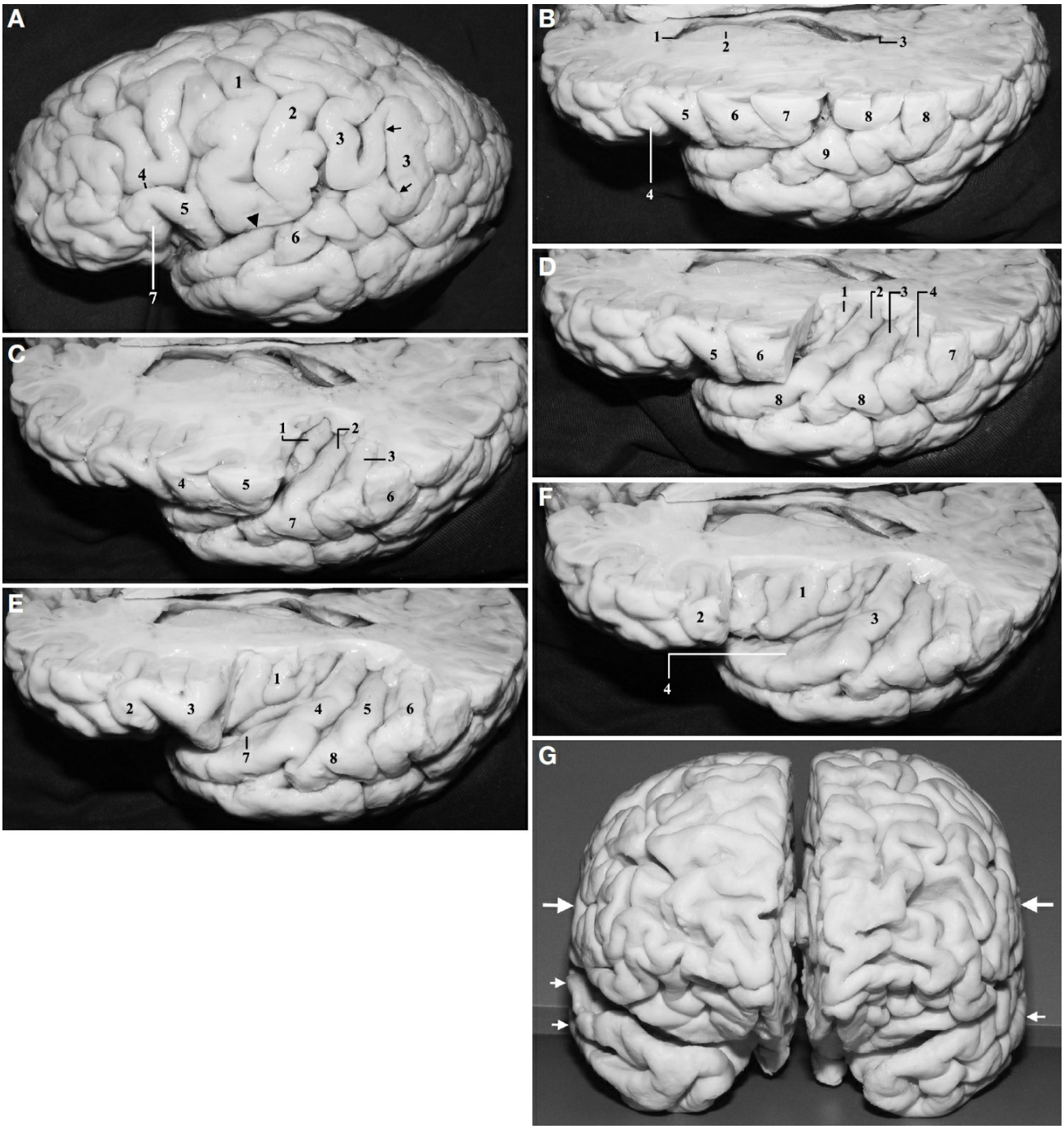

Figure 4. A, superolateral view of the left hemisphere. 1, precentral gyrus; 2, postcentral gyrus; 3, supramarginal gyrus; 4, inferior frontal sulcus; 5, pars opercularis of the inferior frontal gyrus; 6, superior temporal gyrus; 7, pars triangularis of the inferior frontal gyrus. The arrows indicate the ascending and descending terminal branches of the posterior ramus of the sylvian fissure. The arrowhead indicates posterior ramus of the sylvian fissure. The largest transverse diameter of the cerebrum usually corresponds to the level of postcentral gyrus and to the middle and the superior temporal gyri (at the level of the postcentral gyrus). B, superolateral view of the same specimen shown in A. A transverse cut has been made by following a line drawn from the base of the pars triangularis of the inferior frontal gyrus to the supramarginal gyrus, immediately above the posterior ramus of the sylvian fissure. 1, frontal horn; 2, head of the caudate nucleus; 3, atrium; 4, pars triangularis; 5, pars opercularis; 6, precentral gyrus; 7, postcentral gyrus; 8, supramarginal gyrus; 9, superior temporal gyrus. C, the operculum of the supramarginal gyrus has been removed to display the middle and posterior transverse temporal gyri and the medial end of the Heschl's gyrus. 1, medial part of the Heschl's gyrus (anterior transverse temporal gyrus); 2, middle transverse temporal gyrus; 3, posterior transverse temporal gyrus; 4, precentral gyrus; 5, postcentral gyrus; 6, posterior end of the superior temporal gyrus turning around the descending branch of the posterior ramus of the sylvian fissure to become the supramarginal gyrus; 7, superior temporal gyrus. The supramarginal gyrus constitutes the posterior wall of the posterior ramus of the sylvian fissure. D, the operculum of the postcentral gyrus has been removed to display the Heschl's gyrus and posterior end of the insula. 1, posterior long gyrus of the insula; 2, Heschl's gyrus; 3, middle transverse temporal gyrus; 4, posterior transverse temporal gyrus; 5, pars opercularis; 6, precentral gyrus; 7, supramarginal gyrus; 8, superior temporal gyrus. E, the operculum of the precentral gyrus has been removed to display the posterior part of the planum polare, located immediately anterior to the Heschl's gyrus, and also to display the posterior half of the insula. 1, posterior insula; 2, pars triangularis; 3, pars opercularis; 4, Heschl's gyrus; 5, middle transverse temporal gyrus; 6, posterior transverse temporal

gyrus; 7, planum polare; 8, superior temporal gyrus. F, the pars opercularis of the inferior frontal gyrus has been removed to display the anterior portion of the planum polare and the anterior portion of the insula. 1, insula; 2, pars triangularis; 3, Heschl's gyrus; 4, planum polare. G, frontal view of the cerebrum. The largest transverse diameter of the brain in the suprasylvian region corresponds to the postcentral gyrus (large arrows). The largest transverse diameter of the brain in the infrasylvian region corresponds to the superior or middle temporal gyrus, in the coronal plane of the postcentral gyrus (small arrows). (Images courtesy of AL Rhoton, Jr.)

When viewed from the front, the transverse diameter of the poles of the frontal and occipital lobes is smaller than that of the parietal lobe. In a person with a normal cranial configuration, the largest transverse diameter of the cerebrum on an anteroposterior (AP) view is located at the level of the postcentral gyrus in the suprasylvian region and at the level of the middle or superior temporal gyrus in the infrasylvian region, on the same coronal plane as the postcentral gyrus (Fig. 4, A, E, and G).

Sylvian Fissure

The frontotemporal arachnoid membrane covers the basal surface and the lateral surface of the cerebrum. On the basal surface, the frontotemporal arachnoid membrane bridges the anterior portion of the planum polare to the posterior portion of the lateral, posterior, and medial orbital gyri (Fig. 5A). It continues medially with the arachnoidal membrane of the carotid, olfactory, and chiasmatic cisterns (Fig. 5B).

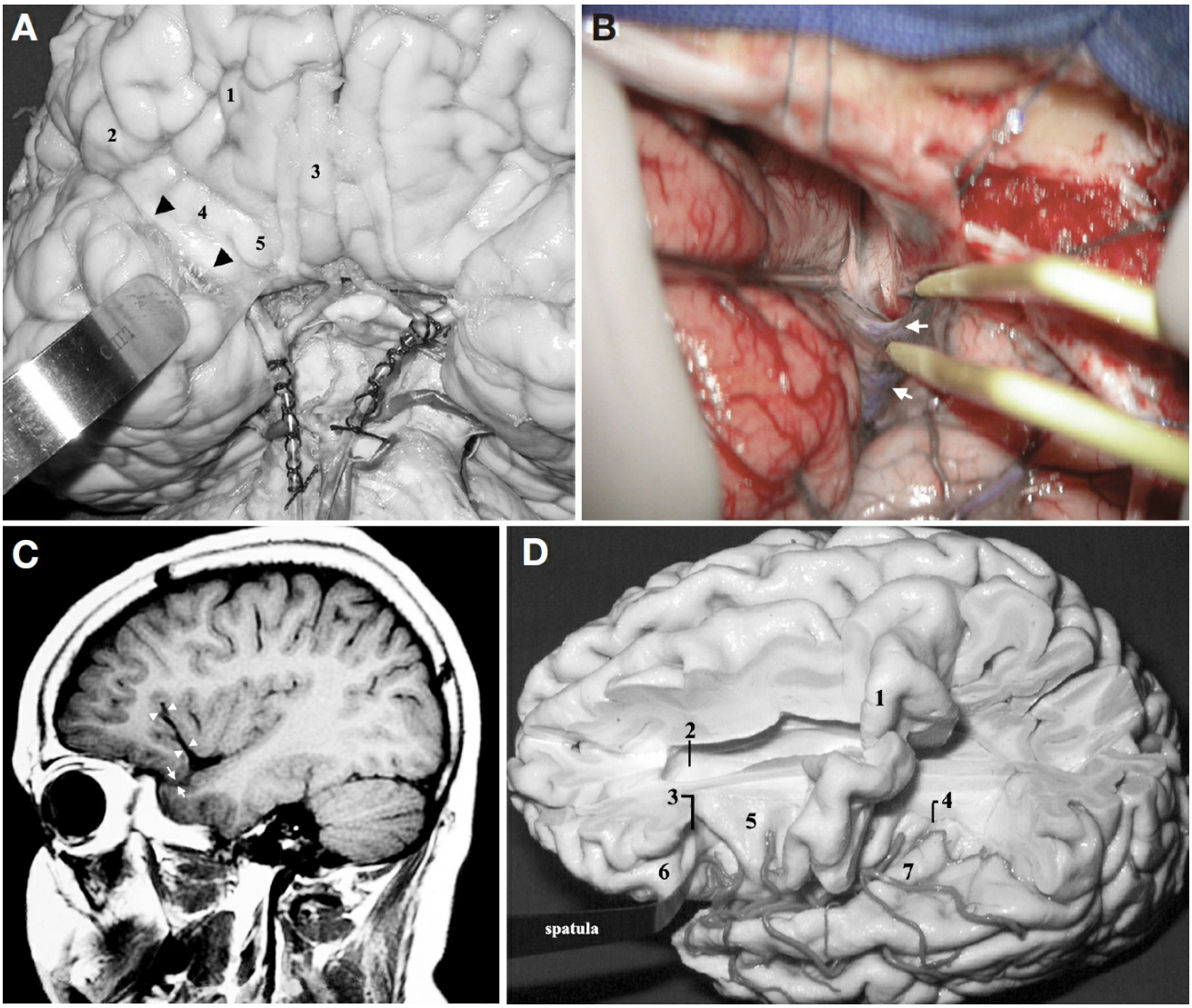

Figure 5. A, anterobasal view of the cerebrum. The arrowheads indicate the frontotemporal arachnoid reflection bridging the orbital surface of the frontal lobe to the planum polare. 1, anterior orbital gyrus; 2, lateral orbital gyrus; 3, rectus gyrus; 4, posterior orbital gyrus; 5, medial orbital gyrus. B, intraoperative photograph showing the basal surface of the right hemisphere after the pterional craniotomy and dural opening. The frontotemporal arachnoid membrane (arrows) in this figure has been stretched between the tip of the bipolar forceps and the suction tube. The frontotemporal arachnoid membrane is continuous with the carotid, chiasmatic, and olfactory cisterns. In this figure, the olfactory tract is shown at the right side of the tip of the suction tube, and the optic nerve is shown at the right side of the olfactory tract. C, sagittal MRI scan. The arrows indicate the intermediate plane of the sylvian fissure on the basal surface, located between the posterior portion of the orbital gyri and the planum polare. The arrowheads indicate the anterior operculoinsular compartment of the sylvian fissure. D, superolateral view of the left

hemisphere. A spatula has been placed in the horizontal ramus of the sylvian fissure that continues medially with the anterior limiting sulcus of the insula. The precentral gyrus is usually related to the mid-posterior portion of the insula. 1, precentral gyrus; 2, frontal horn; 3, anterior limiting sulcus of the insula; 4, junction between the inferior and the superior limiting sulci of the insula; 5, anterior portion of the insula; 6, pars orbitalis; 7, Heschl's gyrus. (Images courtesy of AL Rhoton, Jr.)

The sylvian fissure divides into 3 rami (horizontal, anterior ascending, and posterior) at the level of the tip of the pars triangularis. The transition between the basal and lateral parts of the sylvian fissure can therefore be considered as located at the level of the pars triangularis of the inferior frontal gyrus.

There is an intermediate plane, as stated by Szikla et al. (19), on the basal surface of the anterior portion of the cerebral hemisphere. It is located between the opercular portions of the lateral and posterior orbital gyri on the frontal side and the upper part of the anterior portion of the planum polare on the temporal side.

The deep part of the sylvian fissure on the basal surface is not restricted only to the narrow space posterior to the sphenoid ridge between the frontal and temporal lobes, in front of the insular pole, but it extends upward over the anterior surface of the insula, between the posterior surfaces of the lateral, posterior, and medial orbital gyri anteriorly and the anterior surface of the insula. Because this part of the sylvian fissure is related to the anterior surface of the insula, we named this part of the sylvian fissure the anterior operculoinsular compartment. The sphenoidal compartment is the inferior portion of the anterior insular compartment, and it is related to the lesser wing of the sphenoid bone (Fig. 5C). We also renamed the operculoinsular compartment on the lateral surface of the cerebrum the lateral operculoinsular compartment.

When viewed from its basal surface, the axis of the temporal lobe is initially directed posteriorly to anteriorly, completely covering the parietal operculum. At its anterior portion, the temporal lobe turns medially, having its tip moved under the posterior orbital gyrus (Fig. 2D). The

turning point of this curve is located on the superior temporal gyrus and begins at the level of the posterior margin of the pars opercularis, but the planum polare has its medial curve intensified from the level of the tip of the pars triangularis.

The planum polare therefore presents 2 distinct morphologies. The first, the posterior part, extends from the Heschl's gyrus to the "turning point" located at the level of the pars opercularis but becomes more evident at the level of the pars triangularis. It is related to the precentral gyrus, pars opercularis, and pars triangularis of the inferior frontal gyrus. The second, the anterior part, extends from the level of the pars triangularis to the rhinal incisura that separates the planum polare from the uncus. This part of the planum polare constitutes the pole of the temporal lobe located under the lesser wing and behind the greater wing of the sphenoid. It is related to the lateral and posterior orbital gyri.

The anterior horizontal ramus of the sylvian fissure continues medially as the anterior limiting sulcus of the insula (Fig. 5D). The anterior horizontal ramus separates the pars orbitalis anteriorly from the pars triangularis posteriorly. As mentioned previously, the pars orbitalis occupies both basal and lateral surfaces of the cerebrum; it is composed of the posterior portion of the lateral orbital gyrus and the lateral portion of the posterior orbital gyrus. The anterior horizontal ramus therefore separates the pars triangularis from the pars orbitalis and the lateral orbital gyrus.

Insula

The lateral surface of the insula is convex and presents 2 facets: superolateral and inferolateral. This distinction is more evident in the anterior zone of the insula. These 2 facets are divided by an edge that we called the insular edge in this study. The superolateral facet is composed of short gyri (anterior, middle, and posterior), the central sulcus, the upper part of the anterior long gyrus, the insular apex, and the edge between the anterior short gyrus and the transverse gyrus of Eberstaller that occupies the inferior portion of the anterior surface of the insula. The superolateral facet of the insula is related to the operculum of the pars triangularis, pars opercularis, and precentral and postcentral gyri. The superior lateral

insular cleft is the space between the superolateral facet of the insula and the frontal and parietal opercula (Fig. 6A).

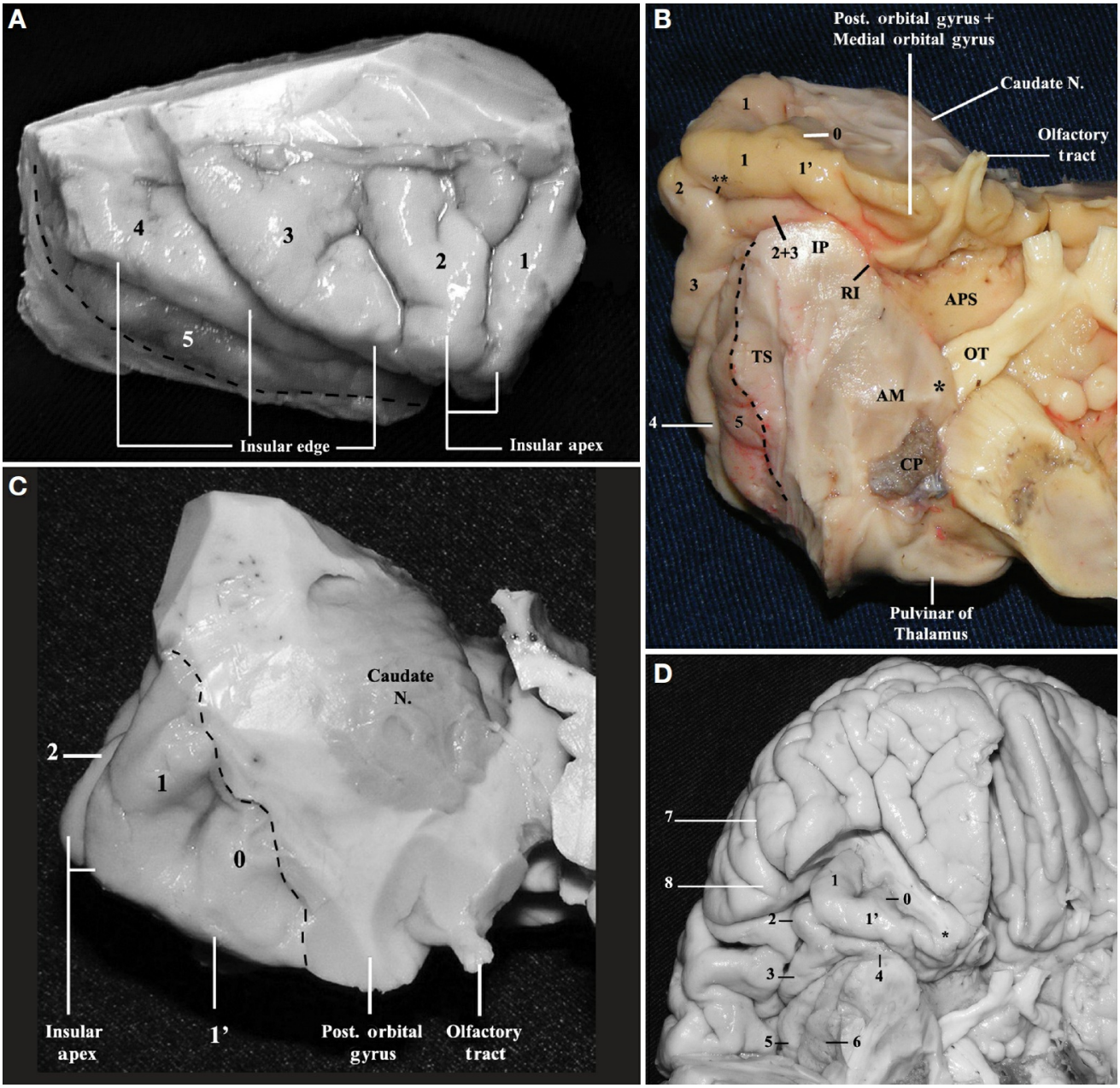

Figure 6 (A–D). A, lateral view of the right insula. In this specimen, the short insular sulcus that separates the anterior and the middle short gyri traverses the insular apex and extends to the limen insulae. 1, anterior short gyrus; 2, middle short gyrus; 3, posterior short gyrus; 4, anterior long gyrus; 5, posterior long gyrus. The central sulcus of the insula is located between the posterior short gyrus and the anterior long gyrus of the insula. The dotted line indicates the inferior limiting sulcus of the insula. B, basal view of the right insula to display the inferolateral facet. In this specimen, the short insular sulcus that runs between the anterior and middle short gyri also traverses the insular apex and extends to the limen insulae. 0, accessory gyrus; 1', transverse gyrus of Eberstaller; 1,

anterior short gyrus; 2, middle short gyrus; 3, posterior short gyrus; 2 + 3, fusion of the middle and posterior short gyri; 4, anterior long gyrus; 5, posterior long gyrus; IP, insular pole; RI, rhinal incisura; APS, anterior perforated substance; TS, temporal stem; OT, optic tract; AM, amygdala; CP, insertion of the choroid plexus at the inferior choroidal point. Double asterisk, short insular sulcus. The dotted line indicates the inferior limiting sulcus of the insula. Asterisk, medial nucleus of amygdala. The medial nucleus of the amygdala is located anterior and slightly superior to the inferior choroidal point, and it is in close proximity to the optic tract and the upper part of the crus cerebri. The posteromedial orbital lobule is composed of the medial portion of the posterior orbital gyrus and by the posterior portion of the medial orbital gyrus. C, frontal view of the right insula. 0, accessory gyrus; 1', transverse gyrus of Eberstaller; 1, anterior short gyrus; 2, middle short gyrus; Caudate N, head of the caudate nucleus. The dotted line indicates the anterior limiting sulcus of the insula. The insular edge and the superolateral and inferolateral facets of the insula are more evident at the anterior portion of the insula as shown in this figure. D, laterobasal view of the cerebrum. The posterior orbital gyrus has been removed to display the overall view of the anterior surface and the inferolateral facet of the insula. 0, accessory gyrus; 1', transverse gyrus of Eberstaller; 1, anterior short gyrus; 2, middle short gyrus and the insular apex; 3, posterior short gyrus; 4, insular pole; 5, anterior long gyrus; 6, posterior long gyrus; 7, horizontal ramus of the sylvian fissure; 8, pars triangularis. Asterisk, posteromedial orbital lobule. The anterior zone of the insula (anterior surface and the short gyri) forms a pyramidal structure with its apex pointing laterally and inferiorly. The insular pole and the limen insulae are located more medially and posteriorly in relation to pars triangularis. 1, frontal horn; 2, accessory gyrus of the insula; 3, lentiform nucleus and the internal capsule; 4, head of the caudate nucleus; 5, genu of the MCA; 6, insular pole; 7, anterior perforated substance; 8, amygdala; 9, head of the hippocampus. (Images courtesy of AL Rhoton, Jr.)

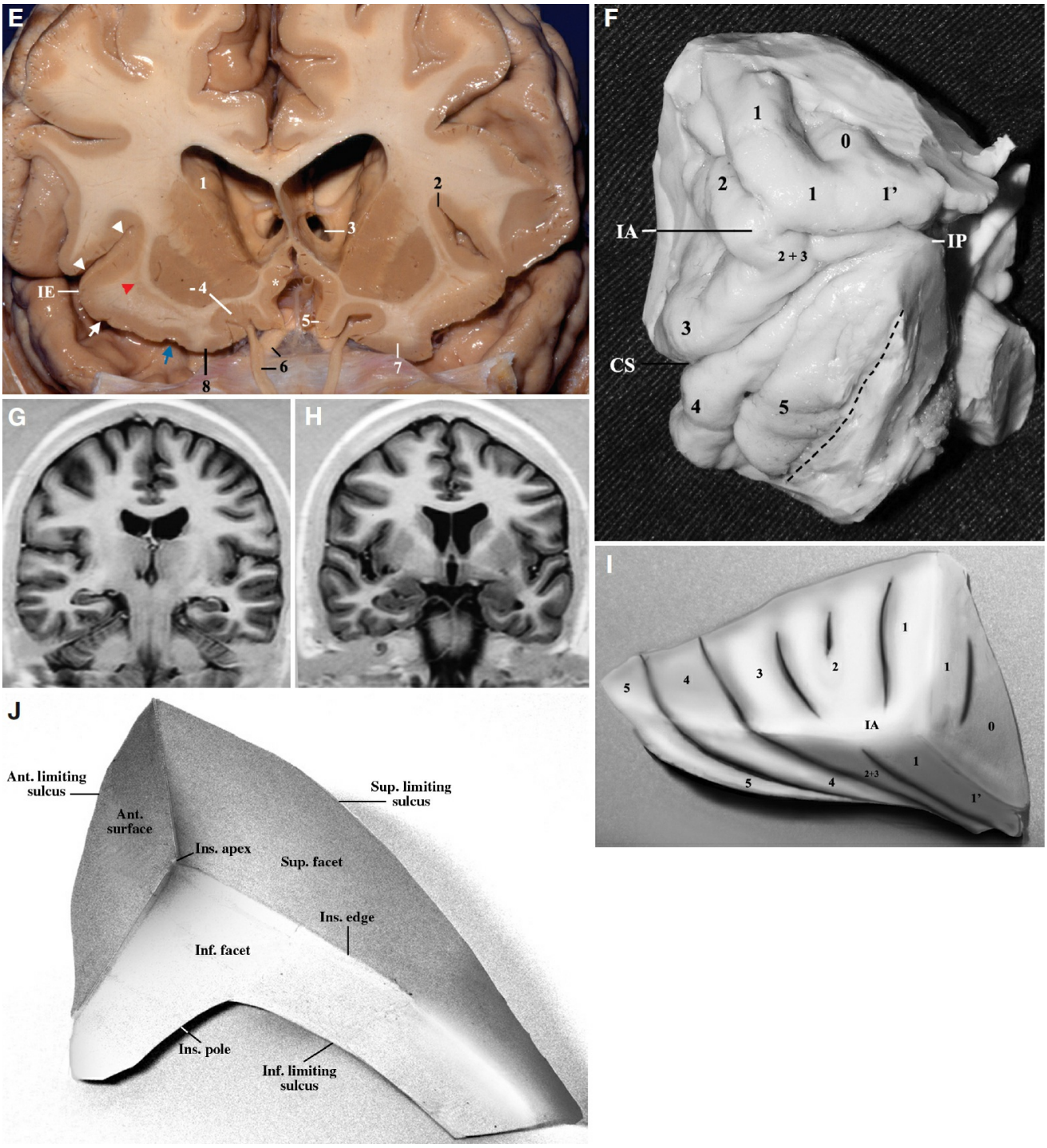

Figure 6 (E–J). E, frontal view. A coronal cut has been made at the anterior portion of the insula at the level of the optic nerves. In the anterior portion of the insula, the superolateral and the inferolateral facets, as well as the insular edge, are more evident. In the right hemisphere, the coronal cut includes the extension of the anterior short gyrus in the inferolateral facet, the transverse gyrus of Eberstaller, and its junction with the posteromedial orbital lobule (blue arrow). In the left hemisphere, a coronal cut has been made more anteriorly and included the posterior orbital gyrus. At this level, the head of the caudate is located immediately above the gray matter overlying the olfactory sulcus and is separated from the latter by a thin layer of white matter. The

lentiform nucleus is located above the posteromedial orbital lobule and above the transverse gyrus of Eberstaller and is separated from the latter by a layer of white matter interposed by the claustrum. 1, head of the caudate nucleus; 2, superior limiting sulcus; 3, foramen of Monro (left); 4, lentiform nucleus and olfactory sulcus; 5, rectus gyrus; 6, optic nerve and olfactory tract; 7, posterior orbital gyrus; 8, posteromedial orbital lobule. The arrowheads indicate superior insular cleft and superolateral facet of insula. The white arrow indicates transverse gyrus of Eberstaller. The blue arrow indicates junction between the transverse gyrus and the posteromedial orbital lobule. IE, insular edge. Asterisk, paraolfactory gyrus. The red arrowhead indicates claustrum. The head and body of the caudate nucleus are located more superiorly than the superior limiting sulcus of the insula. G, coronal MRI scan of the posterior portion of the insula. H, coronal MRI scan of the middle portion of the insula. F, laterobasal view of the right insula. 0, accessory gyrus; 1', transverse gyrus of Eberstaller; 1, anterior short gyrus; 2, middle short gyrus; 3, posterior short gyrus; 2 + 3, junction between the middle and the posterior short gyri; 4, anterior long gyrus; 5, posterior long gyrus; IA, insular apex; IP, insular pole; CS, central sulcus of insula. The dotted line indicates the location of the inferior limiting sulcus of insula. I, schematic drawing of the anterolateral aspect of the right insula. 0, accessory gyrus; 1', transverse gyrus of Eberstaller; 1, anterior short gyrus; 2, middle short gyrus; 3, posterior short gyrus; 4, anterior long gyrus; 5, posterior long gyrus; IA, insular apex. J, schematic drawing depicting a posterosuperomedial view of the walls of the insula. ANT., anterior; SUP., superior; INS., insular; INF., inferior. 1, frontal horn; 2, accessory gyrus of the insula; 3, lentiform nucleus and the internal capsule; 4, head of the caudate nucleus; 5, genu of the MCA; 6, insular pole; 7, anterior perforated substance; 8, amygdala; 9, head of the hippocampus. (Images courtesy of AL Rhoton, Jr.)

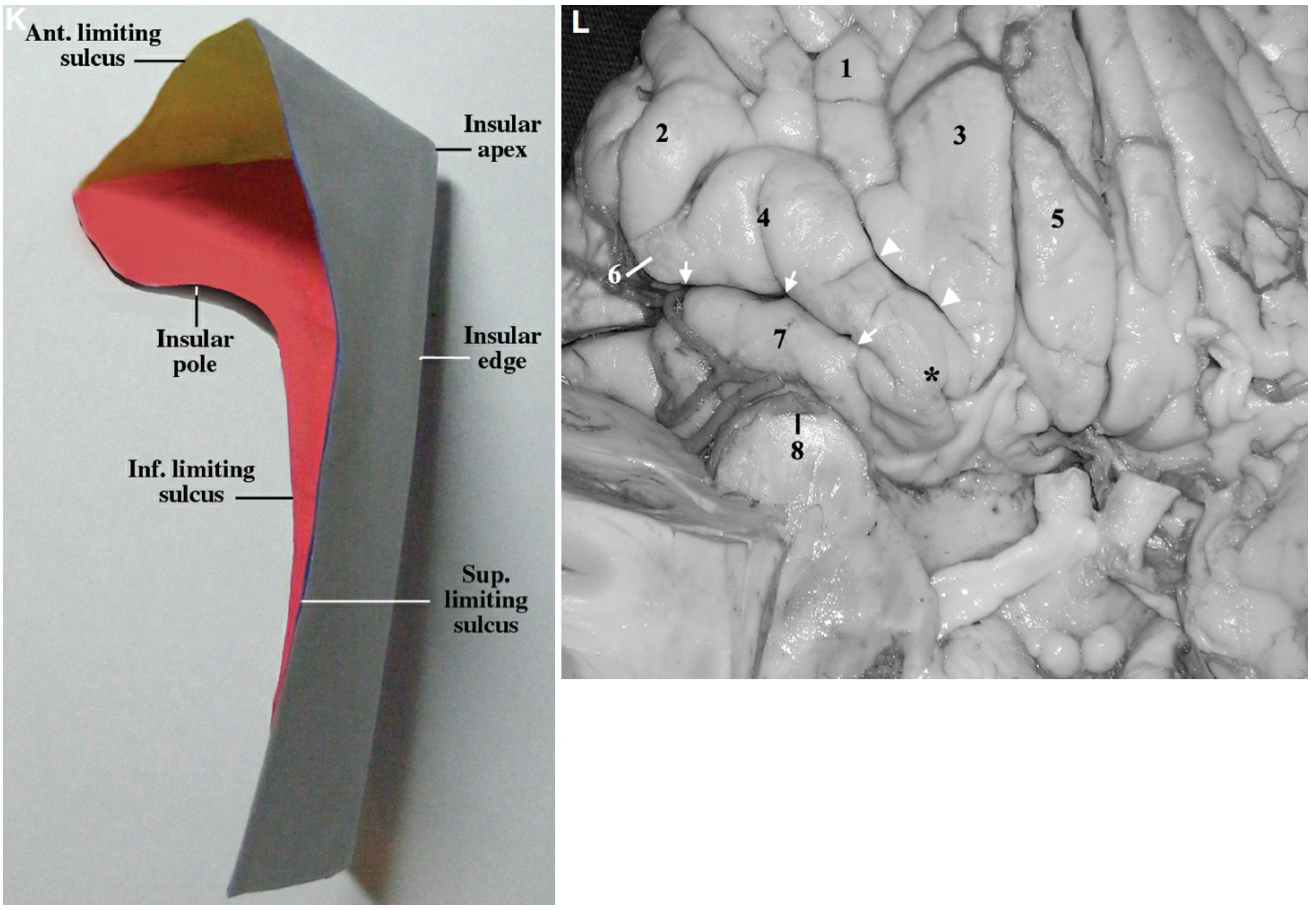

Figure 6 (K–L). K, schematic drawing depicting a posterosuperior view of the walls of the insula. The anterior wall is in yellow, the superolateral facet is in light blue, and the inferolateral facet is in red. L, basal view of the right frontal lobe. 1, anterior orbital gyrus; 2, lateral orbital gyrus; 3, medial orbital gyrus; 4, posterior orbital gyrus; 5, rectus gyrus; 6, pars orbitalis; 7, transverse gyrus; 8, insular pole. The arrows indicate anterior insular cleft. The arrowheads indicate posteromedial limb of the orbital sulcus. Asterisk, posteromedial orbital lobule, just anterior to the lateral olfactory stria and lateral to the olfactory sulcus. 1, frontal horn; 2, accessory gyrus of the insula; 3, lentiform nucleus and the internal capsule; 4, head of the caudate nucleus; 5, genu of the MCA; 6, insular pole; 7, anterior perforated substance; 8, amygdala; 9, head of the hippocampus. (Images courtesy of AL Rhoton, Jr.)

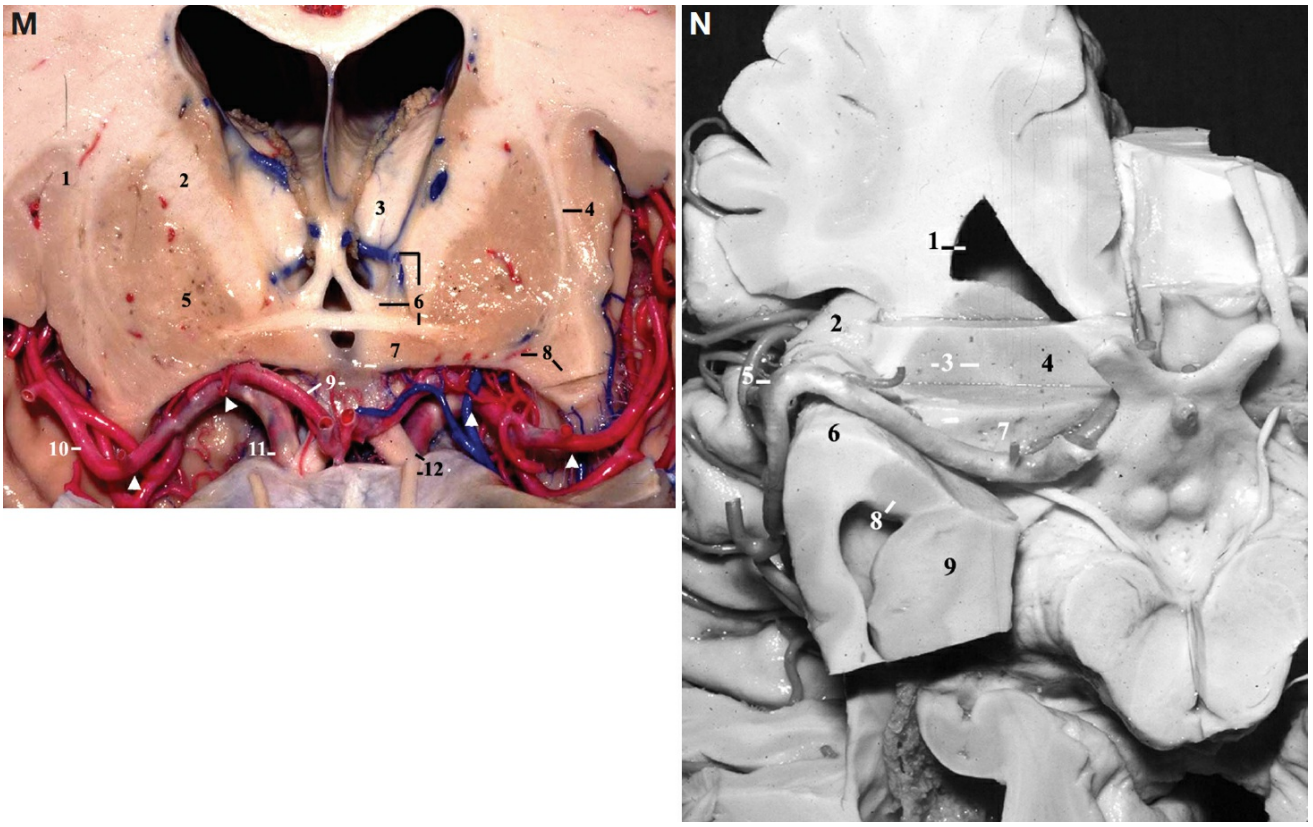

Figure 6 (M–N). M, frontal view. A coronal cut has been made at the level of the bifurcation of the internal carotid artery (anterior perforated substance). 1, insula; 2, internal capsule; 3, thalamus; 4, claustrum, external and extreme capsules; 5, lentiform nucleus; 6, thalamostriate vein, column of the fornix, and anterior commissure; 7, hypothalamus; 8, lateral lenticulostriate arteries and insular pole; 9, lamina terminalis and anterior cerebral artery (A1 segment); 10, middle cerebral artery (MCA) (M2 segment); 11, internal carotid artery (supraclinoid segment); 12, olfactory tract and optic nerve. The arrowheads indicate the extent of the M1 segment of the MCA from the carotid bifurcation to the limen insulae. N, basal view of the right hemisphere. A coronal section, followed by an axial section, has been performed at the level of the anterior perforated substance. 1, frontal horn; 2, accessory gyrus of the insula; 3, lentiform nucleus and the internal capsule; 4, head of the caudate nucleus; 5, genu of the MCA; 6, insular pole; 7, anterior perforated substance; 8, amygdala; 9, head of the hippocampus. (Images courtesy of AL Rhoton, Jr.)

The inferolateral facet of the insula comprises the inferior portion of the anterior and posterior long gyri that continue anteriorly and inferiorly toward the lateral edge of the anterior pole of the insula, the basal

continuation of the short gyri of the superolateral facet of the insula below the insular edge comprises the transverse gyrus of Eberstaller. The basal continuation of the short gyri courses inferomedially toward the superomedial portion of the insular pole, just lateral to the lateral olfactory striae. The anterior portion of the inferolateral facet is actually the base of the anterior surface of the insula. The posterior edge of the medial orbital gyrus and the medial edge of the posterior orbital gyrus, collectively called the posteromedial lobule (22), and the medial end of the transverse gyrus of the insula meet just anterior to the lateral olfactory striae, lateral to the olfactory tract (Fig. 6B). The inferior lateral insular cleft is the space between the inferolateral facet of the insula and the temporal operculum.

The anterior surface of the insula is triangular in shape and composed of an anterior short gyrus, an accessory gyrus, and the transverse gyrus of Eberstaller. The transverse gyrus continues with the part of the anterior short gyrus that is located at the inferolateral facet. The medial limit of the anterior surface of the insula is the anterior limiting sulcus (Fig. 6C). The anterior insular cleft is the space between the anterior surface of the insula and the posterior and lateral orbital gyri. The overall relationship between the anterior surface and the inferolateral facet of the insula is shown in Figure 6D.

Therefore, the insula presents a rather complex shape. The anterior portion of the insula is marked by a prominent edge sharply dividing the superolateral and inferolateral facets; the latter presents a somewhat horizontal obliquity, almost parallel to the floor in the anatomic position (Fig. 6E). The insular edge is less prominent in the posterior portion of the insula: the surface of the posterior insula is slightly convex, almost perpendicular to the floor in the anatomic position (Fig. 6F).

The middle portion of the insula represents a transitional zone between the anterior and posterior portions: the insular edge is still present but less prominent (Fig. 6G).

The classic description of a pyramid with its apex pointing downward seems to be more suitable to describe the shape of the anterior insula, composed of short gyri and the gyri of the anterior surface (Fig. 6, D and

H). The posterior insula presents the shape of a long strip that extends from the retroinsular region, above the insular edge, to the lateral edge of the insular pole on the inferolateral facet of the insula. The anterior and lateral walls of the insula are schematically depicted in Figure 6, I–K.

The superomedial limit of the anterior limiting sulcus of the insula is related to the anterior portion of the anterior limb of the internal capsule, which constitutes the most anterior portion of the lateral wall of the frontal horn, ahead of the head of the caudate nucleus (Fig. 2E).

The anterior insular cleft separates the posterior surface of the lateral and posterior orbital gyri from the anterior short insular, transverse, and accessory gyri; it is shallower in its superior portion. The inferior portion of the anterior insular cleft is deeper and extends all the way to the junction between the posterior end of the medial orbital gyrus and the posteromedial end of the posterior orbital gyrus (posteromedial orbital lobule). The inferior portion of the anterior limiting sulcus of the insula separates the posterior half of the lateral orbital gyrus and the posterior orbital gyrus from the transverse gyrus of Eberstaller (Fig. 6D).

The anterior limiting sulcus and the medial end of the transverse gyrus are the lateral limit of the posteromedial orbital lobule, which can clearly be identified as having the shape of the letter U, intersected by the posteromedial limb of the orbital sulcus (Fig. 6L). Figure 6L clearly shows that the transverse gyrus extends more medially to the insular pole.

The anterior perforated substance resembles a convex cavity extending upward at the posterior end of the basal surface of the frontal lobe. The roof of the anterior perforated substance is located at a higher level than the olfactory striae and the olfactory tract. The medial part of the anterior perforated substance is located more superior than its lateral part.

The anterior perforated substance is limited anteromedially by the posterior edge of the rectus gyrus and by the medial olfactory striae. Anterolaterally it is limited by the lateral olfactory striae, the medial end of the transverse gyrus, and the posteromedial orbital lobule. It is limited posterolaterally by the upper portion of the anteromedial surface of the

uncus and posteromedially by the optic tract (Fig. 6B). The most superior portion of the uncus that corresponds to the medial nucleus of the amygdala is located immediately below the optic tract. The optic tract is located anteriorly to the upper portion of the crus cerebri. The inferior choroidal point is located laterally to the crus cerebri and below the optic tract.

At the level of posteromedial orbital lobule, the gray matter of the orbital gyri is still separated from the anteroinferior portion of the basal ganglia (the head of the caudate nucleus and the lentiform nucleus) by a band of white matter, and the head of the caudate nucleus is projected directly above the posterior half of the olfactory sulcus and tract.

At the level of the roof of the anterior perforated substance, the lentiform nucleus comes almost directly to the cisternal surface, and the globus pallidus is projected directly above the bifurcation of the internal carotid artery (Fig. 6, E, M, and N).

Sylvian Fissure: Topographic Relationships

Sylvian Fissure versus Anterior Perforated Substance Versus Basal Ganglia

The neural structure on the basal aspect of the cerebrum that separates the sylvian fissure from the carotid cistern (sylvian vallecula) is the limen insulae (Fig. 7A). The olfactory tract points posteriorly toward the anterior perforated substance, which is the roof of the carotid cistern (Fig. 6B).

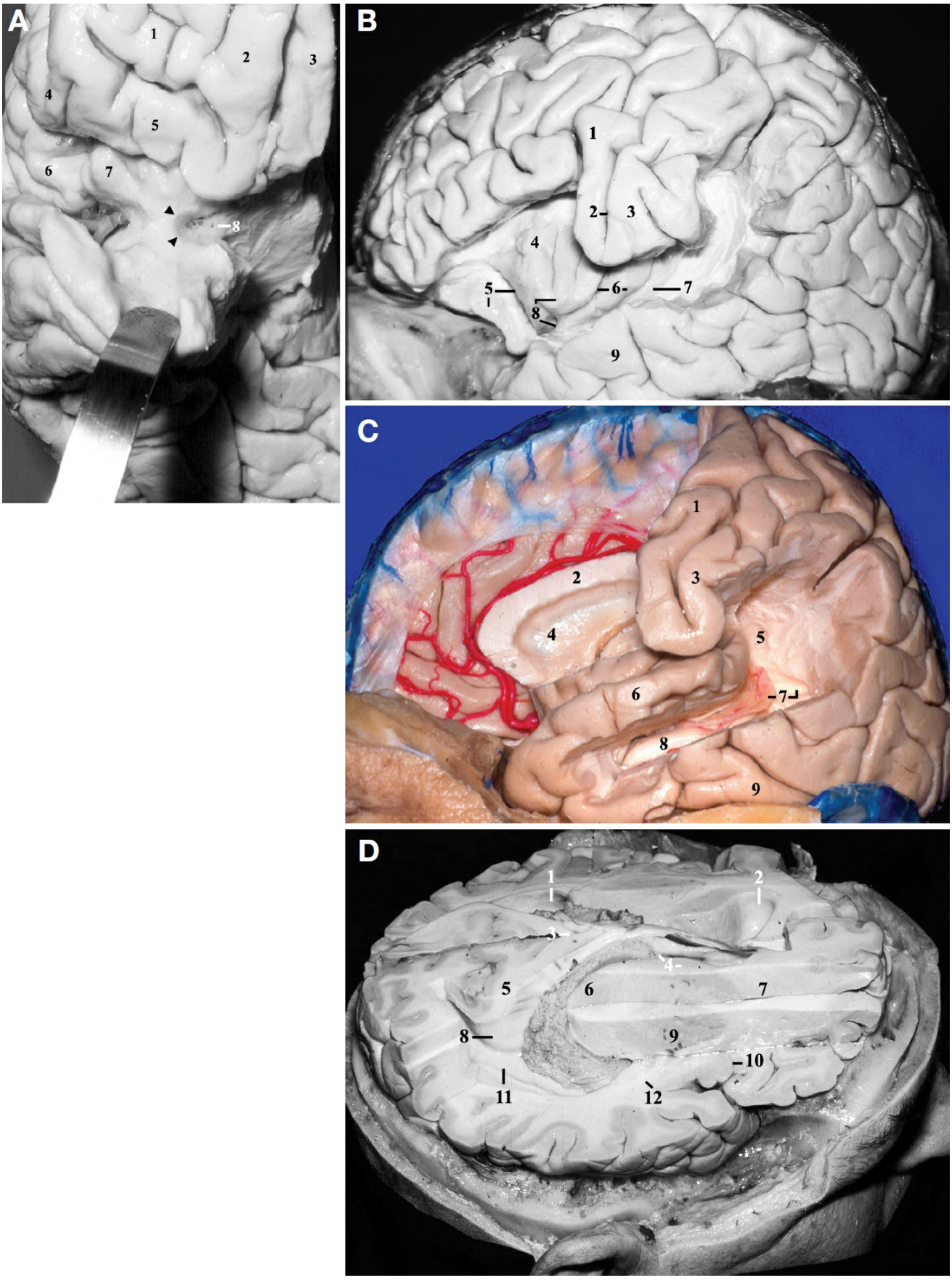

Figure 7. A, frontobasal view of the right hemisphere. The anterior part of the planum polare has been retracted inferiorly to display the anterior aspect of the insular pole. 1, anterior orbital gyrus; 2, medial orbital gyrus; 3, rectus gyrus; 4, pars triangularis; 5, posterior orbital gyrus; 6, pars opercularis; 7, anterior short gyrus of the insula; 8, anterior

perforated substance. The arrowheads indicate the limen insulae. B, lateral view of the left cerebral hemisphere. The inferior frontal and supramarginal gyri have been removed to display the relationship between the insula and the opercula of the precentral and postcentral gyri. 1, precentral gyrus; 2, central sulcus; 3, postcentral gyrus; 4, anterior short gyrus of the insula; 5, posterior orbital gyrus and the anterior insular cleft; 6, central sulcus and the anterior long gyrus of the insula; 7, posterior long gyrus of the insula and the inferior limiting sulcus of the insula; 8, insular apex and insular pole; 9, middle temporal gyrus. C, lateral view of the left cerebral hemisphere. The posterior portion of the superior temporal gyrus, the upper portion of the middle temporal gyrus, and the supramarginal gyrus have been removed. 1, precentral gyrus; 2, corpus callosum; 3, postcentral gyrus; 4, septum pellucidum at the level of the frontal horn; 5, upper portion of the atrium; 6, superior temporal gyrus; 7, calcar avis and the glomus of the atrium (choroid plexus); 8, hippocampus; 9, inferior temporal gyrus. D, superolateral view of the right cerebral hemisphere. 1, left atrium; 2, left frontal horn; 3, splenium of the corpus callosum; 4, foramen of Monro and caudate nucleus; 5, bulb of the callosum; 6, thalamus; 7, anterior extremity of the anterior limb of internal capsule; 8, calcar avis; 9, lentiform nucleus; 10, anterior insular cleft; 11, collateral trigone; 12, sublenticular portion of the internal capsule. (Images courtesy of AL Rhoton, Jr.)

Pars Triangularis, Precentral Gyrus, and Supramarginal Gyrus versus Insula

The lateral surface of the insula is almost evenly covered by these opercula. The frontal and parietal opercula cover the upper half of the lateral surface, and the temporal operculum covers its lower half. The posterior ramus and the lateral opercular compartment of the sylvian fissure divide the insula equidistantly in upper and lower halves (Fig. 6, E–G).

When viewed from a lateral perspective, the anterior zone of the lateral surface of the insula is covered by the pars triangularis, pars opercularis, and precentral gyrus on the frontal side and by the planum polare on the

temporal side. Because of their oblique direction (medially to laterally and posteriorly to anteriorly), the postcentral gyrus on the parietal side and the Heschl's gyrus on the temporal side cover the posterior zone of the lateral surface of the insula and the retroinsular region (Fig. 4, C–E).

Therefore, the posterior limit of the anterior zone of the insula is projected superficially onto the sylvian fissure approximately at the posterior margin of the precentral gyrus. The posterior zone is projected onto the sylvian fissure at ap proximately the level of the postcentral gyrus, and the retroinsular region is projected onto the sylvian fissure ap proximately at the anterior margin of the supramarginal gyrus (Fig. 7B).

The whole AP extent of the insula is therefore projected on the lateral surface of the cerebrum from the horizontal ramus of the sylvian fissure anteriorly to the anterior margin of the supramarginal gyrus posteriorly.

The pars triangularis of the inferior frontal gyrus covers the apex of the insula, and the lentiform nucleus is projected superficially onto the insula from the second short gyrus to the long gyrus, before the retroinsular region.

The precentral gyrus starts in the midline and courses anteriorly and laterally to reach the sylvian fissure. The operculum of the precentral gyrus covers the middle third and the anterior portion of the posterior third of the insula (Fig. 4, D and E). The genu of the internal capsule is projected over the middle third of the insula, whereas the pyramidal tract is projected over the posterior half of the insula. Because of the clockwise rotation of the fibers of the precentral gyrus, the fibers that are more laterally originated in the convexity, namely, fibers from the tongue and face, are located more anteriorly at the genu of the internal capsule. Fibers that are originated close to the midline, namely, fibers from the foot, are located more posteriorly, at the posterior limb.

Lateral Ventricles versus Frontal, Temporal, and Parietal Opercula

The frontal horn can be reached by following the direction of the anterior

limiting sulcus, the body of the lateral ventricle by following the superior limiting sulcus, and the atrium and the temporal horn by following the inferior limiting sulcus of the insula. The temporal horn is projected at the level of the middle temporal gyrus, the inferior portion of the atrium is projected at the posterior portion of the superior temporal gyrus (infrasylvian), and the upper portion of the atrium is projected over the supramarginal gyrus (suprasylvian). The anterior portion of the frontal horn can be reached via the anterior limiting sulcus of the insula (Figs. 5C and 7C).

The projection of the lateral ventricle over the lateral surface of the cerebral hemisphere can be estimated by an axial plane that extends from the base of the pars triangularis anteriorly to the inferior portion of the supramarginal gyrus posteriorly (just above the posterior end of the sylvian fissure), as shown in Fig. 6B.

Basal Ganglia and Thalamus Versus Insula

The insula is the external covering of the central core of the hemisphere, and the lentiform nucleus can be analogous to a short shield that stands between the insula and the internal capsule. The anterior extremity of the lentiform nucleus starts at the level of the second short gyrus of the insula and ends before the posterior long gyrus of the insula. When viewed from the insular side, the lentiform nucleus covers the central portion of the internal capsule; however, the peripheral part around the “short shield” is not covered. The peripheral part is composed of the most anterior, superior, posterior, and inferior portions of the internal capsule (Figs. 6, E–G, and 7D).

Frontobasal Area

The main structures located superior to the basal surface of the frontal lobe are the frontal horn, corpus callosum, and basal ganglia. The beginning of the tip of the frontal horn is located approximately halfway between the frontal pole and the anterior border of the anterior perforated substance, i.e., approximately at the level of the horizontal limb of the orbital sulcus. In this area, the rostrum of the corpus callosum

separates the frontal horn from the posterior and medial orbital gyri, the olfactory tract, and the rectus gyrus (Fig. 8A). At the level of the optic nerves or the anterior border of the anterior perforated substance, the head of the caudate nucleus is located immediately above the gray matter overlying the olfactory tract and is separated from the latter by a thin layer of white matter. At this same level, the lentiform nucleus is located immediately above the posteromedial orbital lobule and above the transverse gyrus of the insula and is separated from the latter by a thicker layer of white matter interposed by the claustrum (Fig. 8B). At the level of the anterior perforated substance or at the level of the optic chiasm, the lentiform nucleus comes directly into the cisternal surface (Fig. 8C).

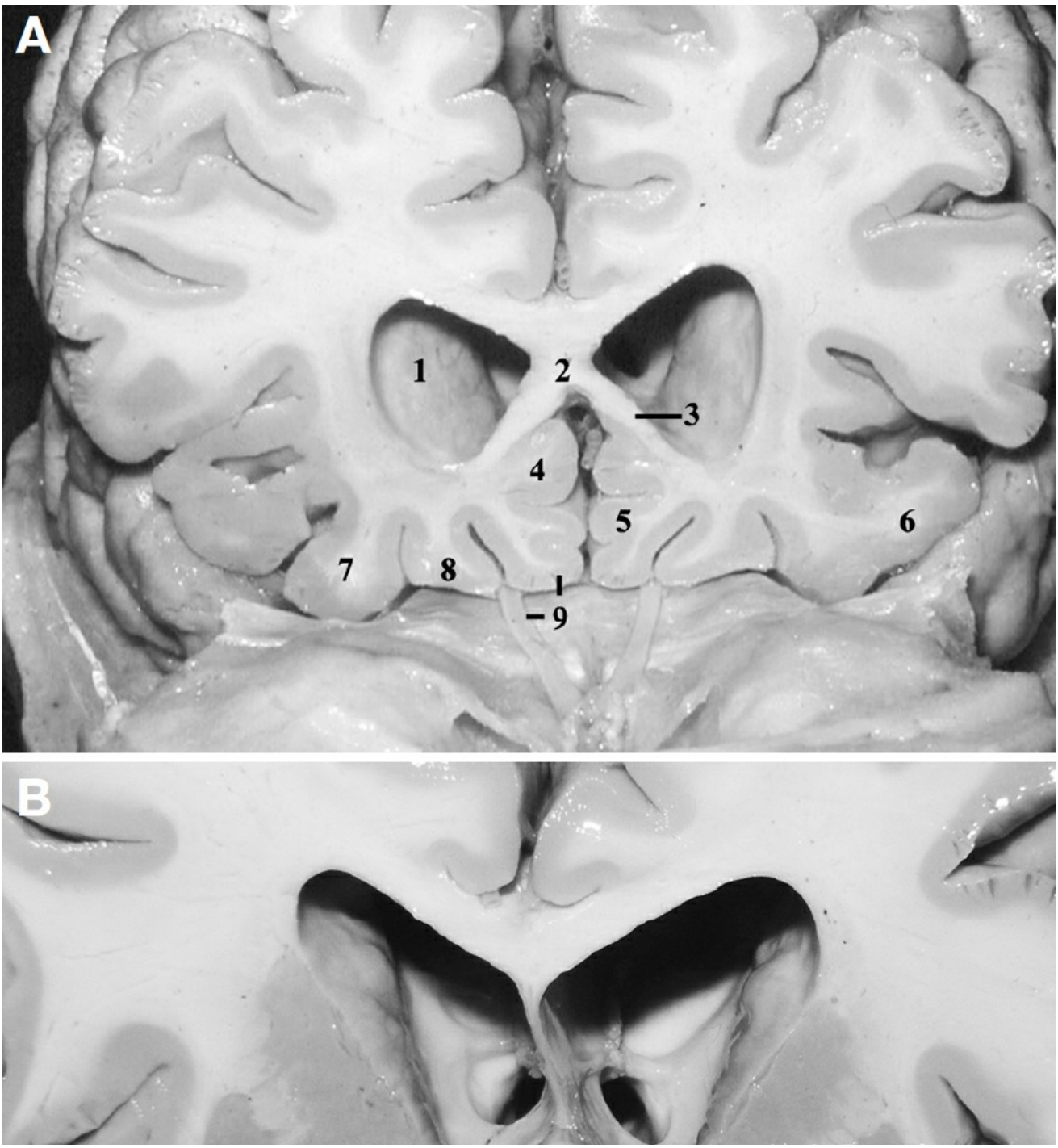

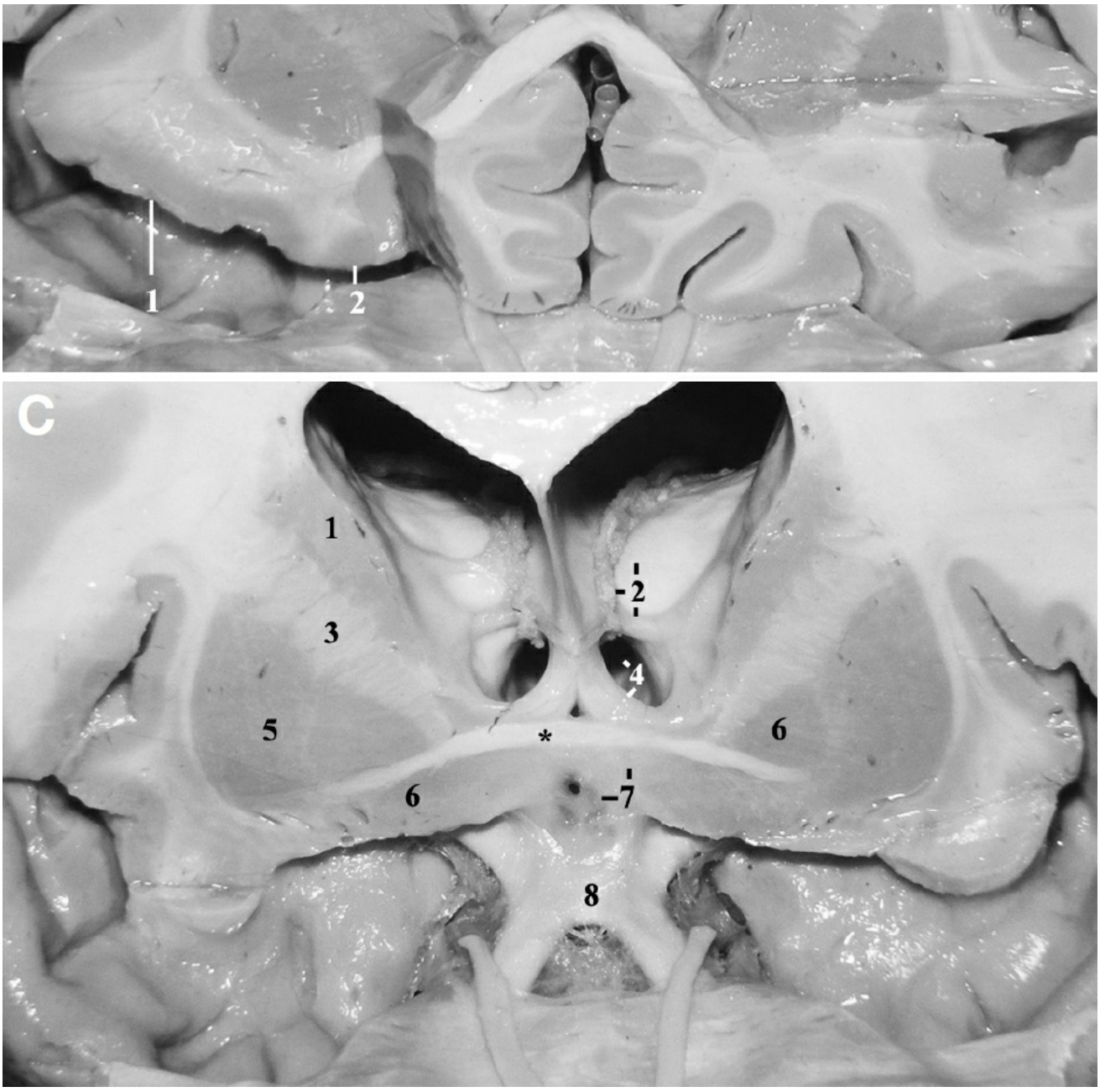

Figure 8. A, a coronal cut at the level of the planum sphenoidale, just anterior to the head of the caudate nucleus has been made. 1, head of the caudate nucleus; 2, genu of the corpus callosum; 3, rostrum of the corpus callosum; 4, inferior continuation of the cingulate gyrus; 5, inferior continuation of the medial frontal gyrus; 6, lateral orbital gyrus; 7, posterior orbital gyrus; 8, medial orbital gyrus; 9, rectus gyrus and the olfactory tract. The superior rostral sulcus is located between the 4 and 5, and the inferior rostral sulcus is located between the 5 and 9. The posteromedial limb of the orbital sulcus is located between the 7 and 8. The olfactory sulcus is located superiorly to the olfactory tract. B, a coronal cut was performed at a level between the cuts shown in Figs. 8A and 6C. 1, transverse gyrus of Eberstaller; 2, posteromedial orbital lobule. C, coronal cut performed at the level of the optic chiasm (at the anterior

perforated substance). 1, caudate nucleus; 2, thalamus, choroidal fissure, and thalamostriate vein; 3, internal capsule, transition between the anterior limb and the genu; 4, foramen of Monro and column of fornix; 5, putamen; 6, globus pallidus; 7, lamina terminalis and hypothalamus; 8, optic chiasm. Asterisk, anterior commissure. (Images courtesy of AL Rhoton, Jr.)

MCA: Anatomic Dissections with Angiographic Correlation

The M1 segment of the MCA extends from the carotid bifurcation to the limen insulae and can be divided into proximal and distal halves. The proximal half is related superiorly to the anterior perforated substance, posteriorly to the upper portion of the anteromedial surface of the uncus, inferiorly to the inferior portion of the anteromedial surface of the uncus, and anteriorly to the stem of the sylvian fissure, the frontotemporal arachnoid reflection, and the lesser wing of sphenoid. The distal half of the M1 is related superiorly to the inferior portion of the anterior surface of the insula, posteriorly to the inferior portion of the insular pole, inferiorly to the anterior portion of the planum polare, and anteriorly to the stem of the sylvian fissure, frontotemporal arachnoid reflection, and the lesser wing of sphenoid (Figs. 6M and 9, A and B).

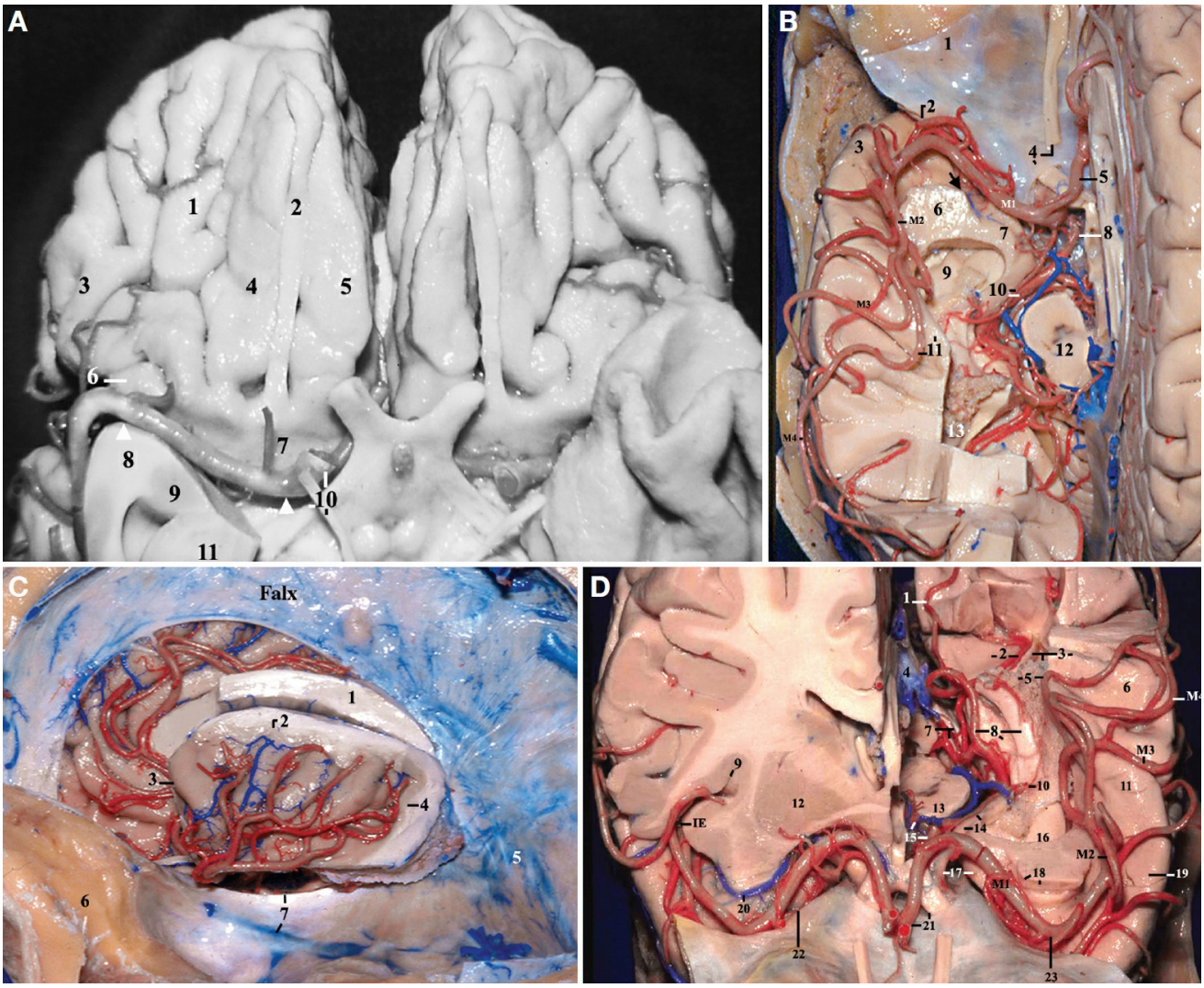

Figure 9. A, basal view of the cerebrum. 1, anterior orbital gyrus; 2, olfactory tract; 3, lateral orbital gyrus; 4, medial orbital gyrus; 5, rectus gyrus; 6, insula; 7, anterior perforated substance; 8, insular pole; 9, amygdala; 10, carotid bifurcation, oculomotor nerve, and the optic tract; 11, head of the hippocampus. The arrowheads indicate the extent of M1 segment. B, superior view. 1, orbit; 2, genu of the MCA; 3, planum polare; 4, olfactory tract and optic nerve; 5, anterior cerebral artery; 6, insular pole; 7, anteromedial surface of the uncus; 8, posterior communicating artery; 9, head of the hippocampus; 10, posteromedial surface of the uncus, anterior choroidal artery, and P2A segment of the posterior cerebral artery; 11, medial end of the Heschl's gyrus and the sylvian point; 12, midbrain; 13, atrium. M1, M2, M3, M4, segments of the MCA. C, lateral view of the left insula and M2 segment of the MCA. 1, corpus callosum; 2, superior limiting sulcus of insula; 3, anterior limiting sulcus of insula; 4, inferior limiting sulcus of the insula; 5, straight sinus; 6, orbit; 7, tentorial edge and middle fossa. D, anteroposterior (AP) view as in angiography. 1, parieto-occipital artery; 2, lingual gyrus and calcarine

artery; 3, calcar avis, atrium, and posterior transverse temporal gyrus; 4, vein of Galen; 5, glomus of atrium and sylvian point; 6, middle transverse temporal gyrus; 7, tentorial edge and trochlear nerve; 8, P2P segment of the posterior cerebral artery, parahippocampal gyrus, and fornix; 9, superior limiting sulcus of the insula; 10, inferior choroidal point (entry point of the anterior choroidal artery in the temporal horn); 11, Heschl's gyrus; 12, lentiform nucleus; 13, crus cerebri; 14, apex and the posteromedial surface of the uncus and the anterior choroidal artery; 15, P1 segment of the posterior cerebral artery and the posterior communicating artery; 16, head of the hippocampus; 17, supraclinoid carotid artery and anteromedial surface of the uncus; 18, limen insulae and insular pole; 19, planum polare; 20, deep middle cerebral vein; 21, anterior cerebral artery and optic nerve; 22, lesser wing of the sphenoid; 23, genu of the MCA; M1, sphenoid segment of the MCA; M2, insular segment of the MCA; M3, opercular segment of the MCA; M4, cortical segment of the MCA; IE, insular edge. (Images courtesy of AL Rhoton, Jr.)

The M2, or insular, segment is related to the surfaces of the insula: it begins at the limen insulae, turns around the insular pole to constitute the genu of the MCA, then sends off branches over the anterior and the lateral surfaces of the insula (they course in the anterior, superolateral, and inferolateral insular clefts). When those branches reach the limiting sulci of the insula (anterior, superior, and inferior), they become the M3 segment (Fig. 9C).

The M3, or opercular, segment of the MCA starts at the anterior, superior, or inferior limiting sulcus of the insula. It then courses between the orbital operculum and the planum polare on the basal surface or between the frontal and parietal opercula above and the temporal operculum below on the lateral surface to exit the sylvian fissure (the sylvian fissure stem on the basal surface and the 3 rami of the sylvian fissure on the lateral surface). Once they exit the sylvian fissure, they become the M4, or cortical, segment (Fig. 9D).

Clinical Application of Anatomic Information and Discussion

One of the most difficult tasks when studying the anatomy of the central

nervous system is to distinguish what information is relevant because what is important to neurosurgeons might not be relevant to anatomists and vice versa. In the authors' experience, most of the time, this distinction can only be made when we are actively examining radiological images, planning surgical strategies, and performing surgeries. The following are some of the clinical applications of sylvian fissure region anatomy.

Angiography

The neural and vascular structures along the trajectory of the M1 segment can be identified easily. At the limen insulae, the M1 becomes M2 and turns around the pole of the insula. This turn is easily recognized angiographically. The insula can be identified as the neural structure located immediately medial to the M2 segment of the MCA. The several loops formed by the M2 when it reaches the superior circular sulcus of the insula can also be identified angiographically. These several loops approximately indicate the location of the superior circular sulcus of insula. The first loop of the M2 is usually located more medially on angiography than the subsequent loops because the first loop usually is located in the anterior insular cleft. The last loop of the M3 segment that loops over the temporal operculum and exits the sylvian fissure constitutes an important angiographic landmark: the sylvian point or the M point (21, 24). The sylvian point is usually located on the most medial aspect of the Heschl's gyrus or even on the most medial aspect of the planum temporale. Besides being the last loop, the sylvian point is usually the most medial loop on the temporal side. This is explained by the anatomy of the retroinsular region because both the Heschl's gyrus and the planum temporale enclose the insula posteriorly and medially toward the atrium of the lateral ventricle and because the retroinsular region is located more medially than the anterior portion of the insula (Figs. 2E and 9, B and D).

The morphology of the other M3 loops on the temporal operculum can also be explained by the anatomy of the temporal operculum: the M3 segment that courses over the planum temporale presents a straight

morphology because it courses between the opercula of the supramarginal and postcentral gyri above and the planum temporale and the Heschl's gyrus below. All these present flat surfaces, allowing no space for curves. Only those M3 segments that course over the temporal opercula ahead of the Heschl's gyrus present a rather curved morphology because, anatomically, the planum polare is a depression and provides space for curves.

Looking at the AP view of the carotid angiography, we can recognize the neural structures located along the trajectory of the M1 and M2. The insula is located medially to the M2, and the frontal, parietal, and temporal opercula are projected laterally to M2, between the M2 and M4 segments. The curvature and morphology of the M3 branches of the frontal and parietal opercula determine the location of that particular M3 branch. In the anterior frontal operculum, they loop shallowly, loop deeply in the central region, and then exit straight with a long course in the postcentral region. In the posterior parietal region, they exit straight with a short course (19).

The sylvian point can provide the location of the following structures: the medial end of the Heschl's gyrus and consequently the retroinsular space, the posterior extremity of the posterior limb of the internal capsule, the atrium because the Heschl's gyrus points toward the atrium of the lateral ventricle, and the pulvinar of the thalamus, which is the anterior wall of the atrium.

The central core of the cerebral hemisphere, composed of the basal ganglia, thalamus, internal, external and extreme capsules, and claustrum, can be identified promptly in an AP view of carotid angiography: it is located in the rectangle limited anteriorly by the A1, M1, and genu of the MCA, medially by the distal anterior cerebral artery (A2–A5 segments), laterally by the M2 segment, and posteriorly by a transverse line drawn from the sylvian or M point.

The location of any angiographically visible vascular lesion in the sylvian fissure of the lateral surface of the cerebrum also can be roughly estimated: the first loop of the M2 usually indicates the location of the

anterior limiting sulcus of the insula (the anterior limit of the insula), the sylvian point indicates approximately the posterior limit of the insula, and the first M3 segment that displays a straight morphology indicates the location of the Heschl's gyrus or the planum temporale (Figs. 9D and 10A).

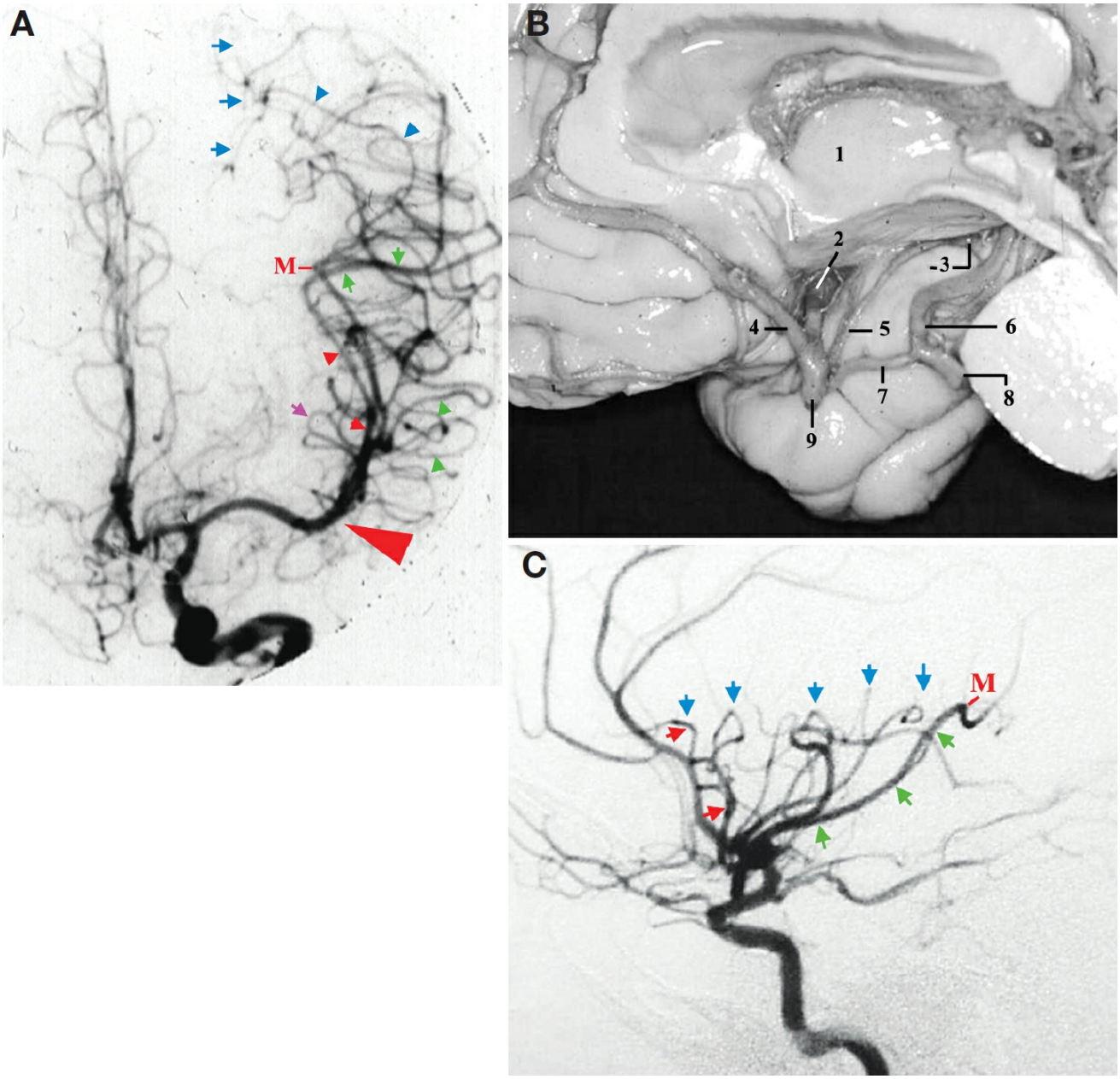

Figure 10. A, carotid angiography, AP view. The small red arrowheads indicate the M2 segment of the MCA. The green arrowheads indicate the M3 segment of the MCA over the planum polare. The green arrows indicate the M3 segment of the MCA over the planum temporale. The blue arrowheads indicate the M4 segment of the MCA over the parietal area. The blue arrows indicate the location of the intraparietal sulcus. The purple arrow indicates the superior limiting sulcus of insula. The large red arrowhead indicates the projection of the location of the tip of the pars triangularis, just distal to the genu of the MCA. B, medial view of the

right cerebral hemisphere with the crus cerebri removed to display the trajectory of the M1 segment in this projection. 1, thalamus; 2, M1 segment of the MCA; 3, uncus and the inferior choroidal point; 4, anterior cerebral artery; 5, anterior choroidal artery; 6, P2A segment of posterior cerebral artery; 7, posterior communicating artery; 8, P1 segment of posterior cerebral artery; 9, supraclinoid carotid artery. C, carotid angiography, lateral view. The red arrows indicate anterior limiting sulcus. Blue arrows indicate superior limiting sulcus. The green arrows indicate inferior limiting sulcus. M, sylvian point. (Images courtesy of AL Rhoton, Jr.)

In an AP view of carotid angiography, the temporal lobe is projected as follows: the planum temporale, Heschl's gyrus, and planum polare are all projected to the outer periphery of the arch formed by the distal half of the M1, the genu, and the whole extent of the M2 up to the sylvian point. The anterior segment of the uncus is projected at the outer periphery and behind the proximal segment of M1. The apex of the uncus is projected behind the supraclinoid carotid artery. The posterior segment of the uncus, the para hippocampal gyrus, the temporal horn, and the hippocampus are all projected inside the square formed by the M1, the A1 anteriorly, the distal anterior cerebral artery medially, the M2 and the sylvian point laterally, and an imaginary line traced horizontally from the sylvian point toward the midline. The medial limit of the parahippocampal gyrus is projected approximately halfway between the distal anterior cerebral artery and the M2 (Figs. 9D and 10A). In an AP view of vertebral angiography, the medial limit of the temporal lobe is the posterior cerebral artery (P2A, P2P, and P3 segments).

Both frontal and occipital poles can be superimposed on MCA branches in an AP view. However, as shown in Figure 4G, the largest transverse diameter of a normal brain (the suprasylvian lateral convexity) is located at the level of the postcentral gyrus. Therefore, the most laterally located vessels over the lateral convexity in an AP view are most likely running on the postcentral gyrus. Both the frontal and occipital poles present a smaller transverse diameter. Therefore, vessels running over those poles are usually not the most laterally located ones in an AP view.

The same consideration can also be applied to the middle temporal gyrus at the level of the postcentral gyrus. The largest transverse diameter of the brain on the infrasylvian convexity is located at the level of the superior or middle temporal gyrus at the same coronal plane as the postcentral gyrus.

In the lateral view of the carotid angiography, it is difficult to visualize the trajectory of the M1 segment because the view angle is the same as the main axis of the M1 (Fig. 10B) and because of the superimposition of the vessels. Also in the lateral view, the loops of the MCA, mainly composed of the M2 and M3 segments over the insula and adjacent frontal, parietal, and temporal opercula, form the sylvian triangle (16, 21).

The sylvian triangle resembles a right triangle with the right angle represented by the junction between the anterior and superior limiting sulci of the insula and the hypotenuse represented by the inferior limiting sulcus of the insula (Figs. 9C and 10C). This triangle basically displays the shape of the insula; this, in turn, approximately indicates the location of the "central core" of the hemisphere. The structures of the central core will be projected inside the triangle except for the caudate nucleus; the head and the body of the caudate nucleus are located above the lateral projection of the superior limiting sulcus of the insula (Fig. 6E).

The lateral ventricle is projected outside the sylvian triangle, the frontal horn is projected ahead and above the anterior limiting sulcus, the body of the lateral ventricle is projected above the superior limiting sulcus of the insula, the atrium is projected behind the junction between the superior and the inferior limiting sulcus of the insula, and the temporal horn is projected below the inferior limiting sulcus of the insula.

As mentioned previously, in normal conditions, the operculum of the precentral gyrus covers the middle third and the anterior portion of the posterior third of the insula. The anterior and posterior limits of the insula can be seen in angiography by identifying, respectively, the first loop of the sylvian triangle and the sylvian point. Thus, it is theoretically possible to determine the middle third between those 2 landmarks and to

determine the location of the precentral gyrus region by analyzing the morphology of the vascular loops.

In the lateral view of carotid angiography, the temporal lobe is projected as follows: the anterior portion of the planum polare and the genu of the MCA are projected anteriorly to the projection of the siphon of the carotid artery, the anterior segment of the uncus is projected at the level of the carotid artery, the apex of the uncus is projected behind the carotid artery, and the temporal horn starts behind the carotid artery and is projected at the level of the middle temporal gyrus (Fig. 9B). In a lateral view of the vertebral angiography, the apex and the anterior segments of the uncus are projected anteriorly to the basilar artery, and the posterior segment of the uncus is projected over the basilar tip and the P2A segment of the posterior cerebral artery. The inferior temporal gyrus is also the lowest part of the temporal lobe in the lateral view. Because of the obliquity of the tentorium cerebelli, the medial part being higher than its lateral part, the medial edge of the parahippocampal gyrus is located higher than the inferior temporal gyrus, approximately at the level of the inferior temporal sulcus or middle temporal gyrus, when viewed laterally.

In a standard AP view of a person with a normal cranial configuration, the largest transverse diameter of the cerebrum is located at the level of the postcentral gyrus (suprasylvian) and the middle temporal gyrus (infrasylvian). Therefore, the most laterally located vessels in an AP view are most likely related to those gyri. The vessels that course on the frontal lobe or occipital lobe will be projected more medially than the vessels coursing on the postcentral and middle temporal gyri (Fig. 4G).

There is controversy about the definition of the M1 segment of MCA. Yaşargil (31) and Taveras and Pile-Spellman (21) have defined M1 as extending from the carotid bifurcation to the limen insulae, and according to Yaşargil (31), the true bifurcation of the proximal M1 always occurs at the highest point of the limen insulae. Gibo et al. (5) and Rhoton (13) have defined the extent of M1 from the carotid bifurcation to the genu of MCA. The word limen comes from a Latin root meaning threshold; the limen was named to describe the medial border of the insula that

separates the sylvian vallecula from the sylvian fissure cistern (8, 30). Earlier publications reported the sylvian vallecula cistern as the hilum of the brain and that the bifurcation of the internal carotid artery, and the first portions of the anterior and middle cerebral arteries lie within it (30). This is actually a precise description of the carotid cistern.

For Krayenbuhl et al. (7), the practical meaning of limen insulae is the entrance to the insula. If one defines the extent of M1 from the carotid bifurcation to the limen insulae, it means that the entire M1 segment courses within the carotid cistern. If the genu of the MCA is defined as the distal end of M1, most of M1 still courses within the carotid cistern, and a small distal part of it courses within the sylvian fissure.

The variations of the trajectory of the M1 segment have been extensively studied by Krayenbuhl et al. (7) and Taveras and Pile-Spellman (21). Regardless the definition of the M1 segment, surgeons should be able to identify it on angiography, recognize its topographical relationships, and identify it intraoperatively.

The morphology of the M1 segment, whether straight or curved, is highly dependent not only on the length of the M1 itself, but also the height of the carotid bifurcation. The M1 segment turns around the insular pole to constitute the genu regardless of M1's morphology or curvature. Therefore, if the carotid bifurcation is low, the M1 tends to be straight; if the carotid bifurcation if high, the M1 tends to be curved; and if the carotid bifurcation is high and the M1 is elongated, the M1 tends to make a double curve.

Pterional Transsylvian Approach

In a standard pterional approach, the usual cerebral exposure can be seen (Fig. 11A).

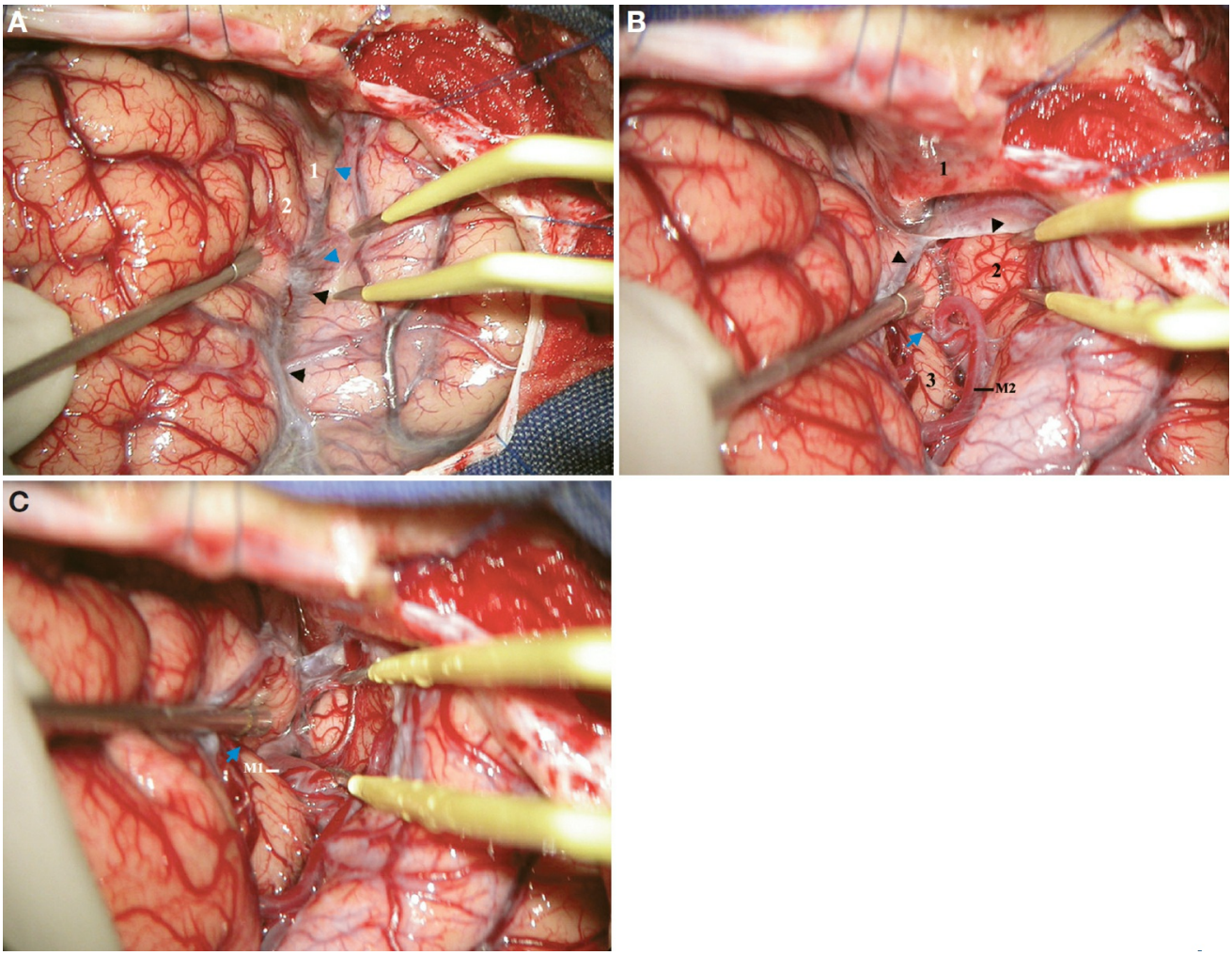

Figure 11. A, intraoperative photograph displaying cerebral exposure after a standard right pterional craniotomy. The tip of the suction tube has retracted the pars triangularis medially. 1, posterior orbital gyrus; 2, lateral orbital gyrus (pars orbitalis). The blue arrowheads indicate frontotemporal arachnoid reflection on the basal surface. The black arrowheads indicate frontotemporal arachnoid reflection on the lateral surface. B, continuation of A. The frontotemporal arachnoid membrane has been split to display the anterior opercular compartment of the sylvian fissure on the basal surface. 1, lesser wing of the sphenoid; 2, planum polare; 3, insular apex. The posterior orbital gyrus is retracted medially by the tip of the suction tube. The black arrowheads indicate the frontotemporal arachnoid membrane. The blue arrow indicates the beginning of the anterior insular cleft. C, continuation of B. The frontotemporal arachnoid membrane and the anterior opercular compartment have been further split to display the anterior insular compartment. The M1 segment of the MCA courses in the lower part of the anterior operculoinsular compartment (sphenoidal compartment). The blue arrow indicates the anterior insular cleft. (Images courtesy of AL

Rhoton, Jr.)

It is possible to see the frontotemporal arachnoid reflection that covers the superficial part of the sylvian fissure. The pars triangularis can usually be determined because it is the only part of the frontal operculum that habitually is retracted upward; this, in combination with the medial deviation of the planum polare, leaves a larger space for arachnoidal opening. However, when the pars triangularis cannot be promptly identified, an alternative is to check the sharp transition between the orbital and the lateral surfaces of the frontal lobe because the edge of this transition can easily be seen on the pars orbitalis, which occupies both lateral and basal surfaces of the cerebrum. On the lateral surface, the tip of the pars triangularis is located approximately 2 cm from the sharp transition between the basal and lateral surfaces (Fig. 12B).

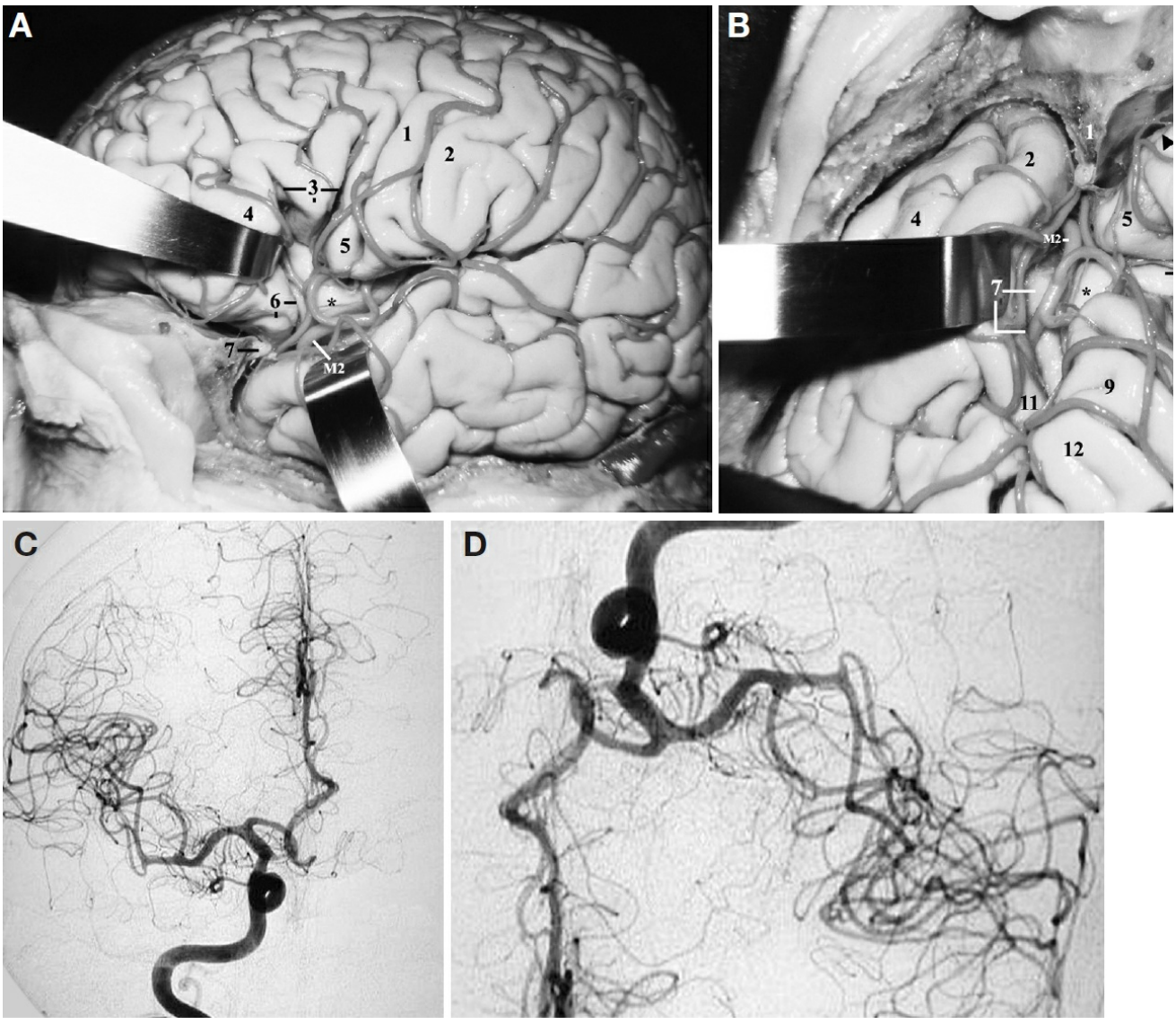

Figure 12. A, lateral view of the left hemisphere. The pars orbitalis has

been retracted anterior and superiorly. 1, precentral gyrus; 2, postcentral gyrus; 3, pars triangularis, anterior horizontal, and anterior ascending rami of the sylvian fissure; 4, orbitalis; 5, pars opercularis; 6, posterior orbital gyrus and the anterior insular cleft; 7, lesser wing of the sphenoid. Asterisk, insular apex. M2, insular segment of the MCA that has just turned around the insular pole (just distal to the genu of the MCA). B, same specimen in A in surgical position (left pterional exposure). The spatula on the left side is retracting the planum temporale, and the spatula on the right side is retracting the posterior portion of the pars orbitalis. 1, lesser wing of sphenoid; 2, superior temporal gyrus; 3, pars orbitalis; 4, middle temporal gyrus; 5, posterior orbital gyrus; 6, anterior insular cleft and anterior short gyrus of the insula; 7, posterior long gyrus and the inferior limiting sulcus of the insula; 8, pars triangularis; 9, precentral gyrus; 10, pars opercularis; 11, Heschl's gyrus; 12, postcentral gyrus; M2, insular segment of the MCA that has just turned around the insular pole (just distal to the genu of the MCA). Asterisk, insular apex. The arrowheads indicate the sharp transition between the basal and lateral surfaces of the cerebrum. C, AP view of a right carotid angiography. Note the laterally deviated supraclinoid carotid artery, the initial upward course followed by a downward curve of the M1, and then a rather horizontal course to turn around the insular pole. D, the expected intraoperative course of the M1 shown in C. (Images courtesy of AL Rhoton, Jr.)

Knowing the location of the tip of the pars triangularis, the approximate location of the frontal horn can be determined as well because it can be reached at the level of the base of the pars triangularis. This information can be helpful when the frontal horn has to be punctured.

Knowing the location of the pars triangularis also allows us to know the approximate location of the anterior limit of the central core because the location of the pars triangularis leads automatically to the horizontal ramus of the sylvian fissure that continues medially with the anterior limiting sulcus of the insula, and this will ultimately determine the anterior limit of the central core or will lead us to the frontal horn.

It is usually very difficult to identify a specific sulcus on the orbital surface of the frontal lobe; only the medial limit of the orbital gyri can be easily identified by the olfactory tract. However, the frontotemporal arachnoid reflection can help in identifying not only the posterior portion of the lateral, posterior, and medial orbital gyri, but also the anterior half of the planum polare in a transsylvian approach because this arachnoidal reflection is attached to those structures (Figs. 5A and 11A).

When it is necessary to release cerebrospinal fluid from the carotid cistern to “relax” the brain before splitting the sylvian fissure, the identification of the posterior portion of the olfactory tract can guide the surgeon to the carotid cistern (Fig. 5B). After opening the superficial part of the sylvian fissure, the intermediate, or opercular, compartment can be exposed (Fig. 11, B and C).

The compartments of the sylvian fissure on the basal surface of the brain have been defined as superficial (sylvian fissure stem) and deep (sphenoidal compartment) (5, 13). Although this is a classic definition, it apparently does not accurately depict the anatomy of the sylvian fissure in that region. It is clear that there is an opercular compartment composed of operculum of the pla num polare and the opposing operculum of the lateral and posterior orbital gyri (Fig. 11, B and C). The term sphenoidal compartment might suggest the close relationship of the lesser wing of the sphenoid to the deep compartment of the sylvian fissure or might depict the relationship of the M1 segment, also called the sphenoidal or horizontal segment, to the lesser wing of the sphenoid bone. However, the sphenoidal compartment actually arises in the region of the limen insulae at the lateral margin of the anterior perforated substance as a narrow space posterior to the sphenoid ridge between the frontal and temporal lobes. It communicates medially with the carotid cistern or sylvian vallecula.

One may automatically associate the term sphenoidal compartment with the term sphenoidal segment, but they represent different structures. The sphenoidal compartment is restricted to the region anterior to the insular pole, and the sphenoidal segment describes the trajectory of M1 behind

the lesser wing of the sphenoid bone, medial to the insular pole, within the carotid cistern.

The deep compartment of the sylvian fissure on the basal surface encompasses the sphenoidal compartment and extends into the anterior insular cleft, a space between the posterior surface of the lateral and posterior orbital gyri and the anterior surface of the insula.

Because of its relationship to the anterior surface of the insula, in this study, we called this compartment the anterior insular compartment and its opercular mate the anterior operculoinsular compartment.

In this article, we propose the introduction of the concept of the anterior operculoinsular compartment and the lateral operculoinsular compartment to describe the deep part of the sylvian fissure on the basal and lateral surfaces, respectively, of the cerebral hemisphere. Because the sylvian fissure is formed by the infolding of the frontal, parietal, and temporal opercula over the anterior and lateral surfaces of the insula, we believe that the term anterior operculoinsular more clearly delivers the information about the anatomy of that region. The classically used term sphenoidal compartment does not describe the entire anatomic situation over the anterior surface of the insula well. Rather, it describes only the inferior portion of the anterior insular compartment where the M1 courses.

MCA Aneurysm Surgery

As in any other aneurysm surgery, in MCA aneurysm surgery, it is very important to evaluate preoperative angiography to establish the surgical strategy and its application in surgery.

Important information can be obtained by evaluating preoperative angiography, including the exact location of the aneurysm and the direction of its dome, the neural structures adjacent to the aneurysm, the morphology (curvatures) of the M1 segment, and the early identification of the parent artery for proximal control.

The location and the direction of the dome of the aneurysm and the

morphology of the M1 segment can be evaluated by analyzing the following questions:

1. Is this aneurysm located before, at, or after the genu of the MCA?
2. If the aneurysm is located before the genu of the MCA, is it in the proximal half, in the distal half, or midway between the two halves of the M1 segment?
3. Is the dome of the aneurysm directed predominantly forward, backward, upward, downward, medially, or laterally?
4. What is the predominant course of the M1 segment? Is it straight or curving upward, downward, forward, or backward?

An MCA aneurysm that is located at or distally to its genu is more superficial and can usually be promptly located intraoperatively. As mentioned previously, the pars triangularis covers the apex of the insula that is located just posterior to the pole of the insula. Therefore, when the surgeon splits the sylvian fissure at the level of the pars triangularis, she or he will expose the portion of the MCA that has just turned around the pole of the insula, that is, just distal to the genu of the MCA (Figs. 10A and 12, A and B). If the aneurysm is located soon after the genu of MCA, it will be promptly identified.

If the aneurysm is located before the genu of the MCA, it can be located in the proximal half, in the distal half, or between the halves of the M1 segment. As mentioned previously, the adjacent neural structures are different in those situations.

The predominant direction of the dome of the aneurysm indicates the surrounding structures to which the dome of the aneurysm might be attached. Retraction on those structures is to be avoided in the beginning of the dissection of the sylvian fissure.

An MCA aneurysm that points laterally, parallel to M1 on an AP view in angiography, means that its dome is directed along the sylvian fissure, usually parallel to the course of the M1 segment, and it is pointing toward

the surgeon intraoperatively during the pterional approach.

It is very important to know beforehand the course of the M1 segment, as demonstrated by Yaşargil et al. (33), not only for intraoperative orientation, but also for the purpose of proximal control.

The course and the shape of the M1 segment, as well as the height of its origin from the supraclinoid carotid artery, can vary considerably (21). However, the MCA always turns around the pole of the insula to constitute its genu to reach the lateral surface of the insula, regardless the variable course of its M1 segment.

When the M1 segment curves inferiorly on angiography, it will be curving toward the temporal lobe. When the M1 segment curves superiorly on angiography, it will curve toward the anterior perforated substance or toward the anterior surface of the insula. The approximate intraoperative course of the M1 segment can be displayed when we turn the standard AP view angiography upside down (Fig. 12, C and D). In some cases, there is no need to expose the entire M1 segment to find the aneurysm or even to find a portion of the M1 segment for proximal control.

The next step is to transport all the information obtained from the angiography to the surgery, and the surgeon's next questions are the following:

1. Toward what direction should I proceed with dissection in the sylvian fissure?
2. Where can I or can I not apply retraction to avoid early rupture of the aneurysm?
3. Where do I expect to find intraoperatively the aneurysm and the M1 segment for proximal control?

After the appropriate positioning and standard pterional craniotomy, the cerebrum is exposed. First, we have followed routinely the olfactory tract posteriorly to locate the carotid cistern and released cerebrospinal fluid from it to relax the brain. After having opened the carotid cistern, the

carotid artery is identified. The sylvian fissure is then split, starting at the level of the pars triangularis.

As the pars triangularis is projected over the apex of the insula, as soon as we split the sylvian fissure at that level, we will encounter the M2 segment that has just turned around the insular pole and the apex of the insula (Fig. 12B).

The anterior pole of the insula and, consequently, the limen insulae are located more medially and posteriorly than the tip of the pars triangularis. The aneurysms that are located soon after the genu of the MCA are located at the level of the pars triangularis, and the aneurysms that are located at the level of the insula pole are projected more medially and posteriorly in relation to the tip of the pars triangularis. Those aneurysms arising before the insula pole are projected even more medially and posteriorly in relation to the pars triangularis (Fig. 6D).

If the aneurysm is located immediately distal to the genu of the MCA, it can be found quickly when the sylvian fissure is split at the level of the pars triangularis. If the aneurysm is located more distally, its location can be estimated by looking at the distance of the aneurysm to the genu of the MCA and to the sylvian point on the AP view angiography. If the aneurysm is located midway between the sylvian point and the genu of MCA, it will probably be located at the level of the precentral gyrus, or it can be located by looking at the lateral view angiography by locating the aneurysm inside the sylvian triangle. The anterior limit of the sylvian triangle is located at the level of the anterior limiting sulcus that continues superficially as the horizontal ramus of the sylvian fissure, and the sylvian point is projected at the anterior margin of the supramarginal gyrus. If it is midway between the two, it probably is located at the level of the precentral gyrus. If it is located at the level of the anterior zone of the insula, it will be related to the pars opercularis or triangularis. If it is related to the posterior zone of the insula, it will be related to the pre- or postcentral gyrus. Therefore, the intraoperative location of a distal MCA aneurysm can be calculated between the pars triangularis and the supramarginal gyrus, and the intraoperative identification of the

operculum of the precentral gyrus can be a helpful landmark.

However, in most cases of MCA aneurysms, the aneurysm is located at or before the pole of the insula, and its intraoperative location can be easily estimated by looking at the distance between the bifurcation of the internal carotid artery and the genu of the MCA. The clinical application of the anatomic information can be illustrated in the following cases.

Case 1. After the carotid bifurcation, the M1 segment curves downward and gives rise to the aneurysm that is directed inferiorly and anteriorly (Fig. 13, A and B). The aneurysm is located before the genu of the MCA, roughly midway between the carotid bifurcation and the genu of the MCA. Therefore, it is more medially and posteriorly located than the genu of the MCA. It is important to keep in mind that opening the sylvian fissure at the level of the pars triangularis will expose the apex of the insula, distal to the genu of the MCA. This aneurysm is located much more medially (proximal) than the level of the pars triangularis (Fig. 13C).

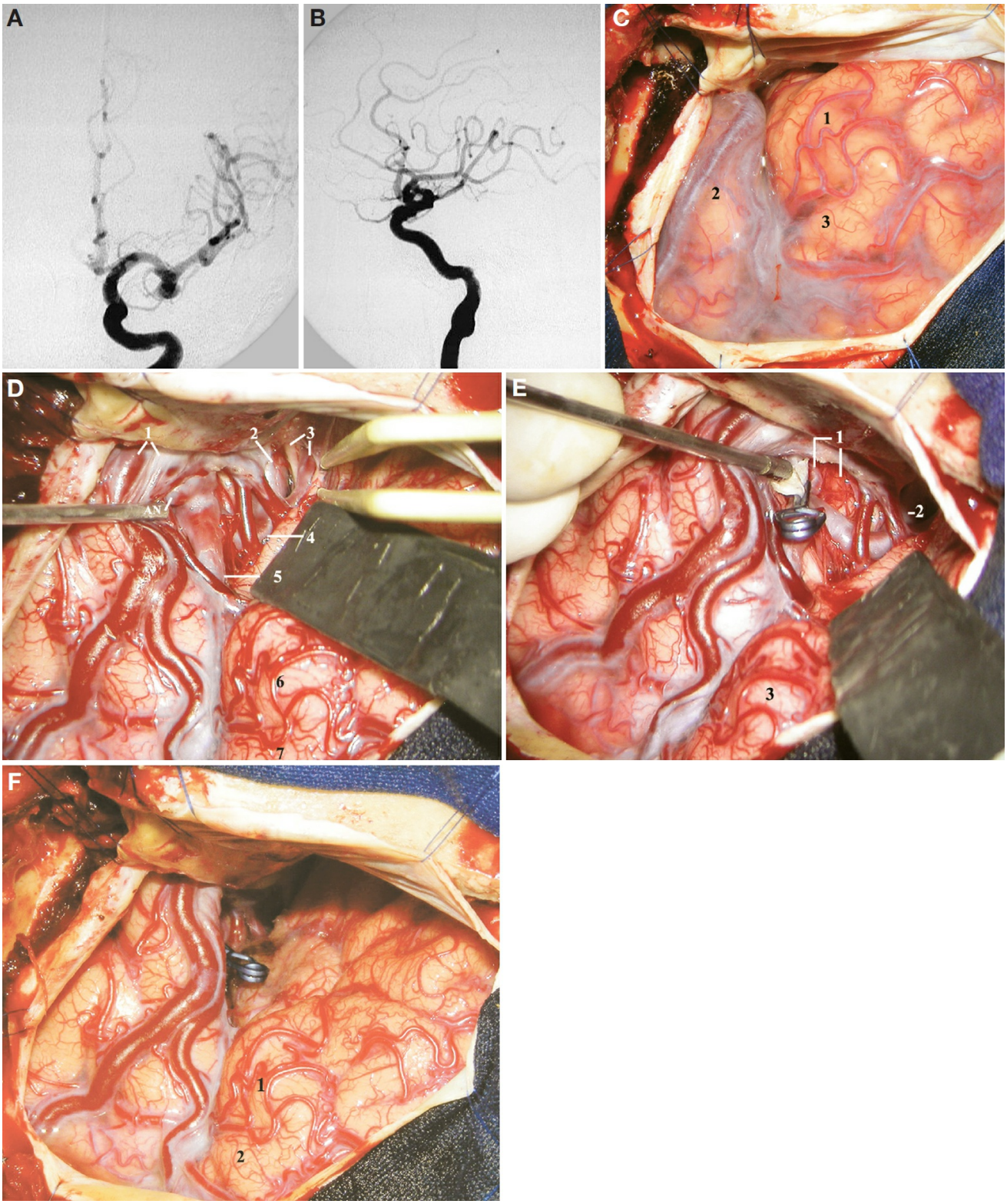

Figure 13. A, AP view of a left carotid angiography depicting an MCA aneurysm pointing downward. B, lateral view of the same angiography shown in A depicting an MCA aneurysm pointing anteriorly and inferiorly. C, surgical exposure after a left pterional craniotomy followed by the dural opening. 1, pars orbitalis; 2, superior temporal gyrus; 3, pars triangularis. D, intraoperative photograph. The sylvian fissure was split proximal to the pars orbitalis to expose the aneurysm. 1, superficial sylvian veins; 2, supraclinoid carotid artery; 3, optic nerve and anterior

cerebral artery; 4, M1 proximal to the aneurysm; 5, MCA distal to the aneurysm; 6, pars orbitalis; 7, pars triangularis. The olfactory tract is located beneath the tip of the bipolar forceps. E, the aneurysm shown in D was clipped and the dome opened and cut (at the tip of the suction tube). 1, temporal branch of the MCA and the planum polare; 2, carotid artery; 3, pars orbitalis. F, overall view of the surgical exposure after aneurysm clipping. Note the location of the clip (which indicates the location of the aneurysm) and the location of the pars triangularis (which indicates approximately the location of the insular apex, just distal to the insular pole and to the genu of the MCA). 1, pars orbitalis; 2, pars triangularis. (Images courtesy of AL Rhoton, Jr.)

Because the dome of the aneurysm is directed inferiorly and anteriorly on angiography, it is expected to be directed anteriorly and superiorly in the surgery (33), and the dome is expected to be in close relation to the anterior half of the planum polare, sylvian fissure stem, frontotemporal arachnoid reflection, and lesser wing of sphenoid. Its dome is expected to be superficially located when viewed intraoperatively. The drilling of the lesser wing and the opening of the dura mater must be performed with caution (Fig. 13, D and E). After originating the aneurysm, the MCA courses almost straight to curve around the insular pole to constitute the genu of the MCA. In this case, the sylvian fissure was split proximal to the pars triangularis because of the location of the aneurysm (Fig. 13F).

Case 2. The M1 segment is almost straight and horizontal. At the distal half of M1, before the insular pole, it bifurcates and gives rise to an aneurysm that points slightly superiorly and laterally. It is difficult to evaluate the lateral view on an angiogram because of the superimposition of the vessels, but in this case, the aneurysm's location was confirmed by angiography–computed tomographic (CT) scan. In the distal half of M1, the aneurysm is related superiorly to the anterior surface of the insula. Slight lateral projection of the aneurysm indicates that it is mostly located inside the sylvian fissure (Fig. 14, A–C).

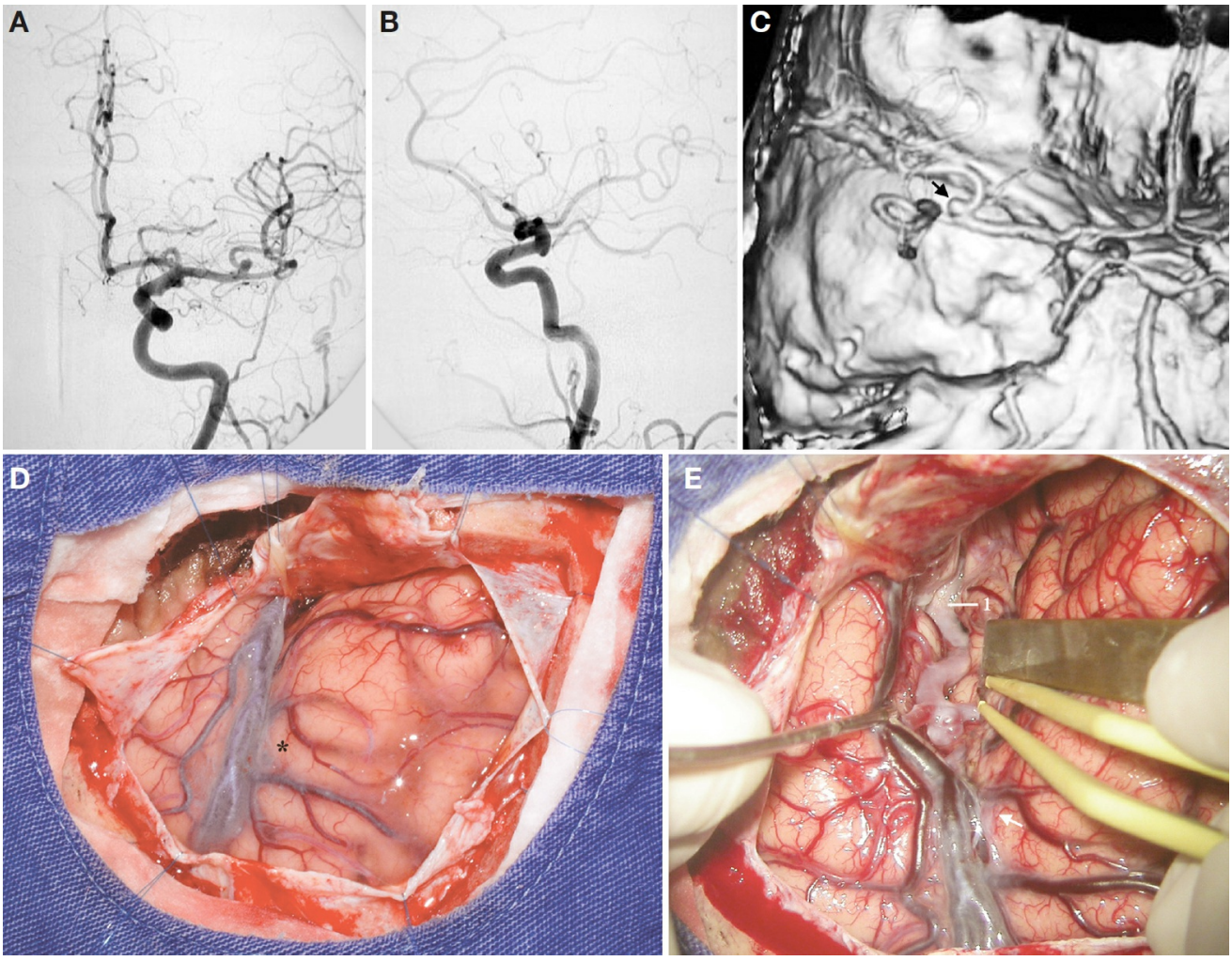

Figure 14. A, AP view of a left carotid angiography depicting an MCA aneurysm arising proximal to the genu of the MCA, in the distal half of the M1 and pointing superiorly in this projection. B, lateral projection of the same carotid angiography shown in A. Because of the superimposition of the vessels, it is difficult to visualize the aneurysm. C, Angiography-CT depicting the aneurysm (arrow) shown in A. D, surgical exposure after a left pterional craniotomy and dural opening. Asterisk, pars triangularis. E, the sylvian fissure was split just proximal to the tip of the pars triangularis (arrow). Note the distance between the aneurysm and the tip of the pars triangularis (arrow). The carotid bifurcation is located at the level of the tip of the spatula. 1, supraclinoid carotid artery. (Images courtesy of AL Rhoton, Jr.)

When the sylvian fissure is split at the pars triangularis, the aneurysm is expected to be located proximally to the insular pole, with most of the aneurysm located inside the anterior insular compartment of the sylvian fissure (Fig. 14, D and E).

Case 3. The M1 segment is initially directed superiorly and laterally. Midway between its proximal and distal halves, M1 gives rise to an aneurysm that is pointing superiorly and slightly anteriorly. After giving rise to the aneurysm, M1 continues downward toward the insular pole (Fig. 15, A–C).

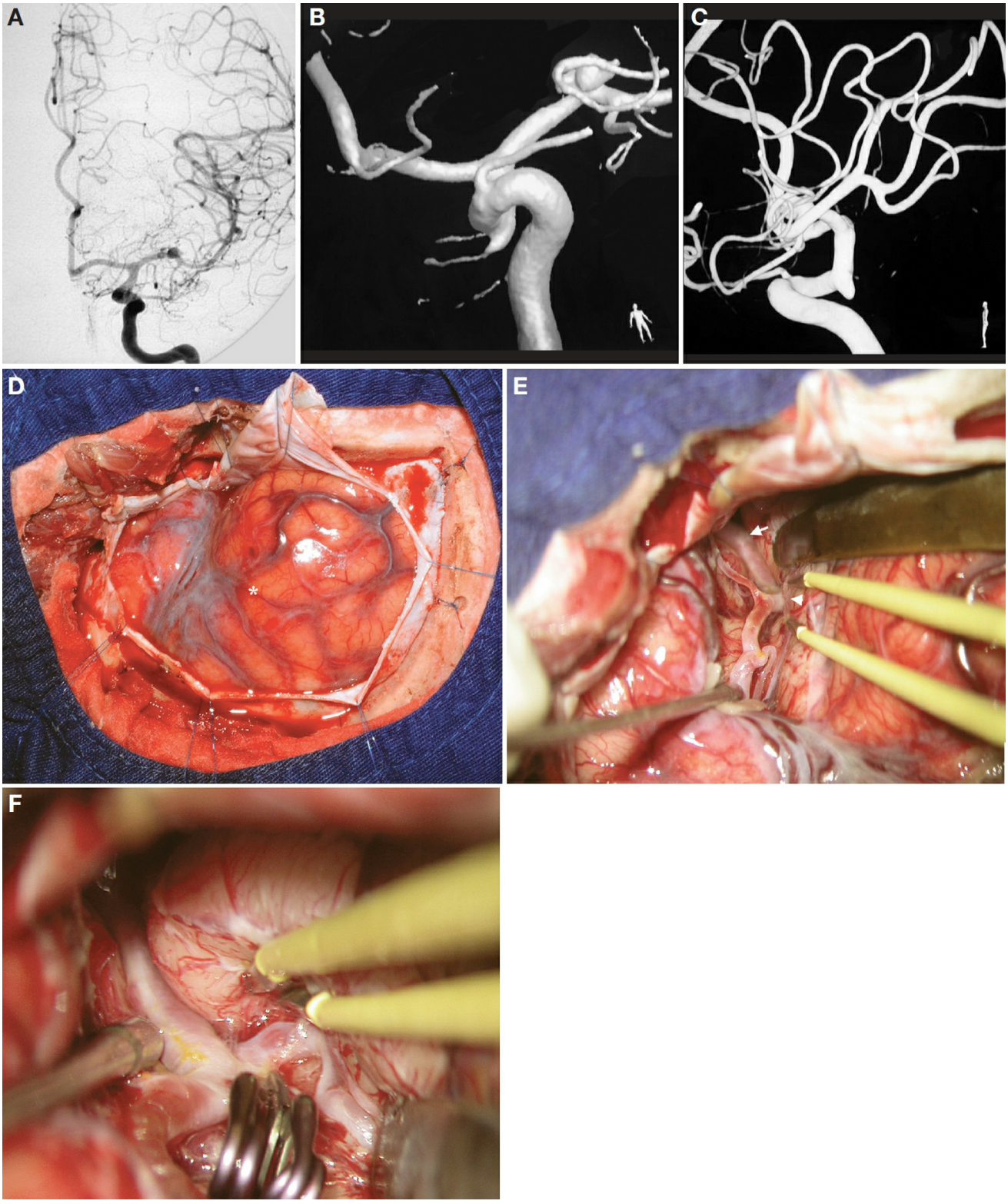

Figure 15. A, AP view of a left carotid angiography depicting an MCA aneurysm arising approximately midway between the carotid bifurcation and the genu of the MCA. B, angiography-computed tomographic (CT)

scan with 3-dimensional reconstruction showing the same aneurysm. C, angiography-CT scan with 3-dimensional reconstruction, lateral view. D, exposure after a left pterional craniotomy and dural opening. asterisk, pars triangularis. E, the sylvian fissure was split proximal to the pars triangularis (asterisk). Arrow indicates the carotid bifurcation. The arrowhead indicates the location of the aneurysm. Note the distance between the pars triangularis and the location of the aneurysm. F, the aneurysm was clipped, and the frontal branch of the MCA bifurcation was identified. (Images courtesy of AL Rhoton, Jr.)

The initial upward curvature of M1 indicates that it is curving toward the anterior perforated substance. Midway between the proximal and distal halves of the M1 is the transition between the anterior perforated substance and the medial limit of the insular pole (Fig. 15, D–F).

In these 3 illustrative cases, the first step in the surgery was to open the carotid cistern to relax the brain and to either expose or estimate the location of the carotid bifurcation. The extent of the MCA from the carotid bifurcation to the genu of MCA, as shown on angiography, is therefore estimated intraoperatively from the carotid bifurcation to the pars triangularis, and the location of the aneurysm is determined according to the angiography. Depending on the location of the aneurysm and the direction of its dome, it will be related to different surrounding neural structures. Knowing the location of the aneurysm and the direction of its dome beforehand, the surgeon can quickly find the aneurysm, thus reducing the risk of its premature rupture because of inadequate brain retraction.

Case 4. A 31-year-old woman had undergone previous surgery for a right MCA aneurysm at another neurosurgical center in 2000. She was admitted to the emergency department on March 23, 2008, with a sudden headache, aphasia, and drowsiness. The CT scan is shown in (Fig.16A). The angiography-CT scan showed a left distal MCA aneurysm (Fig. 16, B and C). Another hemorrhage was present on the morning of the surgery, March 24, and the patient had hemiparesia (Grade 3 strength). Figure 16D shows the brain after an extended pterional craniotomy and dural

opening. The posterior ramus of the sylvian fissure was split, the clot was removed, and the aneurysm was found at the level of the anterior margin of the operculum of the postcentral gyrus (Fig. 16, E and F).

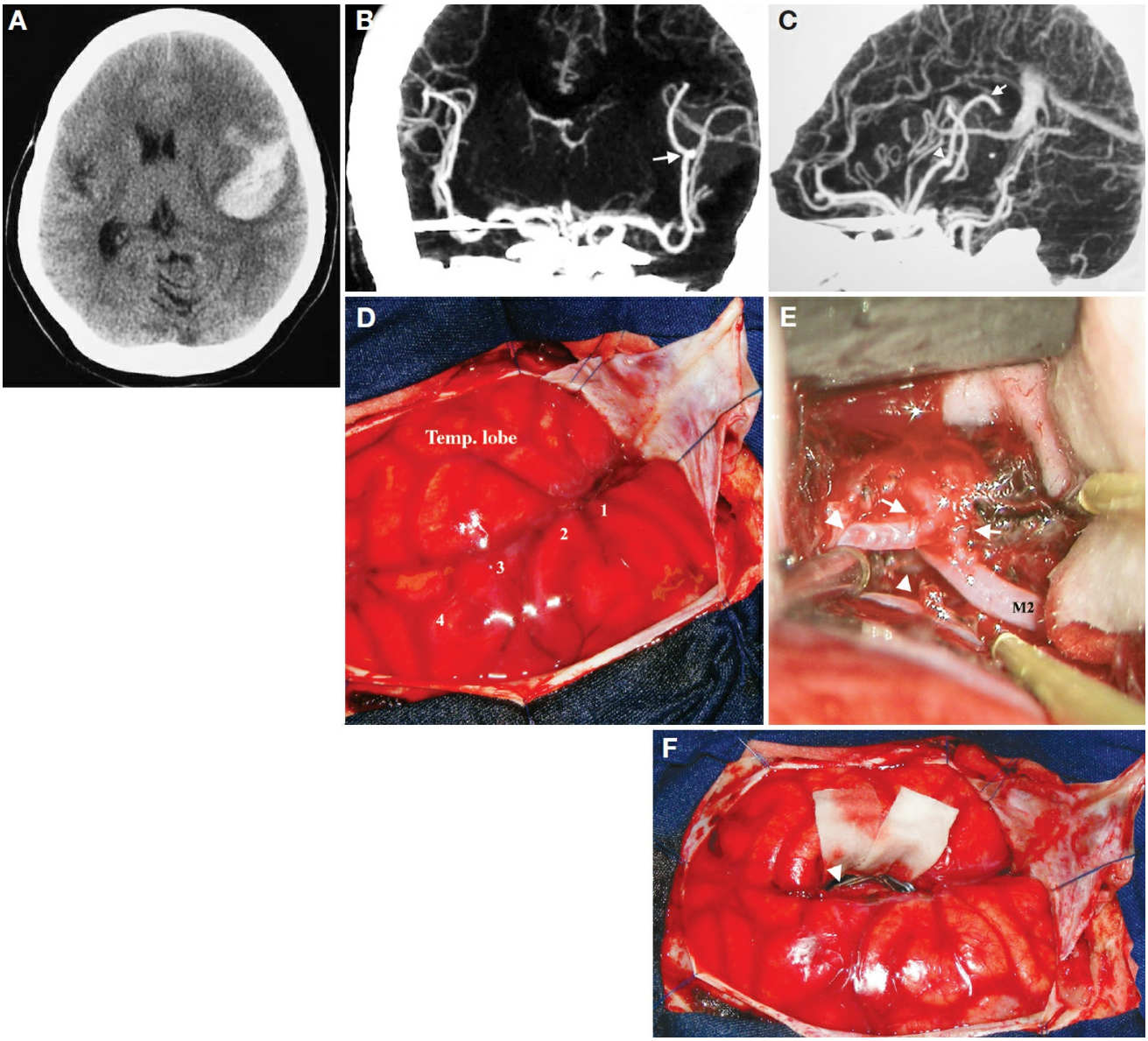

Figure 16. A, axial CT scan. There is a hematoma in the left sylvian fissure. B, Angiography-CT, coronal view. There is a distal MCA aneurysm (arrow); it is located slightly distal to the halfway between the genu of the MCA and the sylvian point. C, Angiography-CT, lateral view. The arrowhead indicates the aneurysm, and the arrow indicates the sylvian point. The aneurysm is located at the level of the transition between the middle third to the posterior third of the insula, close to the inferior limiting sulcus. D, intraoperative photograph depicting the surface of the brain after an extended left pterional craniotomy and dural opening. The intense subpial hemorrhage makes the identification of the sulci and gyri difficult. The authors' interpretation of the case was 1) pars triangularis,

2) pars opercularis, 3) precentral gyrus, 4) postcentral gyrus. Temp., temporal. E, intraoperative photograph showing the aneurysm arising from a bifurcation of an M2 branch. The arrows indicate the neck of the aneurysm. The arrowheads indicate the distal branches of the M2 branch. F, intraoperative photograph. The aneurysm was clipped using only the tip of the clip (Because of a lack of variety of clips available at the time of the surgery), and the clot in the sylvian fissure was removed. The arrowhead indicates the location of the neck of the aneurysm. (Images courtesy of AL Rhoton, Jr.)

In this case, the most difficult part was determining the intraoperative location of the aneurysm by means of angiography-CT scan. The AP view showed a distal MCA aneurysm located slightly distal to the midway point between the genu of the MCA and the sylvian point. The lateral view showed that the aneurysm was arising from an M2 segment that was coursing close to the hypotenuse of the sylvian triangle, close to the inferior limiting sulcus of the insula, and that the aneurysm was related approximately to the transition between the middle and posterior thirds of the lateral surface of the insula.

The middle third and the anterior part of the posterior third of the lateral surface of the insula are usually covered by the operculum of the precentral gyrus. Therefore, preoperative planning entails locating the opercula of the precentral and postcentral gyri along the posterior ramus of the sylvian fissure; the aneurysm must be located at the transition between those gyri or at the level of the posterior margin of the precentral gyrus and close to the inferior limiting sulcus of the insula.

Because of the severe subarachnoid and subpial hemorrhage, it was difficult to identify the sulci and gyri. The location of the pars triangularis was estimated at approximately 2 cm behind the lateral edge of the frontal lobe, and the rest of the operculum was subsequently determined.

The posterior ramus of the sylvian fissure was opened wide from the pars triangularis that covers the insular apex, anterior, and middle short insular gyri to the postcentral gyrus for proximal control and early identification of the parent artery. The intrasylvian clot was removed, and the aneurysm

was soon located and clipped.

Different surgical techniques to clip MCA aneurysms have been reported that can basically be divided into the following 3 categories (3, 17, 18): the medial-to-lateral, lateral-to-medial, and superior temporal gyrus approaches.

The medial-to-lateral approach (31, 35) starts with opening the carotid cistern, followed by opening the stem of the sylvian fissure, which is then opened in a medial-to-lateral direction to expose the aneurysm. This technique allows early proximal control of the parent artery before the aneurysm is exposed.

The lateral-to-medial approach (11) starts with opening the distal sylvian fissure, followed by tracing the MCA branches to the aneurysm and to the MCA trunk.

In the superior temporal gyrus approach (6, 9), the MCA aneurysm is approached through the superior temporal gyrus, and subpial resection is used to expose the MCA branches and the aneurysm neck.

This technique offers the advantage of decreasing brain retraction and manipulation of the MCA trunk and its perforators. The drawback is the potential to increase the risk of postoperative epilepsy, and this technique is not suitable for an aneurysm arising from a short MCA trunk.

The use of image-guidance navigation, thin-slice magnetic resonance imaging (MRI) for image guidance, to locate and treat unruptured MCA aneurysms has been reported by Son et al. (17). The main advantages of this technique include small incision and small craniotomy.

For distal MCA aneurysm, Dashti et al. (4) recommend the use of digital subtraction angiography, 3-dimensional CT-angiography, T2-weighted MRI (coronal, axial) for preoperative planning and the use of neuronavigation, intraoperative noninvasive digital subtraction angiography, and color Doppler ultrasonography for MCA aneurysms arising distal to the M2-M3 junction.

In our surgical technique, the angiogram is analyzed and the location of the aneurysm relative to the genu of the MCA and the direction of its dome are established. This information is taken into consideration in the pterional approach. To locate distal MCA aneurysms intraoperatively, it is important to know the relationship between the frontal, parietal, and frontoparietal opercula to the lateral surface of the insula and to the temporal operculum. It is also important to understand that these relationships are not a perfect match. For instance, the operculum of the postcentral gyrus is in opposition to the Heschl's gyrus. This does not mean that the anterior and posterior edges of the postcentral gyrus will precisely meet the anterior and posterior edges of the Heschl's gyrus, but most of the parts will be in opposition. This can also be extended to the insula and its overlying opercula: the operculum of the precentral gyrus most likely will cover the middle third and part of the posterior third of the lateral surface of the insula.

Aneurysms pointing upward are related to lenticulostriate arteries when located in the proximal half of M1 or to orbitofrontal arteries when located in the distal half. Those that point downward are related to the anterotemporal arteries.

Insular Resections

It is necessary to split the sylvian fissure wide and separate the frontal and parietal opercula from the temporal operculum to expose the insula.

Although the insula is almost evenly covered by frontal, parietal, and temporal opercula, it is more difficult to expose the lesions located in the superolateral facet of the insula than in the inferolateral facet. It is easier to approach the anterior half of the insula than its posterior half, mainly because of the morphology of the temporal operculum; the morphology of the frontal and parietal opercula is roughly constant, except for the pars triangularis, throughout the lateral sylvian fissure. It can increase risks to retract these opercula to expose the upper portion of the insula, especially with the insula of the dominant hemisphere. Hence, the alternative is to retract the temporal operculum. Among the 3 parts of the temporal operculum, only the planum polare (opposite pars triangularis, opercularis,

and precentral gyrus) presents a formidable depression that allows retraction, creating more space to approach the superolateral facet of the anterior zone. From the planum polare posteriorly, the opercula of the postcentral, supramarginal gyri, Heschl's gyrus, and planum temporale present flat surfaces on the sylvian fissure, making their retraction more difficult and consequently making access to the posterior half of the insula more difficult.

Case 1. The patient was a 17-year-old boy with a 4-year history of complex partial seizures. MRI revealed a right-side insular tumor and a right frontal arachnoid cyst (Fig. 17A). The insular tumor was well circumscribed and occupied the posterior two-thirds of the insula (Fig. 17B). The superior limit was located at the same level of the lateral opercular compartment of the sylvian fissure (Fig. 17C). The patient underwent right pterional craniotomy with intraoperative electrocorticography in August 2000 (Fig. 17D). The tumor was totally removed through sylvian fissure (histology revealed pilocytic astrocytoma) (Fig. 17E). The frontal cortex under the arachnoid cyst was resected as well because of persistent spikes. The postoperative course was uneventful, and the patient remains free of seizures, anticonvulsant medication, and tumors (Fig. 17, F and G).

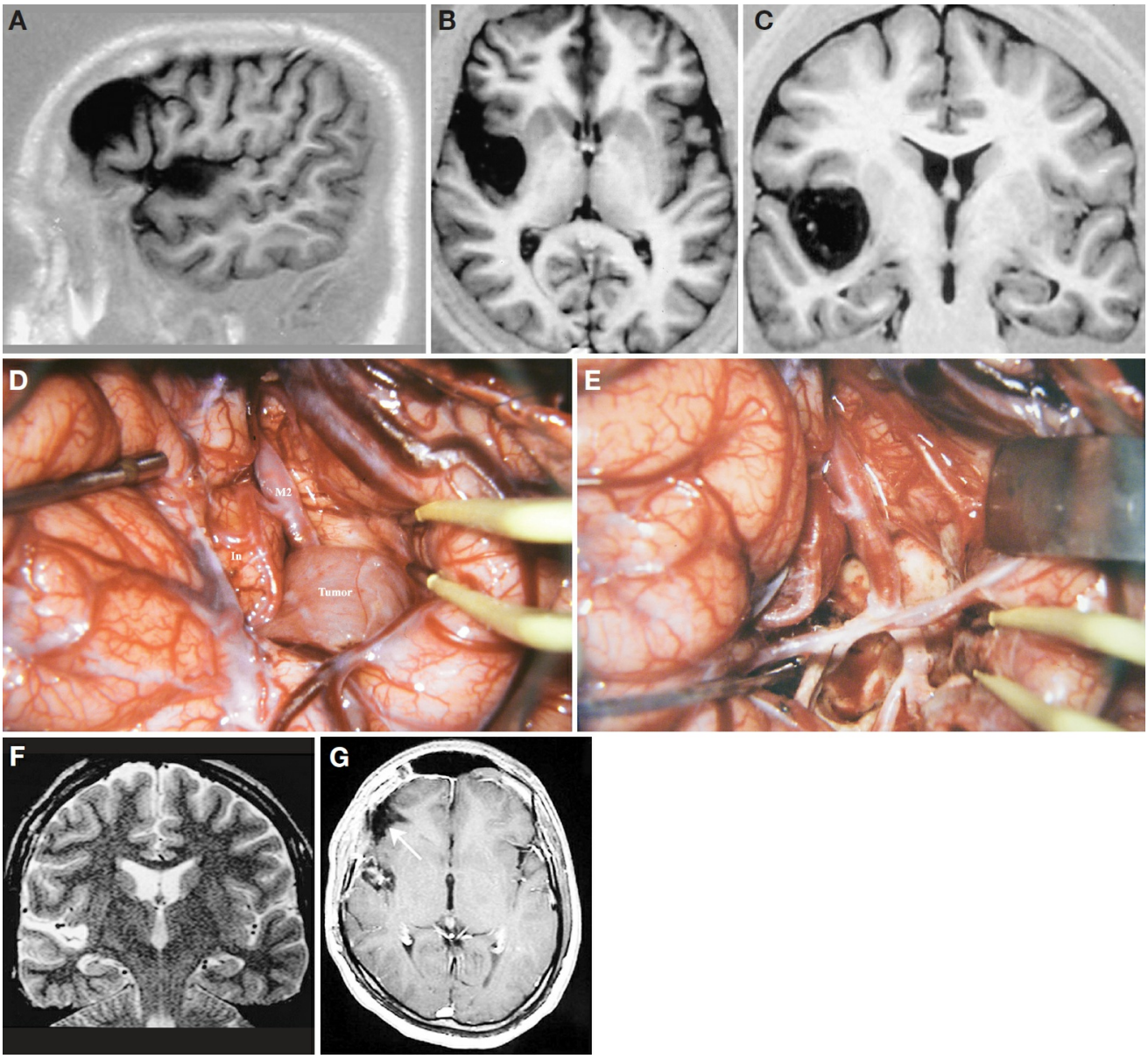

Figure 17. A, sagittal MRI scan of the right hemisphere, depicting an insular tumor and a frontal arachnoidal cyst. B, axial MRI scan. The tumor occupies the posterior two-thirds of the insula, sparing the first 2 short gyri (anterior and middle short gyri) and also sparing the posterior long gyrus. The tumor is limited medially by the lentiform nucleus. C, coronal MRI scan. The superior limit of the tumor is located at the same level of the lateral opercular compartment of the sylvian fissure. D, surgical exposure after an extended right pterional craniotomy, followed by the dural opening and the sylvian fissure splitting. M2, insular segment of the MCA; In, insula. Note that the tumor has encased the MCA. E, final aspect of the brain after tumor removal. The branches of the MCA were preserved. The whitish color of the arteries was owing to frequent application of the papaverine to prevent vasospasm. F, postoperative coronal MRI scan performed 8 months after surgery. G, postoperative

axial MRI scan performed 8 months after surgery. The arrow indicates the frontal resection. (Images courtesy of AL Rhoton, Jr.)

In this case, the relatively low upper limit of the tumor made the surgery easier. The upper limit of the tumor could be reached as soon as the sylvian fissure was split; there was no need to retract the frontal and parietal opercula during the surgery.

Case 2. A 15-year-old girl had daily seizures since 1 year of age. MRI revealed an image compatible with cortical dysplasia, composing the anterior margin of the anterior insula cleft, pars triangularis, and opercularis and the anterior half of the insula on the right hemisphere (Fig. 18, A and B). She underwent a right pterional craniotomy followed by a transsylvian approach and removal of suspicious tissue in March 2006 (histology revealed cortical dysplasia) (Fig. 18, C and D). The postoperative course was uneventful, and postoperative MRI performed 8 months after the surgery showed resection of the dysplasia (Fig. 18, E and F). She presented significant improvement in seizure frequency (1 nocturnal seizure every 3–4 weeks) but is still on anticonvulsants.

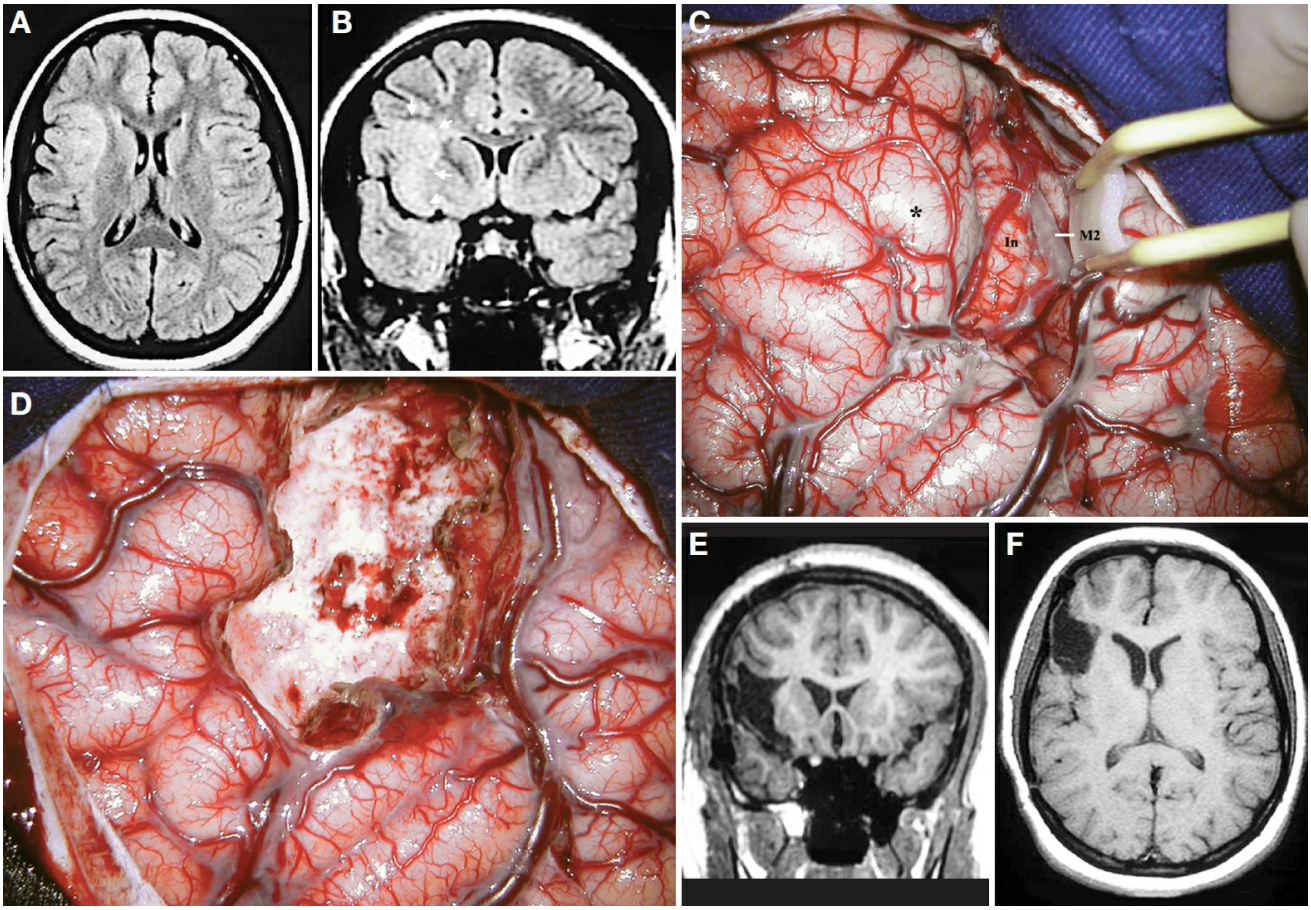

Figure 18. A, axial MRI scan. B, coronal MRI scan at the anterior part of the insula. Note that the superolateral insular cleft on the right side is lacking. Arrows indicate the cortical dysplasia. C, surgical exposure after right pterional craniotomy, dural opening, and sylvian fissure splitting. M2, insular segment of the MCA; In, insula. Asterisk, cortical dysplasia. D, intraoperative photograph after the removal of the cortical dysplasia. E, postoperative coronal MRI scan showing the resection of the cortical dysplasia. F, postoperative axial MRI scan. (Images courtesy of AL Rhoton, Jr.)

Case 3. The patient was a 26-year-old woman with complex partial seizures since the age of 10 years. MRI revealed a small cavernoma located on the long gyrus of the right insula; it was difficult to identify the posterior long gyrus in this case (Fig. 19, A–C). In March 2001, she underwent surgery via a right pterional transsylvian approach with total removal of the lesion (histology revealed cavernoma) (Fig. 19, D and E). The postoperative course was uneventful, but she presented 2 complex partial seizures in the first month after the surgery, after which she had no more seizures (Fig. 19, F and G). Currently, she is anticonvulsant free as well.

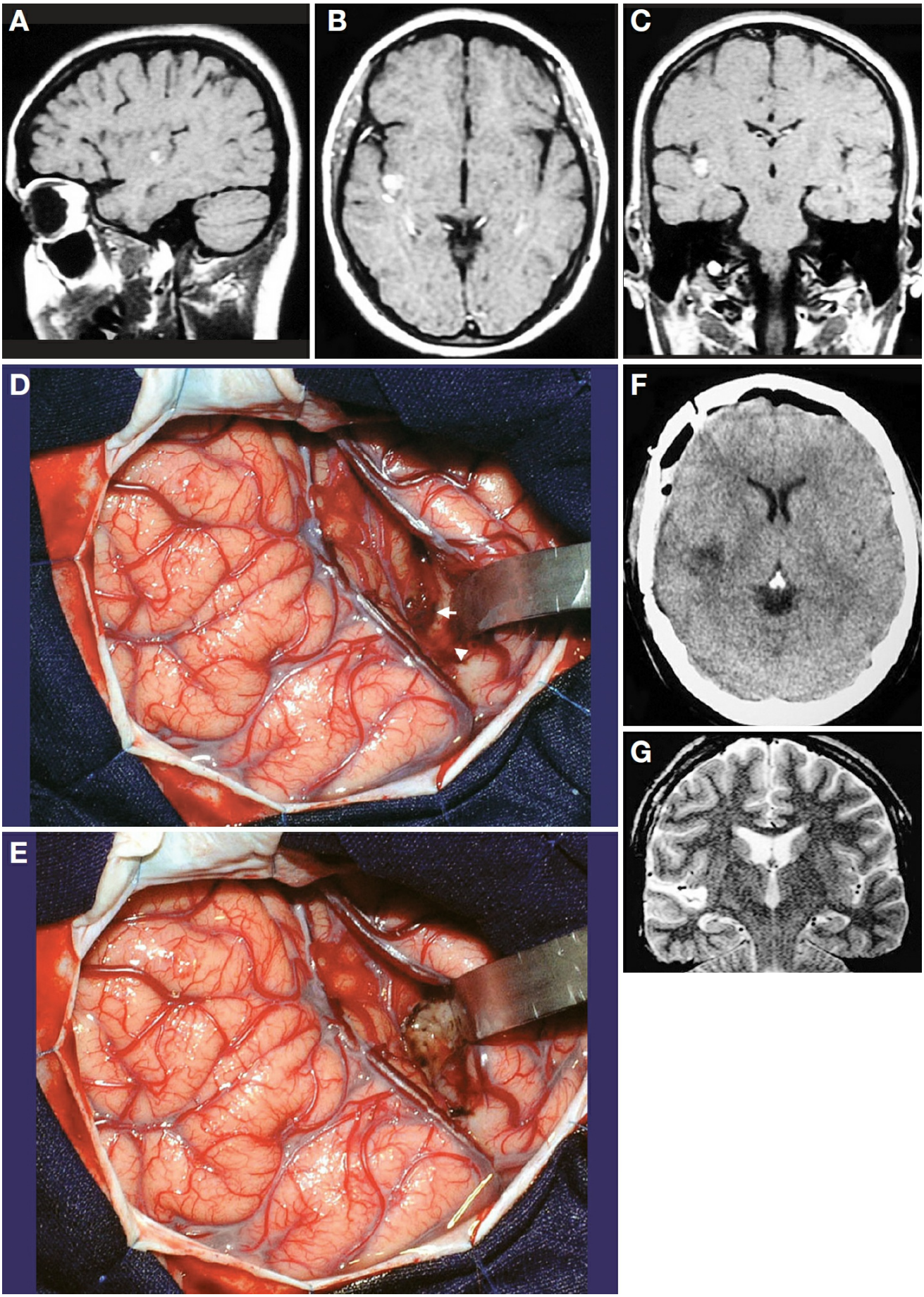

Figure 19. A, sagittal MRI scan depicting a cavernoma located in the long gyrus of the insula, approximately halfway between the superior and the inferior limiting sulci. B, axial MRI scan. C, coronal MRI scan. D, intraoperative photograph after the right pterional transsylvian approach.

The arrow indicates the cavernoma located on the sole long gyrus of the insula. The arrowhead indicates the Heschl's gyrus that prevented further lateral retraction of the temporal lobe. E, intraoperative photograph after the removal of the cavernoma. F, postoperative CT scan 1 day after surgery. Note the proximity of the resection cavity to the posterior limb of the internal capsule. G, postoperative MRI performed 3 months after the surgery showed total resection of the cavernoma. (Images courtesy of AL Rhoton, Jr.)

In this case, the low location of the cavernoma in the insula favored the transsylvian approach. It was easier to retract the temporal lobe than the frontal or parietal opercula because of the planum polare. The proximity of the cavernoma to the retroinsular region made this surgery more dangerous to the posterior portion of the posterior limb of the internal capsule; as discussed earlier, at this location, there is no interposition of the lentiform nucleus between the insula and the posterior limb of the internal capsule (Fig. 19F).

Case 4. A 4-year-old boy had complex partial seizures since the age of 3 years. He underwent brain surgery previously at another neurosurgical center, but apparently no sample of the tumor could be obtained, and the seizure frequency remained unchanged. MRI revealed a tumor arising from the posterior half of the right insula (Fig. 20, A and B). Apparently, the previous surgery reached only the anterior zone of the insula (Fig. 20C). He underwent an extended pterional craniotomy (extended posteriorly to include the posterior end of the posterior ramus of the sylvian fissure) and transsylvian approach in September 2005 with adequate removal of the tumor (Fig. 20, D and E) (histology revealed a grade II astrocytoma). The postoperative course was uneventful; he remains seizure-free since the surgery and still takes anticonvulsant medication (Fig. 20F).

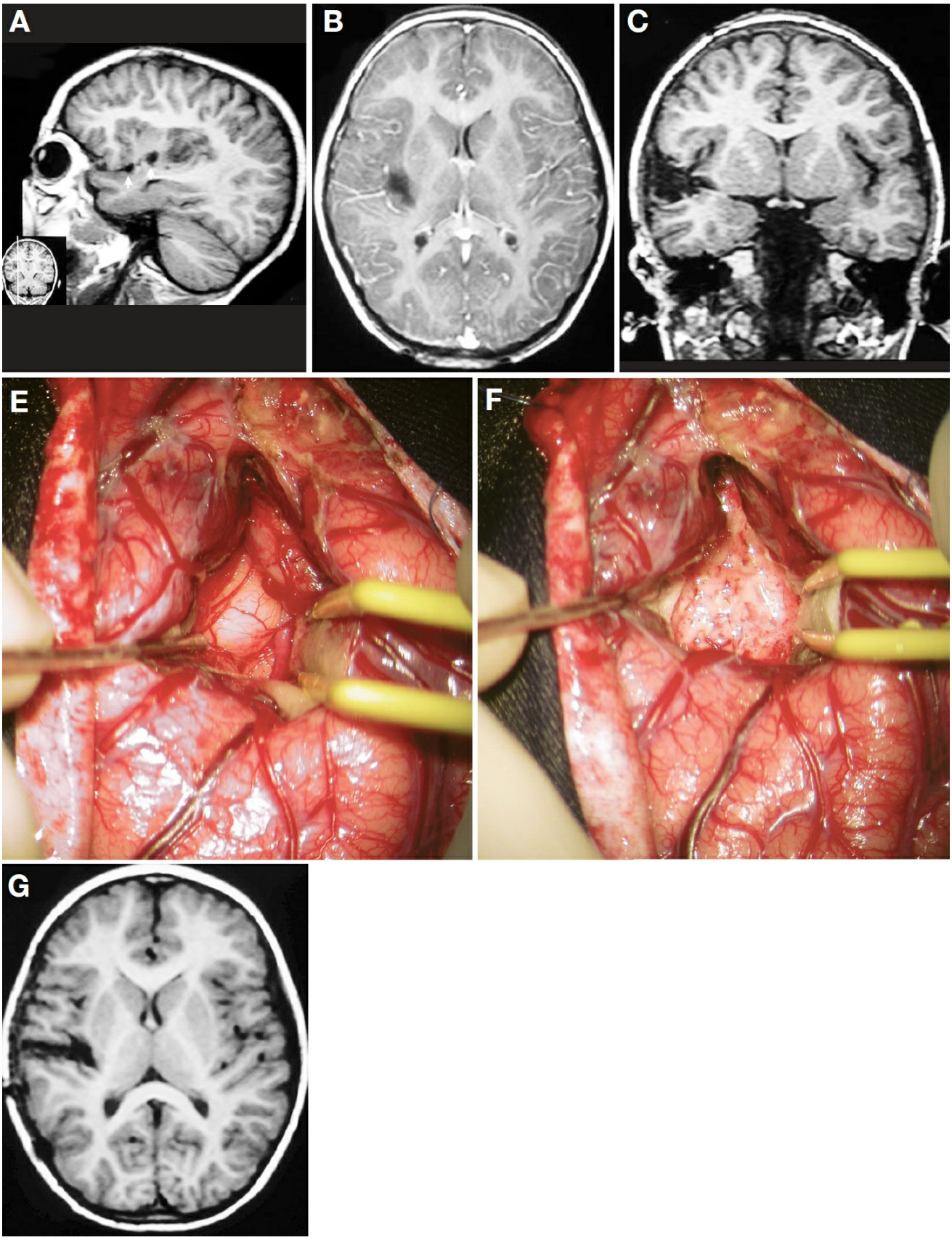

Figure 20. A, sagittal MRI scan. The tumor occupies the posterior zone of the right insula. The previous surgery apparently reached the anterior portion of the insula (arrows). B, axial MRI scan. The tumor occupies the posterior part of the insula. The posteromedial limit of the tumor is closely related to the posterior limb of the internal capsule; there is no intervening lentiform nucleus at this point. C, coronal MRI scan. The

previous surgery removed both the temporal and frontal opercula and also the anterior portion of the insula. Note that the insula edge is still prominent at this cut on the left side, indicating that this is the anterior insula. D, intraoperative photograph after opening the posterior ramus of the sylvian fissure. The tumor (whitish tissue) occupies the posterior zone of the insula. E, intraoperative photograph after the tumor removal. F, postoperative axial MRI scan depicting the resection of the tumor. (Images courtesy of AL Rhoton, Jr.)

In this case, the knowledge of the anatomy of the insula and the surrounding frontal, parietal, and temporal opercula could have helped the surgeon who performed the first surgery. MRI clearly showed that the tumor was located in the posterior half of the insula; the middle and posterior portions of the insula were covered on the surface by the operculum of the precentral and postcentral gyri. The latter meets the junction of the superior temporal gyrus and the Heschl's gyrus at the coronal plane above the external acoustic meatus. Therefore, after opening wide the posterior ramus of the sylvian fissure, the approach to the tumor should have been centered at the level of the junction between the postcentral gyrus and the Heschl's gyrus and not at the level of the planum polare.

Once again, as stated in Case 3, the posteromedial limit of the tumor was immediately adjacent to the posterior limb of the internal capsule, without the intervening lentiform nucleus.

Knowledge of the overall shape of the insula is very important in resecting intrinsic lesions that stay inside the boundaries of the insula, as in some gliomas of the insula. It is important for surgeons to bear in mind that the anterior insula is composed of a pyramid with its apex pointing downward and the posterior insula extends from the retroinsular region to the anterior pole of the insula.

The superomedial, inferomedial, and the posteromedial limits of insular resection are the normal white matter, i.e., the corona radiata superiorly, retrolentiform portion of the internal capsule and temporal stem inferiorly, and retrolentiform portion of the internal capsule posteriorly. At the

central region of the lateral surface of the insula, white matter (extreme and external capsules) or gray matter (claustrum and lentiform nucleus) will be encountered as the medial limits of the resection, depending on the medial extension of the lesion.

The resection involving the anterior surface of the insula is equally challenging. It is very important to bear in mind the overall sickle shape of the inferolateral facet of the insula. It is also important to keep in mind especially the medial boundary of the anterior surface of the insula: it is shallower in its upper portion that ends at the very anterior limb of the internal capsule and deeper in its lower portion that ends at the posteromedial orbital lobule, located laterally to the olfactory sulcus and above the apparent posterior end of the olfactory tract.

Hence, the theoretical limits for anterobasal insular resections are as follows: the anteromedial limit is the anterior portion of the anterior limb of the internal capsule, the posterolateral limit is the insular pole, and the posteromedial limit is the anterior perforated substance. The intraoperative anatomic landmark for the posterior limit of the anterobasal resection is the M1 segment of the MCA. The medial limit of the inferomedial resection of the anterior surface of the insula is the olfactory tract. Obviously, the limits of resection must be very well evaluated preoperatively and tailored according to each particular case.

Although quite similar, the actual microsurgery differs from the anatomic dissection in that the former requires additional information acquired from imaging. An intrinsic insular lesion will remain confined within the insula in most cases and will still be projected on the lateral surface of the cerebrum from the horizontal ramus to the supramarginal gyrus. It is interesting to evaluate the thickness of the medial extent of the tumor as well as the maximum AP length and height of the tumor on the preoperative MRI.

The technical nuances of intrinsic insular tumor resection have been magnificently pioneered and reported by Yaşargil (32) and Yaşargil and Fox (34), and some details are still worth mentioning.

Some important aspects involving insular resection can be pointed out. The early identification of MCA branches is very important because the surgeon has to work between and also preserve the branches of the M2 segment. Usually, the expanded insula with a tumor will come into the surgeon's view as soon as the sylvian fissure is split. Sometimes the major M2 branches cannot be identified promptly be cause each insular gyrus will be expanded, and the insular sulci containing the M2 branches will be trapped between the enlarged gyrus, hiding the MCA branches. In this case, early debulking of the tumor or debulking of the enlarged gyri can facilitate identification of the insular sulci and MCA branches.

Once the tumor has been debulked and the major M2 branches identified, it is advisable to first find the inferior and anterior limiting sulci of the insula to establish the inferior, inferoposterior, and anterior limits of the insula. Frequently, the transition between the insula and the planum polare is also infiltrated by the tumor. Hence, the early removal of this portion of the tumor will create additional room in the planum polare, facilitating the work in the insula.

Removing the upper portion of the tumor is challenging, especially in the dominant hemisphere, because the retraction over the frontal and parietal opercula can cause neurological deficits. It is sometimes advisable to debulk the tumor as much as possible and then try to pull out the pial surface of the upper insula like the capsule of an extrinsic tumor, followed by debulking the tumor again. This maneuver can be performed successively rather than retracting the frontal and parietal opercula to resect the upper insula.

To establish the medial limit of the resection for insular tumors can be challenging as well. The lentiform nucleus can serve as a barrier preventing surgeons from trespassing toward the internal capsule. The lentiform nucleus presents the look of gray matter. How ever, the lentiform nucleus is a small shield leaving the anterior (anterior limb), superior (corona radiata), posterior (retrolentiform), and inferior (sublentiform) parts of the internal capsule uncovered.

The resection of a posterior insular lesion can be difficult because of the

retraction over the Heschl's gyrus and the planum temporale and the supramarginal and postcentral gyri. Caution should be used because there have been reports of branches originating from the M2 segment of this region that directly supply the internal capsule (23).

Under normal conditions, the length of the superior limiting sulcus, the AP extent, of the insula is approximately 5 cm, and the height of the anterior limiting sulcus of the insula is approximately 3 cm. The length of the insula and the limiting sulci of each patient can be determined accurately by preoperative MRI.

Ausman et al. (1) reported an intraoperative localization technique for resecting vascular lesions around the sylvian point by following major ar teries that exit the posterior portion of the sylvian fissure, e.g., the angular artery, and splitting only the necessary extent of the sylvian fissure.

Case 1. The patient was a 17-year-old girl with mental retardation and refractory epilepsy (complex partial seizures) since the age of 5 years. At the age of 10 years, she underwent partial left temporal lobectomy with removal of a tumor (pilocytic astrocytoma) and evacuation of a postoperative extradural hematoma at another neurosurgical center, without adequate postoperative seizure control. At the age of 11 years, she underwent another temporal resection for residual tumor. At the age of 13 years, she was referred to our hospital. MRI revealed a tumor growing from the left frontobasal area pushing the insula backward (Fig. 21, A–C), with good identification of the anterior insular cleft (Fig. 21D). In December 2003, she underwent left pterional craniotomy and intraoperative electrocorticography (Fig. 21E). The anterior insular cleft was split to determine the posterior limit of resection (Fig. 21F). The residual medial temporal structures also were removed (histology revealed pilocytic astrocytoma). The postoperative course was uneventful, and she has remained seizure free since the surgery and is on a gradual withdrawal regimen of anticonvulsant medication (Fig. 21, G–I).In resections involving the basal portion of the frontal lobe, it is important to evaluate the superior and posterior limits of the lesion because of its proximity to the anterior surface of the insula and to the anteroinferior surface of the basal

ganglia.

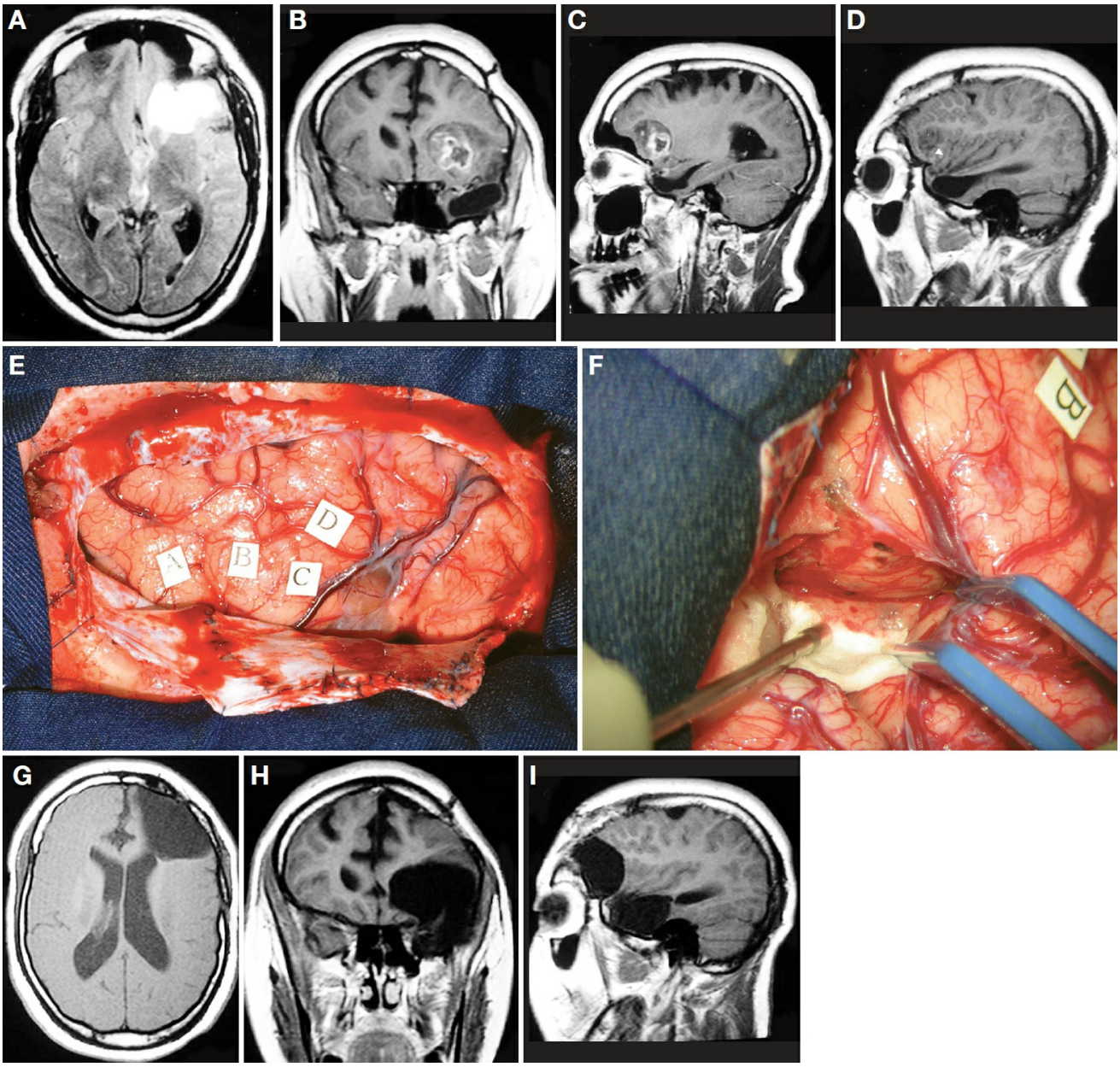

Figure 21. A, axial MRI scan depicting a left frontal tumor. B, coronal MRI scan. C, sagittal MRI scan depicting a tumor arising from the frontobasal region. D, sagittal MRI scan. The arrowhead indicates the anterior insular cleft. The tumor is confined in the fronto-orbital area. E, intraoperative photograph after a left pterional craniotomy and dural opening. The letters indicate epileptiform spikes in the left frontal lobe. F, intraoperative photograph showing the opening of the anterior insular cleft. The anterior surface of the insula was covered by the cottonoid. G, postoperative axial MRI scan. H, postoperative coronal MRI scan. I, postoperative sagittal MRI scan. The mediotemporal structures also were removed. (Images courtesy of AL Rhoton, Jr.)

In this case, the initial approach was to identify the horizontal ramus that continues medially with the anterior insular cleft to determine the anterior limit of the insula and to estimate the location of the head of the caudate nucleus. The entry into the tumor was performed via the pars orbitalis. Because of the very distinctive aspect of the tumor, which was quite different from normal brain tissue, it was not difficult to remove the whole tumor.

Case 2. A 17-year-old girl had 3 different types of daily seizures (complex partial, tonic, and generalized tonic-clonic) since the age of 5 years. The preoperative investigation included electroencephalography, video-electroencephalographic monitoring, and ictal and interictal single-photon emission CT, but did not indicate precisely the origin of the seizures. MRI showed an increased signal on the right frontobasal area (Fig. 22, A and B). In July 2003, she underwent right pterional craniotomy with electrocorticography, and the lateral orbital gyrus, where the epileptiform spikes were evident, and the lateral part of the posteromedial orbital lobule, with no spikes, were resected. Despite the surgery, her epilepsy remained unchanged. In August 2007, after a completely new preoperative workup for epilepsy, the neurologists still could not determine precisely the origin of the seizures. Because of the severity of the illness, she again underwent a right pterional craniotomy (Fig. 22C) with total resection of the frontobasal area and removal of the frontal pole (Fig. 22, D and E). The postoperative course was uneventful, but the seizures gradually resumed 1 week after the surgery, and the histology results remained unclear.

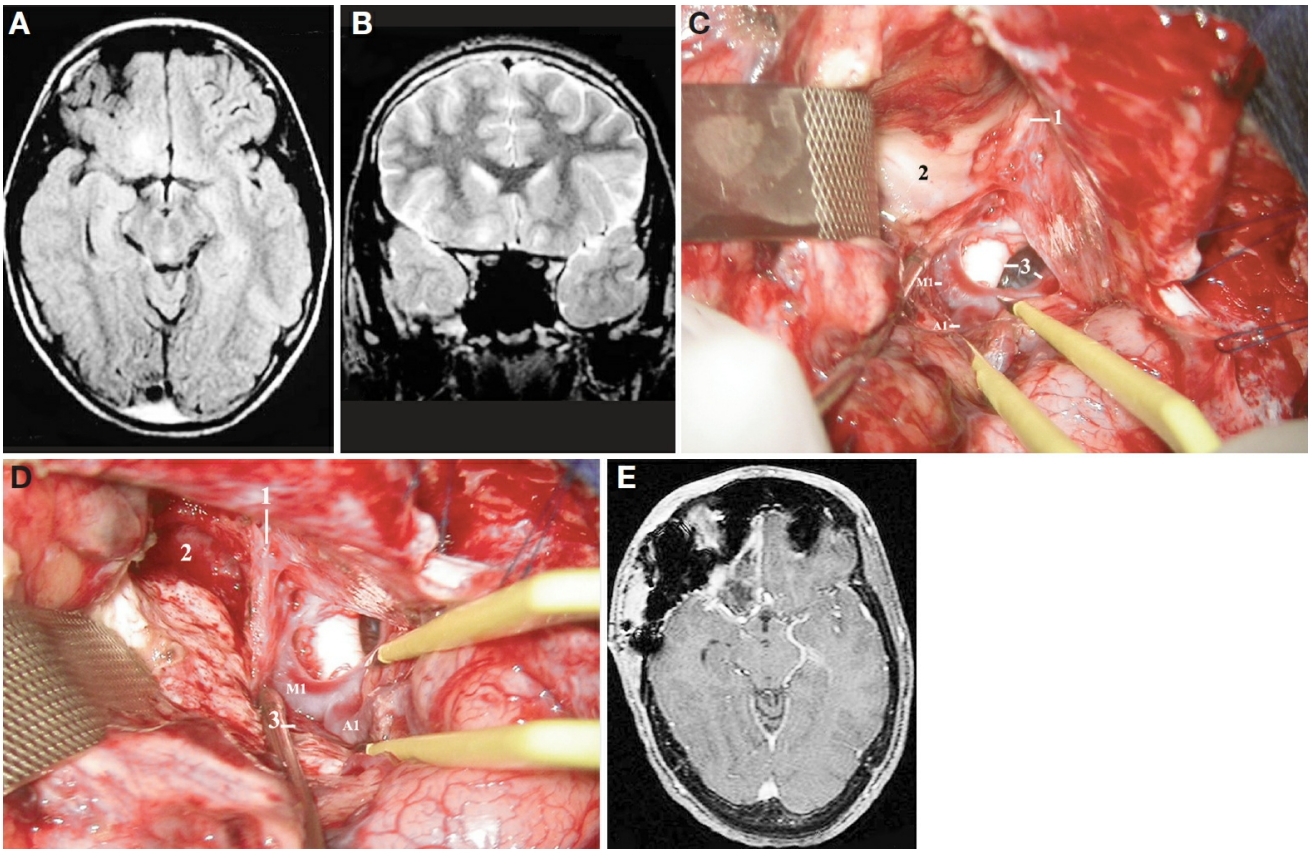

Figure 22. A, axial MRI scan. There is an increase in signal over the posteromedial orbital lobule. B, coronal MRI scan. There is a thin layer of white matter separating the suspicious area (corresponding to the posteromedial orbital lobule) from the inferior portion of the caudate nucleus. C, intraoperative photograph of the second operation, after a right pterional craniotomy and dural opening. 1, olfactory tract; 2, suspicious tissue; 3, optic chiasm and carotid artery; M1, M1 segment of the MCA; A1, precommunicating segment of the anterior cerebral artery. At the tip of the suction tube is the posterior part of the olfactory tract. D, intraoperative photograph after removal of the posteromedial orbital lobule and the rectus gyrus. 1, olfactory tract; 2, anterior cerebral artery in the interhemispheric fissure; 3, lenticulostriate arteries arising from the carotid bifurcation; M1, M1 segment of the MCA; A1, precommunicating segment of the anterior cerebral artery. E, postoperative MRI scan performed 5 days after surgery showed the resection of the frontobasal area, just anterior to the carotid artery bifurcation. (Images courtesy of AL Rhoton, Jr.)

In cases such as this, when the resection of the suspicious tissue is solely based on anatomic landmarks, the knowledge on the anatomy of the frontobasal area becomes essential.

The major areas of concern in dealing with frontobasal lesions are the anterior perforated substance and lenticulostriate arteries and the anteroinferior portion of the basal ganglia.

The anterior limit of the anterior perforated substance has been classically described as medial and lateral olfactory striae (12, 15). However, it is extremely difficult to identify the striae intraoperatively.

From a practical viewpoint, the anterior limit of the perforated substance can be considered the accessory gyrus of Ebertaller laterally and the posterior edge of the rectus gyrus medially.

It is interesting to note that even in the frontobasal area, the claustrum accompanies the inferolateral facet of the insula and stays interposed between the extreme and external capsules. There is no claustrum above the posteromedial orbital lobule (Fig. 6E).

From a microneurosurgical standpoint, the anterior perforated substance indicates more than just the entry site for the lenticulostriate arteries to the basal ganglia or the exit site for the inferior striate vein from the basal ganglia; it is the site where the anteroinferior portion of the lentiform nucleus (the globus pallidus medially and the putamen laterally) comes to the surface. Part of the anterosuperior portion of the basal ganglia, i.e., the caudate nucleus, also comes to the surface intraventricularly as the lateral walls of the frontal horn and the body of the lateral ventricle.

Intraoperatively, the presence of lenticulostriate vessels and a sudden increase in bleeding indicate entry into basal ganglia.

Amygdalohippocampectomy and Hemispherotomy

The inferior limiting sulcus of the insula as the preferred route to enter the temporal horn in transsylvian amygdalohippocampectomies has been advocated and popularized by Yaşargil et al. (36). Figure 23, A–D, shows the sequence of a right transsylvian selective amygdalohippocampectomy.

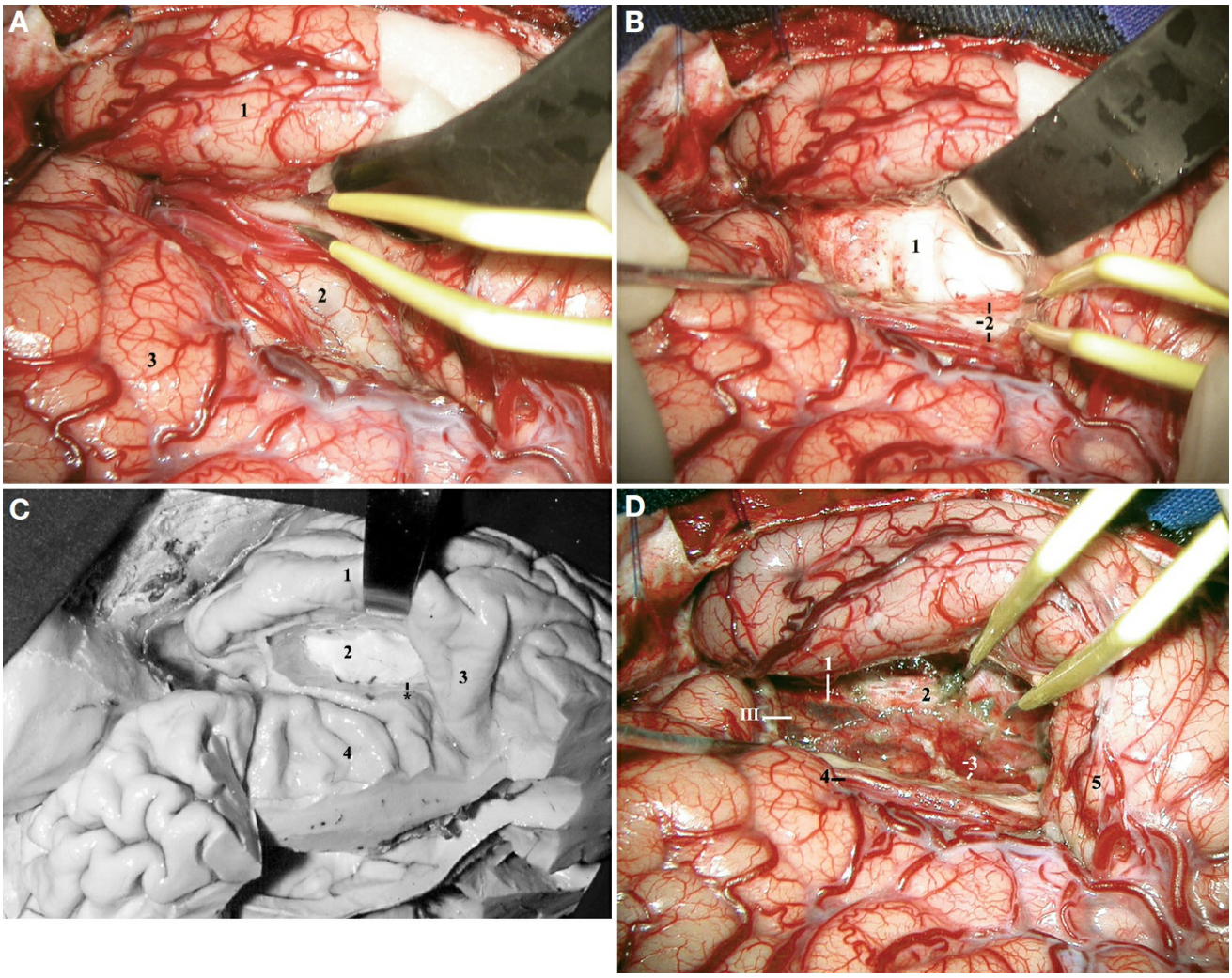

Figure 23. A, intraoperative photograph after an extended right pterional transsylvian approach, depicting the inferior limiting sulcus of the insula (between the tips of the bipolar forceps). 1, temporal lobe; 2, insula; 3, frontal lobe. B, intraoperative photograph after entering the temporal horn. 1, head of the hippocampus; 2, choroid plexus, temporal stem, and the M2 segment of the MCA. The Heschl's gyrus has been retracted posteriorly by the bipolar forceps. C, anatomic dissection mimicking the surgical approach shown in B. 1, superior temporal gyrus; 2, head of the hippocampus; 3, Heschl's gyrus; 4, insula. Asterisk, choroid plexus of the temporal horn. D, intraoperative photograph after a right pterional transsylvian selective amygdalohippocampectomy. 1, free edge of the tentorium; 2, dura mater of the floor of the middle fossa; 3, P2A segment of the posterior cerebral artery, and the choroid plexus of the temporal horn; 4, M2 segment of the MCA; 5, Heschl's gyrus; III, oculomotor nerve. (Images courtesy of AL Rhoton, Jr.)

The first author (HTW) has performed most of the amygdalohippocampectomies via the superior temporal gyrus. In these

cases, the temporal horn is entered by following the gray matter overlying the occipitotemporal sulcus (27, 29). The superior temporal gyrus is then peeled off subpially from the arachnoidal membrane of the sylvian fissure to reach the inferior limiting sulcus of the insula (Fig. 24A). The next step is to connect the bottom of the inferior limiting sulcus of the insula to the temporal horn by cutting the temporal stem.

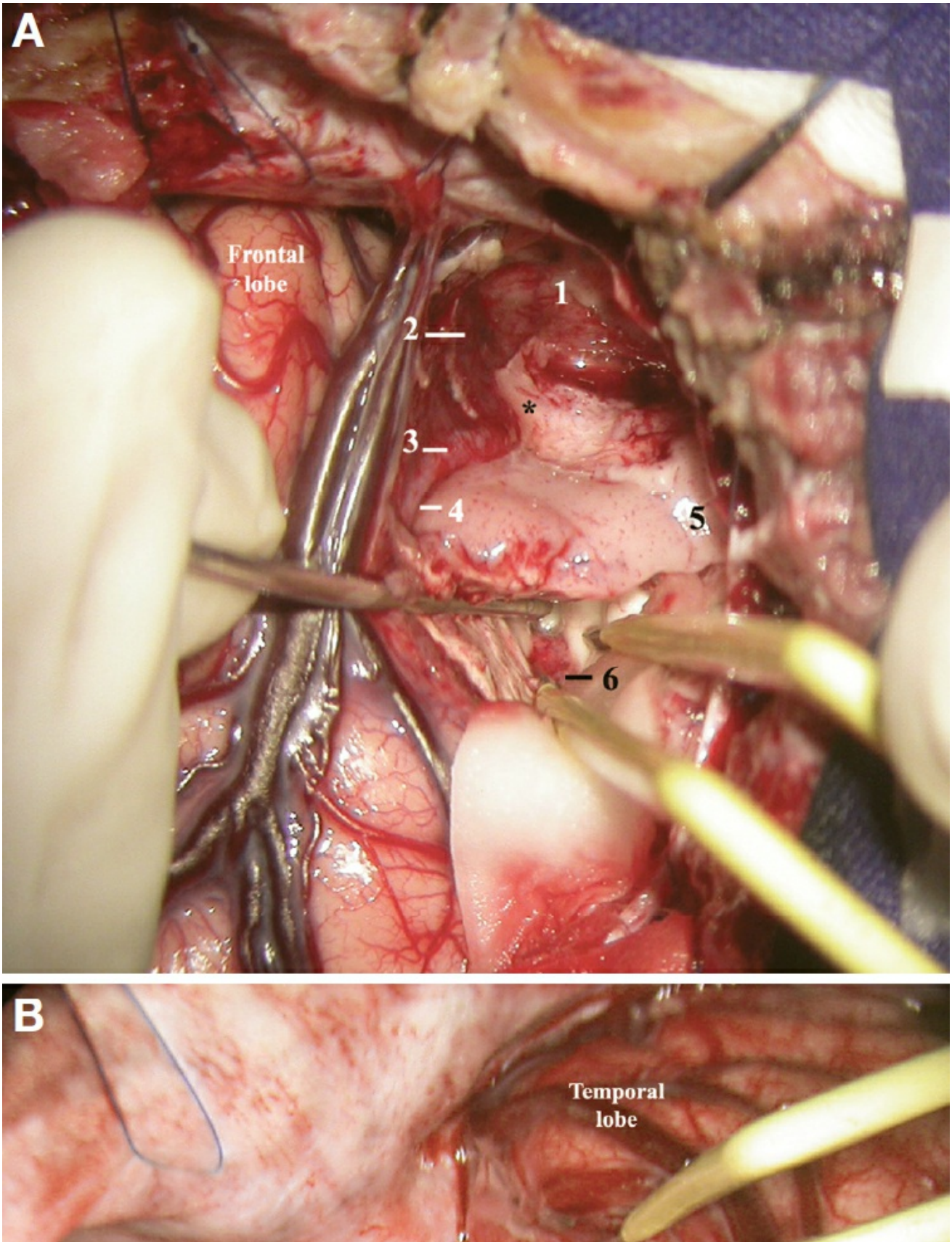

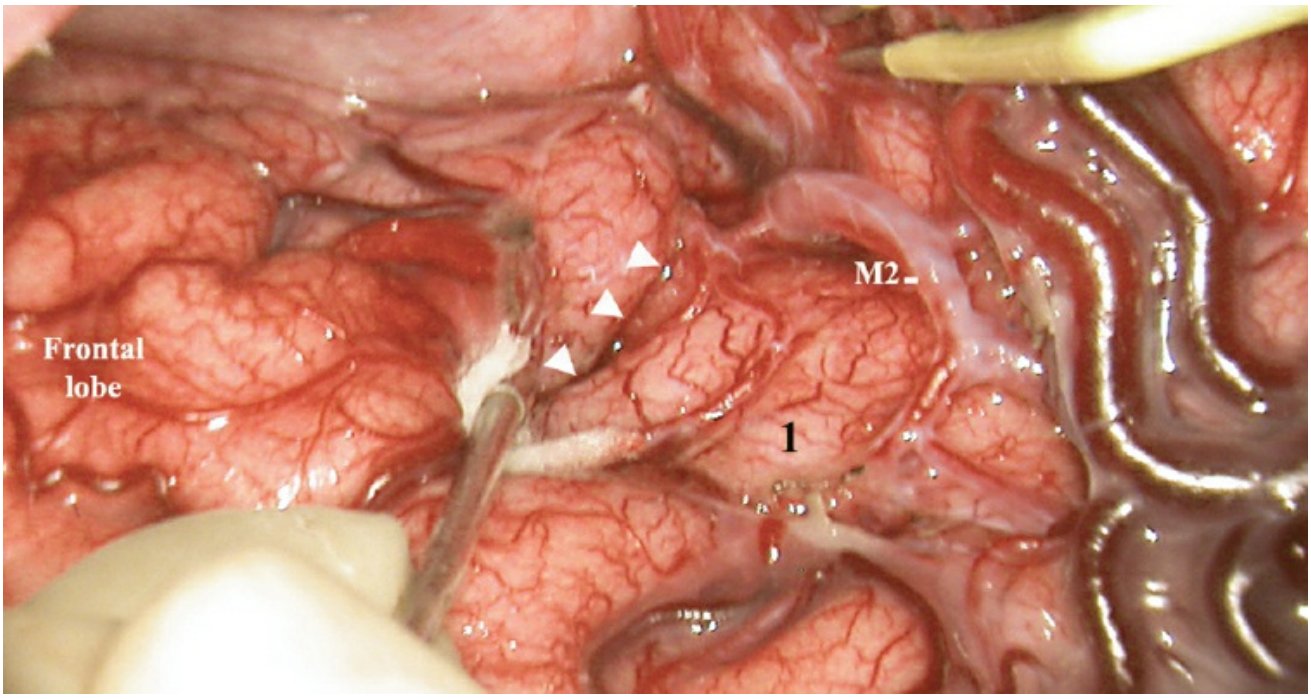

Figure 24. A, intraoperative photograph showing a right amygdalohippocampal resection via superior temporal gyrus. The right temporal horn, superior temporal gyrus, and uncus have been peeled off from the arachnoidal membrane of the sylvian fissure and carotid cistern. The tip of the suction tube (on the left) is located immediately ahead of the inferior choroidal point. Both tips of the bipolar forceps are inside the temporal horn. 1, arachnoidal membrane of the temporal pole; 2, carotid artery (covered by arachnoidal membrane); 3, M1 segment of the MCA just before the genu of the MCA; 4, beginning of the inferior limiting sulcus of the insula; 5, superior temporal gyrus; 6, choroid plexus of the temporal horn. Asterisk, anteromedial surface of the uncus that has been peeled off from the arachnoidal membrane of the carotid cistern. B, intraoperative photograph of the initial phase of a right hemisphere deafferentation (after splitting the sylvian fissure). 1, insula; M2, insular segment of the MCA. The arrowheads indicate anterior insular cleft. (Images courtesy of AL Rhoton, Jr.)

In peri-insular hemispherotomy or hemispherical deafferentation, the rationale of the procedure is to disconnect the cerebral hemisphere around its central core (26). As part of this procedure, the early identification of the anterior insular cleft indicates the anterior limiting sulcus of the insula, which, in turn, ultimately indicates the anterior limit of the basal ganglia that should not be trespassed on during the procedure

(Fig. 24B).

The resection of the amygdala can be performed either subpially or intracisternally. The relationships between the temporal amygdala and the globus pallidus and the landmarks for resecting the temporal amygdala have been reported in an earlier publication by Wen et al. (29). Because of the proximity of the inferior choroidal point and the anatomic complex formed by the optic tract, apex of the uncus, and upper portion of the crus cerebri (Fig. 6B), the resection of the apex of the uncus should not extend above the level of the inferior choroidal point because of the risk of entering the globus pallidus and the risk of injuring the optic tract and the anterior choroidal artery.

In this article, we aimed to share our experience in anatomic dissection combined with its application in neuroimaging, surgical planning, and microsurgery performed in and around the sylvian fissure region. We hope that the information in this article can help a younger generation of neurosurgeons learn as much as we did, but in less time.

CONCLUSION

The anatomic information regarding the sylvian fissure region has been very helpful for the authors in preoperative planning and has provided reliable intraoperative navigation landmarks in microsurgeries involving that region performed over the past 15 years.

Despite the current technological advances in targeting, navigating, and controlling surgical procedures, many anatomic, imaging, preoperative planning, and surgical details are still out of reach using these technologies. When well trained, the surgeon's own mind seems to be the best available computer for analyzing the nuances of neuroimages, defining the operative approach, planning a treatment strategy, performing microsurgery, and optimizing the benefits provided by currently available technology.

Contributors: Hung Tzu Wen, MD, Albert L. Rhoton, Jr, MD, Evandro de Oliveira, MD, Luiz Henrique M. Castro, MD, Eberval Gadelha Figueiredo,

MD, and Manoel Jacobsen Teixeira, MD

Content from Wen HT, Rhoton AL, Jr, de Oliveira E, Castro LHM, Figueiredo EG, Teixeira MJ. Microsurgical anatomy of the temporal lobe: part 2—sylvian fissure region and its clinical application. *Oper Neurosurg (Hagerstown)* 2009;65:ons1–ons36. doi.org/10.1227/01.NEU.0000336314.20759.85. With permission of Oxford University Press on behalf of the Congress of Neurological Surgeons. © Congress of Neurological Surgeons.

The Neurosurgical Atlas is honored to maintain the legacy of Albert L. Rhoton, Jr, MD.

REFERENCES

1. Ausman JI, Dias FG, Malik GM, Tomecek F: A new microsurgical approach to cerebrovascular lesions of the sylvian point: Report of two cases. **Surg Neurol** 34:48–51, 1990.
2. Berry M, Bannister LH, Standring SM: Nervous system, in Williams PL (ed) *Gray's Anatomy*. New York, Churchill Livingstone, 1995, ed 35, p 1111.
3. Chyatte D, Porterfield R: Nuances of middle cerebral artery aneurysm microsurgery. **Neurosurgery** 48:339–346, 2001.
4. Dashti R, Hernesniemi JA, Niemelä M, Rinne J, Lehecka M, Shen H, Lehto H, Albayrak BS, Ronkainen A, Koivisto T, Jääskeläinen JE: Microneurosurgical management of distal middle cerebral artery aneurysms. **Surg Neurol** 67:553–563, 2007.
5. Gibo H, Carver CC, Rhoton AL Jr, Lenkey C, Mitchell RJ: Microsurgical anatomy of the middle cerebral artery. **J Neurosurg** 54:151–169, 1981.
6. Heros RC, Ojemann RG, Crowell RM: Superior temporal gyrus approach to middle cerebral artery aneurysms: Technique and results. **Neurosurgery** 10:308–313, 1982.
7. Krayenbühl H, Yaşargil MG, Huber P, Bosse G: *Cerebral Angiography* Stuttgart, Thieme, 1982, ed 2, pp 105–121.

8. *Microsoft Bookshelf 1999 Computer and Internet Dictionary*. Redmond, Microsoft Corp., 1999.
9. Ogilvy CS, Crowell RM, Heros RC: Surgical management of middle cerebral artery aneurysms: Experience with transsylvian and superior temporal gyrus approaches. **Surg Neurol** 43:15–24, 1995.
10. Ono M, Kubik S, Abernatehey CD: *Atlas of the Cerebral Sulci*. Stuttgart, Thieme, 1990, pp 94–110.
11. Pritz MB, Chandler WF: The transsylvian approach to middle cerebral artery bifurcation/trifurcation aneurysms. **Surg Neurol** 41:217–220, 1994.
12. Rhoton AL Jr: The cerebrum. **Neurosurgery** 53 [Suppl 2]:29–148, 2003.
13. Rhoton AL Jr: The supratentorial arteries, in *Rhoton Cranial Anatomy and Surgical Approaches*. Baltimore, Lippincott Williams & Wilkins, 2003, pp 81–148.
14. Ring BA: The middle cerebral artery, in Newton TH, Potts DG (eds): *Radiology of the Skull and Brain*. St. Louis, CV Mosby, 1974, pp 1442–1478.
15. Rosner SS, Rhoton AL Jr, Ono M, Barry M: Microsurgical anatomy of the anterior perforating arteries. **J Neurosurg** 61:468–485, 1984.
16. Schlesinger B: The insulo-opercular arteries of the brain, with special reference to angiography of striothalamic tumors. **Am J Roentgenol Ther Nucl Med** 70:555–563, 1953.
17. Son YJ, Han DH, Kim JE: Image-guided surgery for treatment of unruptured middle cerebral artery aneurysms. **Neurosurgery** 61 [Suppl 2]:266–272, 2007.
18. Stoodley MA, Weir BKA: Surgical treatment of middle cerebral artery aneurysms in Le Roux PD, Winn HR, Newell DW (eds): *Management of Cerebral Aneurysms*. Philadelphia, Saunders, 2004, pp 795–807.
19. Szikla G, Bouvier T, Hori T, Petrov V: The sylvian fissure, in

Angiography of the Human Brain Cortex. Berlin, Springer, 1977, pp 101–125.

20. Tanriover N, Rhoton AL Jr, Kawashima M, Ulm AJ, Yasuda A: Microsurgical anatomy of the insula and the sylvian fissure. **J Neurosurg** 100:891–922, 2004.
21. Taveras JM, Pile-Spellman J: *Neuroradiology*. Baltimore, Williams & Wilkins, 1996, pp 948–961.
22. Türe U, Yaşargil DCH, Al Mefty O, Yaşargil MG: Topographic anatomy of the insular region. **J Neurosurg** 90:720–733, 1999.
23. Türe U, Yaşargil MG, Al Mefty O, Yaşargil DCH: Arteries of the insula. **J Neurosurg** 92:676–687, 2000.
24. Waddington MM: *Atlas of Cerebral Angiography with Anatomic Correlation*. Boston, Little Brown and Company, 1974, ed 1, pp 38–41.
25. Wen HT, Mussi AC, Rhoton AL Jr: Surgical anatomy of the brain, in Winn HR, Youmans JR (eds): *Youmans Neurological Surgery*. Philadelphia, WB Saunders, 2003, ed 5, pp 5–44.
26. Wen HT, Rhoton AL Jr, Marino R Jr: Anatomical landmarks for hemispherotomy and their clinical application. **J Neurosurg** 101:747–755, 2004.
27. Wen HT, Rhoton AL Jr, Marino R Jr: Gray matter overlying anterior basal temporal sulci as an intraoperative landmark for locating the temporal horn in amygdalohippocampectomies. **Neurosurgery** 59 [Suppl 4]:221–227, 2006.
28. Wen HT, de Oliveira E, Tedeschi H, Andrade FC Jr, Rhoton AL Jr: The pterional approach: Surgical anatomy, operative technique, and rationale. **Operative Techniques in Neurosurgery** 4:60–72, 2001.
29. Wen HT, Rhoton AL Jr, de Oliveira EP, Cardoso AC, Tedeschi H, Baccanelli M, Marino R Jr: Microsurgical anatomy of the temporal lobe: Part 1. Mesial temporal lobe anatomy and its vascular relationships as applied to amygdalohippocampectomy. **Neurosurgery** 45:549–592, 1999.

30. Wolf BS, Huang YP: The insula and deep middle cerebral venous drainage system: Normal anatomy and angiography. **Am J Roentgenol Radium Ther Nucl Med** 90:472–489, 1963.
31. Yaşargil MG: Operative anatomy, in *Microneurosurgery*. Stuttgart, Thieme, 1984, pp 36–39, 72–91, vol 1.
32. Yaşargil MG: Limbic and paralimbic tumors, in *Microneurosurgery*. Stuttgart, Thieme, 1996, pp 252–290, vol 4B.
33. Yaşargil MG: A legacy of microneurosurgery: Memoirs, lessons, and axioms. **Neurosurgery** 45:1025–1092, 1999.
34. Yaşargil MG, Fox JL: The microsurgical approach to intracranial aneurysms. **Surg Neurol** 3:7–14, 1975.
35. Yaşargil MG, Cravens GF, Roth P: Surgical approaches to "inaccessible" brain tumors. **Clin Neurosurg** 34:42–110, 1988.
36. Yaşargil MG, Teddy PG, Roth P: Selective amygdalo-hippocampectomy operative anatomy and surgical technique, in Symon L, Brihaye J, Guidetti B, Loew F, Miller JD, Nornes H, Pásztor E, Pertuiset B, Yaşargil MG (eds): *Advances and Technical Standards in Neurosurgery*, Vienna, Springer-Verlag, 1985, pp 93–123, vol 12.